Filtering Antennas Based on Rectangular Dielectric Resonators

by

Xiangqi Su

A thesis submitted to the
School of Graduate and Postdoctoral Studies in partial
fulfillment of the requirements for the degree of

Master of Applied Science in Electrical and Computer Engineering

The Faculty of Engineering and Applied Science

University of Ontario Institute of Technology (Ontario Tech University)

Oshawa, Ontario, Canada

December, 2023

THESIS EXAMINATION INFORMATION

Submitted by: **Xiangqi Su**

Master of Applied Science in **Electrical and Computer Engineering**

Thesis title: Filtering Antennas Based on Rectangular Dielectric Resonators

An oral defense of this thesis took place on December 6th, 2023 in front of the following examining committee:

Examining Committee:

Chair of Examining Committee	Dr. Shahram ShahbazPanahi
Research Supervisor	Dr. Ying Wang
Examining Committee Member	Dr. Ming Yu
Thesis Examiner	Dr. Min Dong

The above committee determined that the thesis is acceptable in form and content and that a satisfactory knowledge of the field covered by the thesis was demonstrated by the candidate during an oral examination. A signed copy of the Certificate of Approval is available from the School of Graduate and Postdoctoral Studies.

ABSTRACT

Filters and antennas are essential components in communication systems. Being able to simultaneously realize filter and radiation functions, filtering antennas have attracted much attention due to their compactness and low loss. This thesis focuses on different methods of realizing compact filtering antennas using rectangular dielectric resonator antennas (DRAs). First, four designs of DRA to increase bandwidth have been proposed. Low dielectric constant posts are inserted in DRA in different orientations so that the effective dielectric constant can be readily lowered and adjusted. An integrated design of a waveguide dielectric resonator filter and a DRA with an air post shows significant bandwidth improvement. Next, conducting posts are inserted in the DRA to realize radiation cancelation. Radiation nulls, or filtering responses, have been achieved for both linear polarization and dual polarization. All designs have been simulated and optimized using a full wave electromagnetic (EM) simulator, and results are compared and discussed.

Keywords: Filtering antenna; dielectric resonator antennas; dual polarization.

AUTHOR'S DECLARATION

I hereby declare that this thesis consists of original work of which I have authored. This is a true copy of the thesis, including any required final revisions, as accepted by my examiners.

I authorize the University of Ontario Institute of Technology (Ontario Tech University) to lend this thesis to other institutions or individuals for the purpose of scholarly research. I further authorize University of Ontario Institute of Technology (Ontario Tech University) to reproduce this thesis by photocopying or by other means, in total or in part, at the request of other institutions or individuals for the purpose of scholarly research. I understand that my thesis will be made electronically available to the public.

Xiangqi Su

STATEMENT OF CONTRIBUTIONS

I hereby certify that I am the sole author of this thesis and that no part of this thesis has been published or submitted for publication. I have used standard referencing practices to acknowledge ideas, research techniques, or other materials that belong to others. Furthermore, I hereby certify that I am the sole source of the creative works and/or inventive knowledge described in this thesis.

ACKNOWLEDGEMENTS

I would like to express my gratitude to my supervisor Professor Ying Wang for her continuous guidance and unwavering support throughout the completion of this thesis. During my graduate study and research, Professor Ying Wang is always supportive and patient. I am grateful for the opportunity she has provided me. Furthermore, I would like to thank my friends and colleagues for their support. In the end, I would like to acknowledge my parents for their constant support and never-ending love.

Xiangqi Su

Oshawa, Ontario

December, 2023

TABLE OF CONTENTS

LIST OF FIGURES

CHAPTER 2

CHAPTER 3

CHAPTER 4

LIST OF ABBREVIATIONS AND SYMBOLS

DRA	Dielectric Resonator Antenna
RDRA	Rectangular Dielectric Resonator Antenna
EM	Electromagnetic
mm-wave	Millimetre-wave
Q	Quality Factor
Q_{EXT}	External Quality Factor
SIW	Substrate Integrated Waveguide
FBW	Fractional Bandwidth
HFSS	High-Frequency Structural Simulator
ADS	Advanced System Designs

Chapter 1

Introduction

1.1 Overview

As wireless communication technologies are going through rapid development, RF front-end systems are also evolving significantly. Compactness, low loss, and ease to fabricate are among some of the general requirements. Conventionally, filters and antennas, key components in communication systems, are designed independently and connected through connectors or adaptors. Thus, designs are usually bulky, lossy and costly. As a new type of component, filtering antennas have attracted much attentions in recent years since they can simultaneously realize filtering and radiation functions.

Different from the conventional cascaded connection of filters and antennas, there are generally two methods to implement filtering antennas, namely the synthesis method and the fusion method [1]-[3]. The synthesis method follows the synthesis of a standalone filter design. However, an antenna replaces the last resonator of the filter to realize an integrated design without using extra connectors. The approach of fusion design is to modify the antenna, for example, by introducing parasitic elements, to cancel radiation at certain frequencies to achieve filtering responses.

1.2 Motivations

Dielectric resonator antennas have been widely accepted as an ideal candidate for communication systems, due to its many advantages, such as compactness and low loss. Using dielectric material with high dielectric constant further reduces the size. For filter antenna integration using the synthesis method, the external quality factor is controlled by the antenna, which needs to be the same as that for the standalone filter. With high dielectric constant, thus limited bandwidth, such an integration becomes difficult, which is especially true when the filter bandwidth is greater than the antenna bandwidth. Earlier research shows limited control over the external quality factor of the DRA by varying the dimensions only.

The new concept of modifying the antenna or adding parasitic components directly on the antenna further reduces the overall size of the design, since the filtering circuits are no longer needed. However, the design complexity will increase, causing difficulty in fabrication, and realization of dual polarizations can be challenging.

1.3 Contributions

In this thesis, different filtering antenna designs have been developed using rectangular DRA. Both the synthesis method and the fusion method of realizing filtering antenna have been investigated. The center frequency is 3.6 GHz for all designs, which is within the microwave band for 5G wireless networks.

Firstly, the synthesis method has been applied to filter antenna integration with dual polarization, in which the last resonator of a dielectric resonator bandpass filter is replaced with a DRA. The material considered has high dielectric constant of 20. Using high dielectric constant material results in a compact design, but limits the bandwidth. Thus, bandwidth improvement and control are the main focus on this design. Different methods are proposed based on the concept that by inserting low dielectric constant post/posts in the DRA, the effective dielectric constant is lowered. Doing so, the external quality factor is reduced and thus the bandwidth of the antenna is increased. Four different designs to increase bandwidth are presented with low dielectric constant posts inserted in DRA in different orientations. The effects of varying DRA dimensions and post dimensions on external quality factor have been studied in parametric studies. The concept is further validated using a dual polarized integrated design of a DRA with a 3-pole waveguide filter centered at 3.6 GHz. After inserting an air post in the DRA, the bandwidth is increased to 300 MHz, which is 50% higher than the design without an air post.

In addition, fusion method has been investigated to realize linearly polarized and dual polarized designs using rectangular DRA. Instead of having both an antenna and part of a filter, this method uses an antenna only. Conducting posts/loops are inserted in the DRA to realize radiation cancelation at frequencies outside of the passband, resulting in filtering response. Materials with different dielectric constants are investigated at a center frequency of 3.6 GHz. Parametric studies are performed to find out how the radiation nulls are affected by adjusting different dimensions of the DRA and the parasitic components. Both linearly and dual polarized designs are shown to have achieved filtering antenna responses.

The dual polarized design further shows good isolation between ports. Limitations due to the complexity of the structure are also discussed.

1.4 Outline

Chapter 1 provides the overview, motivations and contributions of the thesis.

In Chapter 2, literature review consists the review of dielectric resonator antennas, filtering antennas, and methods of DRA bandwidth improvement. The properties and advantages of dielectric resonator antennas are covered. Different methods of filtering antenna designs are discussed, including the cascaded method, the synthesis method, and the fusion method.

In Chapter 3, details of design process of using the synthesis method for integrating a filter and an antenna have been explained. Structures of the proposed designs of rectangular DRAs with increased bandwidth are presented. Parametric studies on design variable are performed. Design example using a proposed structure is presented showing significant bandwidth improvement and validating the concept. Simulation results using full electromagnetic (EM) simulation software HFSS are presented.

In Chapter 4, the fusion method has been studied and applied to both linearly polarized and dual polarized filtering antenna designs. DRAs with different dielectric constants are studied. Parametric study results and design examples are shown. The design challenges and limitations are also discussed.

Chapter 5 summarizes the filtering antenna designs and results presented in Chapter 3 and Chapter 4. Future research has also been suggested.

Chapter 2

Literature Review

In this chapter, an overview of dielectric resonator antennas (DRAs) is given first, which offers many advantages and is the focus of the thesis. Next, recent technologies and different methods of filter antenna integration are presented. Methods of bandwidth improvement for DRA are also discussed.

2.1 Dielectric Resonator Antenna

In late 1960s, dielectric resonator was introduced and developed as high-quality (Q) factor and compact elements in microwave circuit applications [4]. Then in 1980s, the first study of DRA was presented by Long, McAllister and Shen [5]. DRAs offer many advantages, such as light-weight, low loss, high radiation efficiency, ease of excitation, ease of integration, and diverse feeding techniques [6]. Various shapes have been reported, such as rectangular [7-9], cylinder [10-12], square [13-15], and super shaped [16-18]. DRAs have been designed in frequency range of 1-60 GHz and with dielectric constant (ε_r) 5-30 [19]. Different excitation methods also have been developed, such as waveguide [20-23], microstrip [24-26], aperture coupling [27-29], coaxial probe [30-32], and substrate integrated waveguide [33].

In this thesis, rectangular dielectric resonator antennas are used, which offers design flexibility. Feeding methods of waveguide and microstrip line are applied to antenna designs.

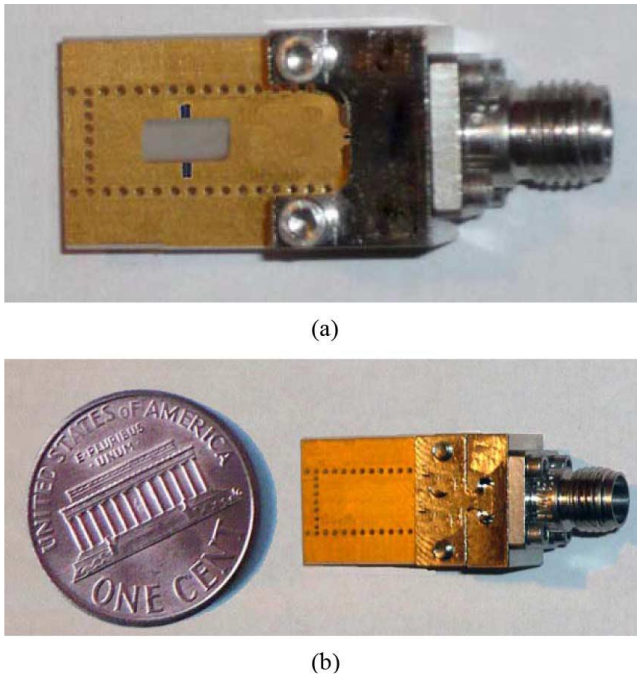

Figure 2-1 Rectangular DRA Fed by Substrate Integrated Waveguide © 2010 IEEE [33]

2.2 Filter and Antenna Integration Methods

Filters and antennas are both important components in any wireless communication systems. Filters and antennas can be connected using the conventional cascaded method. More recently, filtering antennas, a new type of components, have be developed that simultaneously realize filtering and radiation functions. Filtering antennas are generally developed using the synthesis method, or the fusion method [34].

Synthesis Method

To surmount the disadvantages of the cascaded method, the synthesis method follows the synthesis method for filter design. Once a filter is synthesized, the last resonator of the filter is replaced by an antenna. The antenna thus serves as both the radiator and the last resonator of bandpass filter in this method. Different types of antennas have been reported using the synthesis method for filter antenna integration, such as slot antennas [35-37], dielectric resonator antennas [38], [39], and microstrip patch antennas [40-42]. Comparing with the cascaded method, the advantages of this method are much reduced overall size and lower loss.

In [43], the SIW filtering antenna design are proposed and the configuration is shown in Figure 2-2. Short-ended coaxial feeding is used as external coupling. First, a four-pole filter is designed using four coupled substrate integrated waveguide cavities. To achieve the filtering antenna, a slot antenna is then placed on top of the filter, replacing the coaxial connector and last cavity of the four-pole filter. The center frequency is 9.96 GHz and the bandwidth is 6.0%.

In [44], dual polarized filtering microstrip patch antenna and DRA are studied. Fist, a dual polarized bandpass filter is designed. Then, a rectangular DRA is applied to the design replacing the last resonator. The external quality factor of antenna is same/similar to the last resonator's external quality factor. The dielectric constant of the DRA is 20. The center frequency of the design is 3.6 GHz, and the bandwidth is 200 MHz.

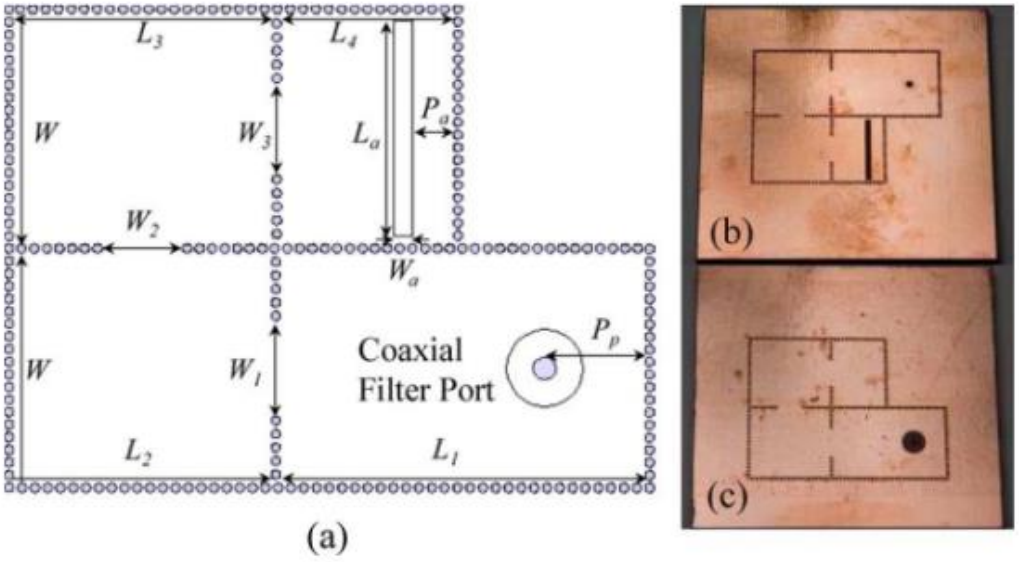

Figure 2-2 Compact Low-Loss Integration of High-Q 3-D Filters with Highly Efficient Antennas © 2011 IEEE [43]

Fusion Method

The fusion method is mainly focused on the antenna. The method is to integrate resonant structures in parallel with the antenna to generate band-stop functions at both sides of the passband [34]. In this method, filtering antennas are designed without adding any extra filtering circuit by modifying the antenna directly [45][46]. Reported approaches include modifying the antenna feeding method with open stubs [47][48], adding parasitic strips [49-51], and inserting shorting post [52-55]. In addition to offering low insertion loss, and high efficiency, this method further reduces the size and complexity of the system by removing the filter circuits. However, generating and controlling transmission zeros can be challenging.

In [51], a filtering rectangular DR antenna with dielectric constant 10 is designed at center frequency 5 GHz and bandwidth approximately 20.4%. The feeding method is microstrip feedline. In order to achieve transmission zeros, placing two parallel strips on the ground plane can excite three modes, which are TE_{111} mode, TE_{311} mode and the hybrid mode. The transmission zeros can be controlled by adjusting length of open stub. In [56], single and dual polarized filtering rectangular DRA with dielectric constant ε_r=9.5 have been designed and microstrip line is also the feeding method. The center frequency is 1.9 GHz and bandwidth is 22.1%. By placing hybrid microstrip line/conformal strip, transmission zeros are generated. The feed network may be difficult to fabricate due to extremely narrow strip width.

The filtering antenna design with fusion method in [57] is shown in Figure 2-3. Linearly and circularly polarized filtering cylinder DR antennas are designed with dielectric constant of 10. The center frequency is 2.45 GHz and the bandwidth is 7.2%. The transmission zeros are generated by posts and strip forming loops, which help to achieve the cancelation of radiation at certain frequencies. Similar concept is applied to rectangular DRA for filtering antennas with linear and dual polarizations in Chapter 4.

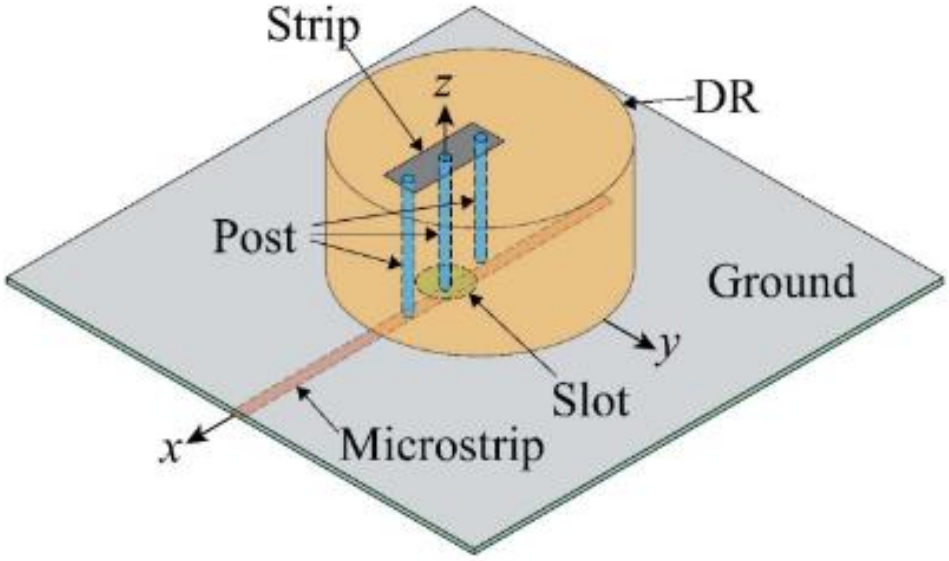

Figure 2-3 Linearly and Circularly Polarized Filtering Dielectric Resonator Antennas© 2019 IEEE [57]

2.3 Bandwidth Improvement of DRA

The quality factor (Q) of DRA depends on the dielectric constant and dimensions of the DRA. Decreasing the dielectric constant of the material will increase the bandwidth. However, the size of the antenna increases with lower dielectric constant. When high dielectric constant material is used, the bandwidth is reduced. Varying the dimensions of the DRA can change the bandwidth, but within limited range [44]. This can further cause difficulty in antenna filter integration using the synthesis method, because both the last resonator of the filter and the antenna need to have the same external quality factor.

Different methods of increasing DRA bandwidth have been proposed [58]-[61]. A wideband low-profile single and dual polarized DRA design is proposed in [58] as shown in Figure 2-4. Posts with lower dielectric constant than that of the DRA, including air posts,

are inserted in the DRA. The design approaches are to maintain the DRA size and to control the bandwidth by adjusting the posts. The dielectric constant of DRA is 20, and the dielectric constant of dielectric posts is 10.2. The bandwidth can achieve 47.5%. The design is rather complicated and thick due to two substrate layers. In this thesis, the concepts of DRA bandwidth improvement have been applied to the dual polarized filtering antenna design in Chapter 3, using, however, much simpler structures.

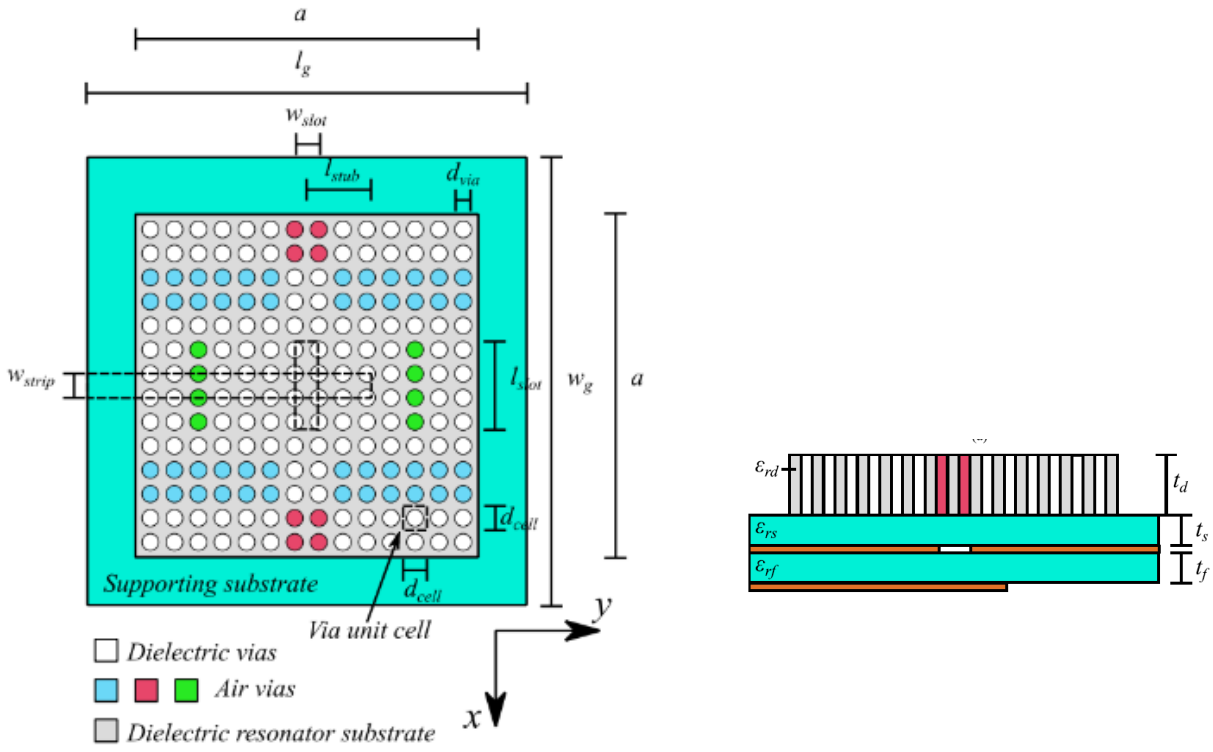

Figure 2-4 Compact Wideband Low-Profile Single- and Dual-Polarized Dielectric Resonator Antennas Using Dielectric and Air Vias. © 2021 IEEE [58]

Chapter 3

Dielectric Resonator Filter Antenna Integration with Increased Bandwidth

In this chapter, filter antenna integrations are implemented using rectangular dielectric resonators. Using dielectric material with high dielectric constants results in compact designs, which, however, limits the bandwidth at the same time. Different methods to increase design bandwidth are investigated.

3.1 Filter Antenna Integration

Filter antenna integration following the synthesis method starts with the separate designs of the filter and the antenna. The two designs are subsequently combined together [37].

Firstly, a three-pole dual mode bandpass filter is designed, consisting of dielectric filled waveguide cavity resonators for compactness and low loss, as shown in Figure 3-1. In the thesis, square cavities operating in TE_{101} and TE_{011} modes are used due to the symmetrical shape to achieve dual polarization [44].

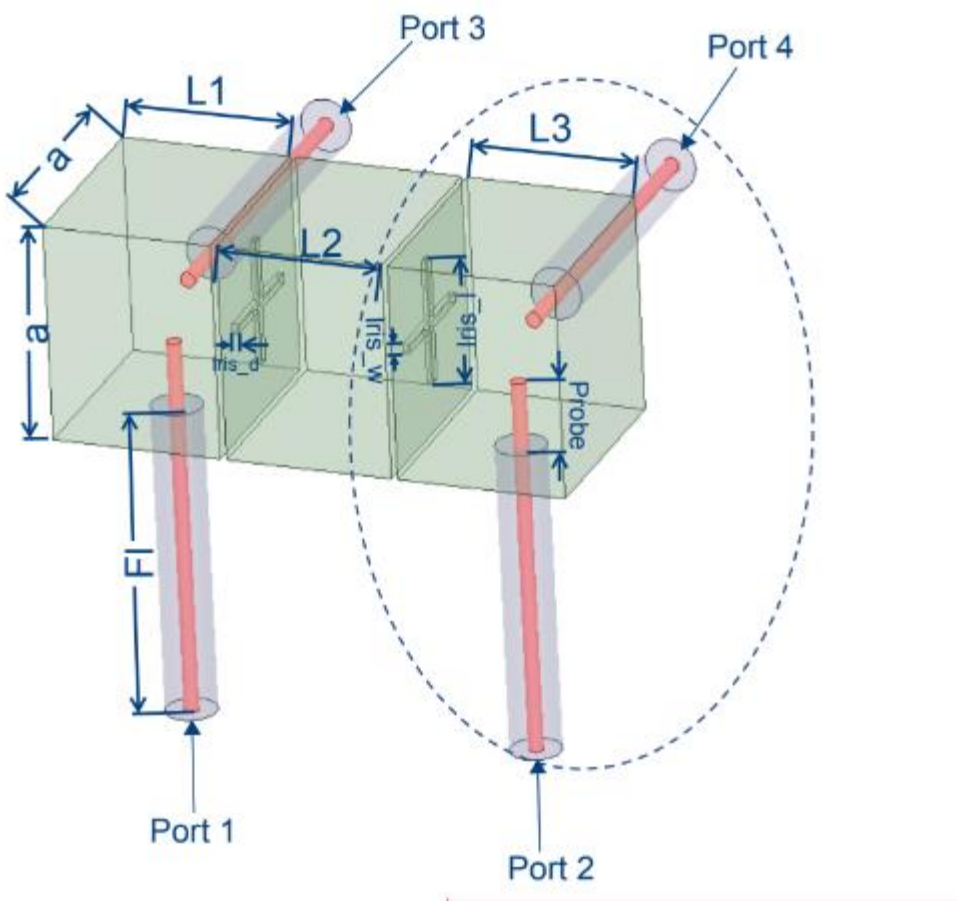

Figure 3-1 Waveguide filter for TE_{101} and TE_{011}modes (a = 13.98 mm, L_1 = 11.34 mm, L_2 = 11.2 mm, L_3 = 11.34 mm, Iris_l = 7.97 mm, Iris_w = 0.4064 mm, Iris_d = 0.635 mm, probe = 4.16 mm, probe radius = 0.5 mm, F_l radius = 1.7mm and F_l = 20 mm)

For antenna design, the DRA shown in Figure 3-2 is used. DRAs are a good candidate for communication applications due to their high efficiency, flexibility in their shapes, and low cost [19]. The dimensions of the DRA are calculated based on the following equations [62]:

$$k_x = \frac{\pi}{DRA\_a} \tag{3.1}$$

$$k_y = \frac{\pi}{DRA\_b} \tag{3.2}$$

$$k_z tan\left(\frac{k_z DRA\_d}{2}\right) = \sqrt{(\varepsilon_r - 1){k_0}^2 - {k_z}^2} \tag{3.3}$$

$${k_x}^2 + {k_y}^2 + {k_z}^2 = \varepsilon_r {k_0}^2 \tag{3.4}$$

where DRA_a is the length, DRA_b is the width, and DRA_d is the height of the DRA. k_o is the free-space wavenumber at the center frequency, f_0. ε_r is the dielectric constant of the DRA.

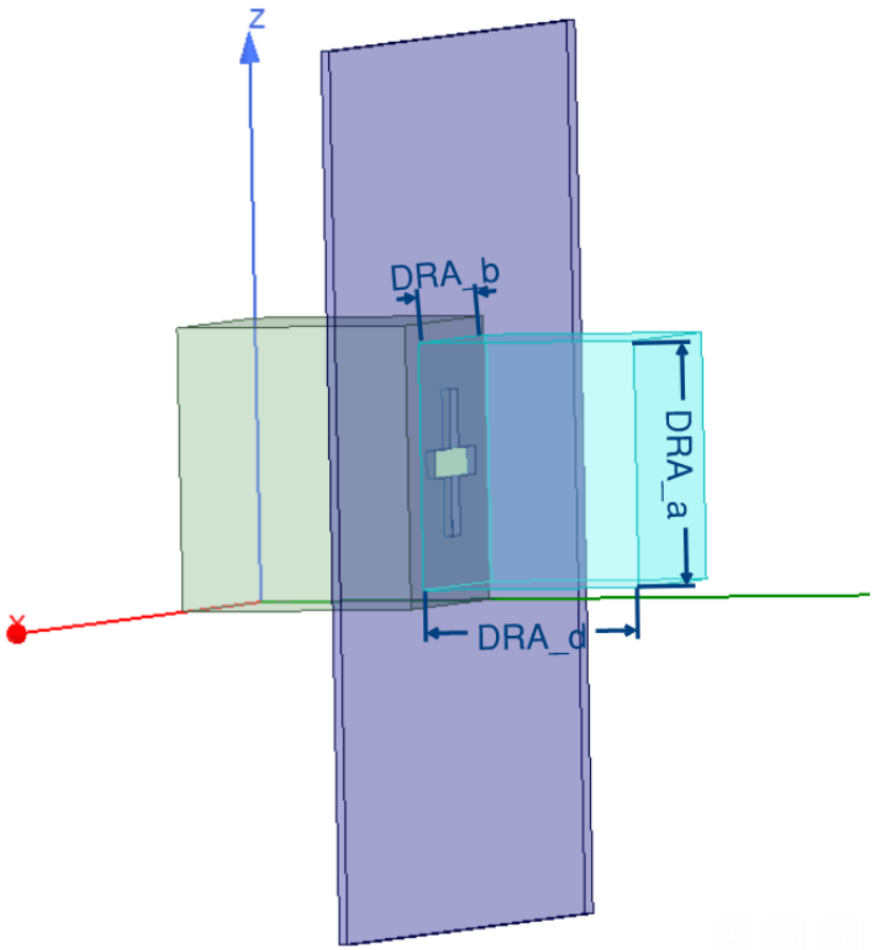

Figure 3-2 Structure of DR antenna (DRA_a = 12.15mm; DRA_b = 12.15mm; DRA_d = 11mm; $L_3 = 11.66mm$; a = 13.98mm; Iris_d = 0.016in; Iris_w = 1.39 mm; Iris_l = 7.25mm)

In the next step, the filter and the DRA are combined together. There are generally two methods to implement the filter antenna integration [37]:

1. Using antenna design in lieu of the last resonator of the filter.
2. Using antenna design in lieu of the output port of the filter.

The design is based on the first method, in which the DRA acts as both a radiator and the last resonator of the filter. As shown in Figure 3-1, the last cavity and ports in the dashed line circle can be replaced by the structure in Figure 3-2. There are two conditions that need to be satisfied. The last resonator of filter and antenna need to have the same external quality factor (Q_{EXT}). And the coupling between the resonator *N*-1 of the filter and antenna is the same internal coupling coefficient $K_{N-1,N}$ as the original filter, where *N* is the filter order. Once the conditions are met, the S_{11} response of the filtering antenna is similar to the standalone filter, while maintaining the radiation characteristic of the antenna.

Q_{EXT} of the antenna is related to the bandwidth, as $Q_{EXT} = f_0/Bandwidth$. Using the structure in Figure 3-2, Q_{EXT} can be calculated using steps shown below [37].

First, the loaded quality factor Q_L is determined using the reflection coefficients at the waveguide port in Figure 3-2. S_{11}^{min} is the minimum reflection coefficient at the resonant frequency f_0. f_1 and f_2 correspond to the frequencies when $|S_{11}| = S_{11}^{\Phi}$, where S_{11}^{Φ} can be determined by using following equation:

$$S_{11}^{\Phi} = \sqrt{\frac{1+|S_{11}^{min}|^2}{2}} \tag{3.5}$$

The coupling coefficient, *K*, between the input port and the resonator can be calculated using the following equations:

$$K = \frac{1-|S_{11}^{min}|}{1+|S_{11}^{min}|} \text{ (resonator is under-coupled)} \quad (3.6)$$

$$K = \frac{1+|S_{11}^{min}|}{1-|S_{11}^{min}|} \text{ (resonator is over-coupled)} \quad (3.7)$$

Q_L can be determined using the following the equation.

$$Q_L = (1+K)\frac{f_0}{f_2-f_1} \quad (3.8)$$

$$\frac{1}{Q_L} = \frac{1}{Q_U} + \frac{1}{Q_{EXT}} \quad (3.9)$$

When the unloaded quality factor Q_U is infinity, i.e. assuming DRA lossless, $Q_L = Q_{EXT}$.

3.2 Antenna Designs with Increased Bandwidth

To make the antenna compact, the DRA is made of high dielectric constant material. High dielectric constant results in narrow bandwidth for the antenna. There is also limited tuning rang for Q_{EXT}. In [58], it has been shown that Q_{EXT} (or bandwidth) can be changed by varying DRA height, while slot length and slot width do not have significant impact on bandwidth improvement. In order to adjust Q_{EXT} and increase bandwidth, using posts filled with low dielectric constant material is considered in this section. These posts are embedded in the DRA. Different configurations are investigated. In the following designs, all posts are filled by air (dielectric constant $\varepsilon_r = 1$) for ease of fabrication. For all designs, the DR antennas have dielectric constant of 20.

Design 1:

Design of DRA with one air post is presented in Figure 3-3, and parametric study is performed with results shown in Figures 3-4 to 3-9.

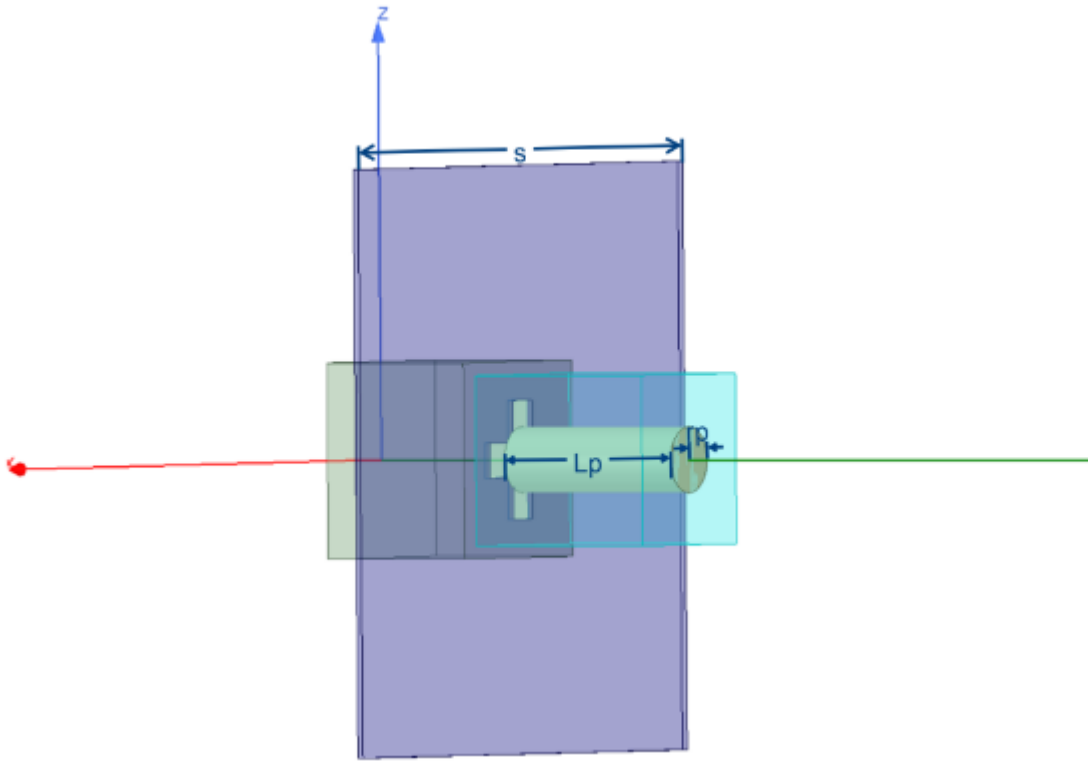

Figure 3-3 DR antenna with one air post (DRA_a = 12.15mm; DRA_b = 12.15mm; DRA_d = 14.2mm; $L_3 = 11.66mm$; a = 13.98mm; Iris_d = 0.016in; Iris_w = 2.35 mm; Iris_l = 8.5mm; r_p =2.36mm; L_p = 14.2mm)

In the first case, slot length of 8.5 mm, and slot width of 2.35 mm and post radius of 2.36 mm are selected, and the impact of varying DRA height on K_{23} and Q_{EXT} is studied. The analysis is shown in Figures 3-4 and 3-5. In the next case, the impact of varying slot width and the post radius on K_{23} and Q_{EXT} is studied, while the DRA height of 14.2 mm and slot length of 8.5 mm are fixed. The results are compared in Figures 3-6 and 3-7. In the last

case, slot width of 2.35 mm and DRA height of 14.2 mm are selected and the impact of varying slot length on K_{23} and Q_{EXT} is studied. The analysis is shown in Figures 3-8 and 3-9.

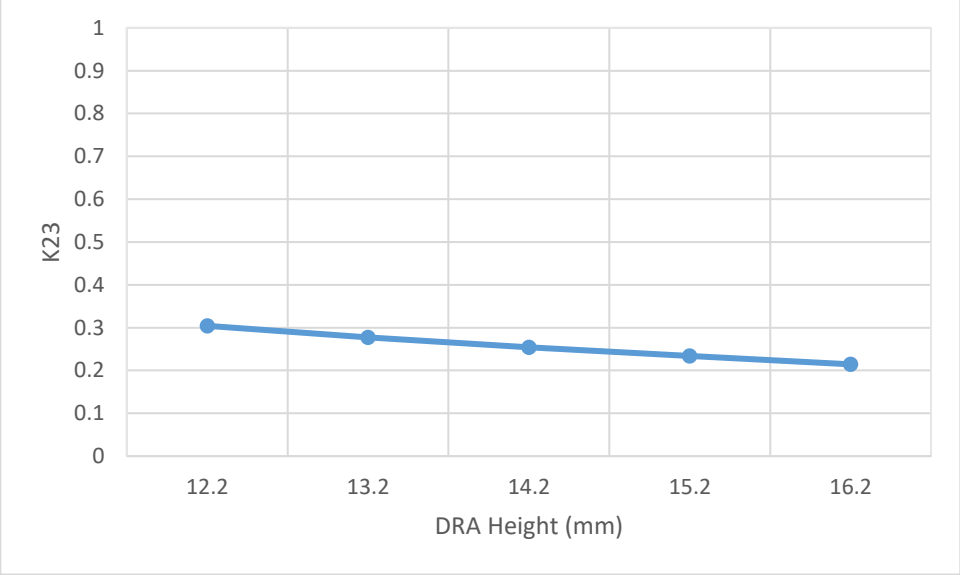

Figure 3-4 The impact of DRA height variation on K_{23}, where slot length = 8.5mm, slot width = 2.35mm and radius of post = 2.36mm

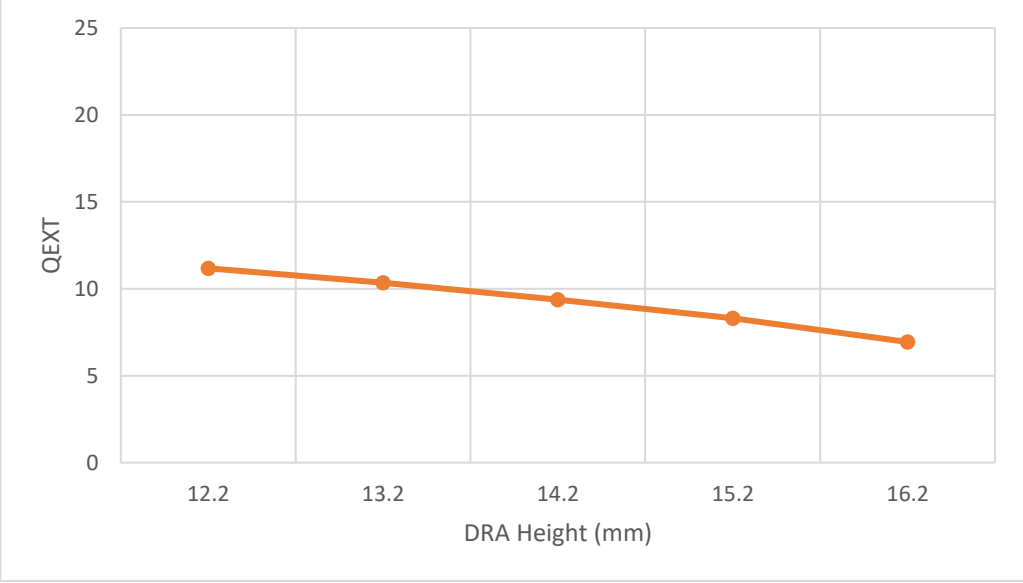

Figure 3-5 The impact of DRA height variation on Q_{EXT}, where slot length = 8.5mm and slot width = 2.35mm and radius of post = 2.36mm

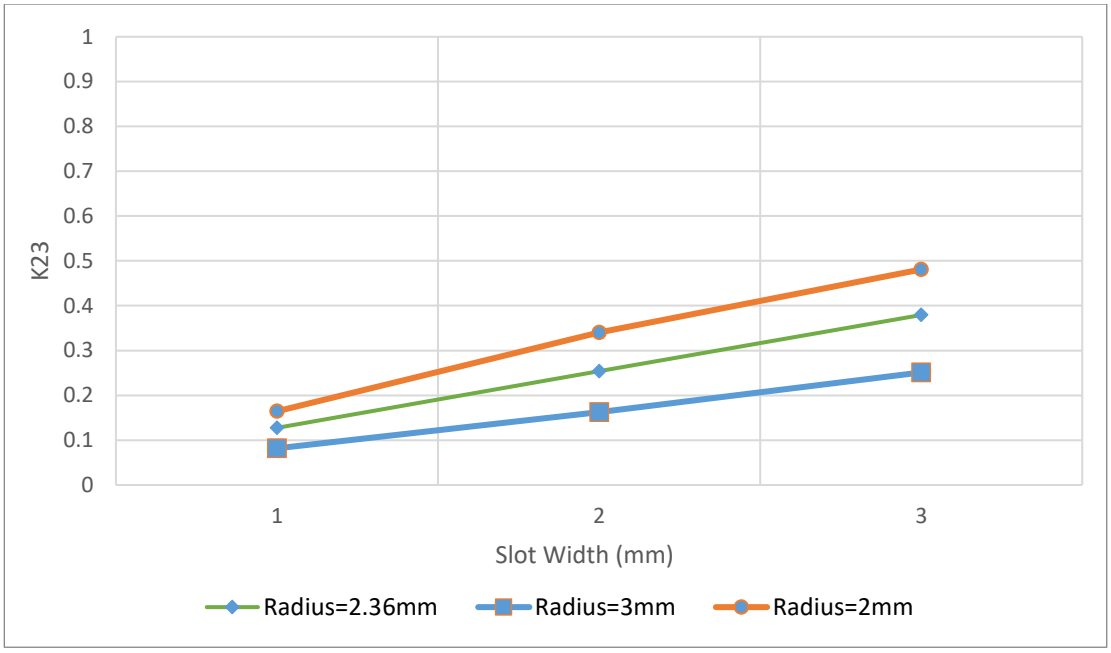

Figure 3-6 The impact of slot width variation on K_{23}, where DRA height = 14.2mm, slot length = 8.5mm and radius of post = 2mm, 2.36mm and 3mm

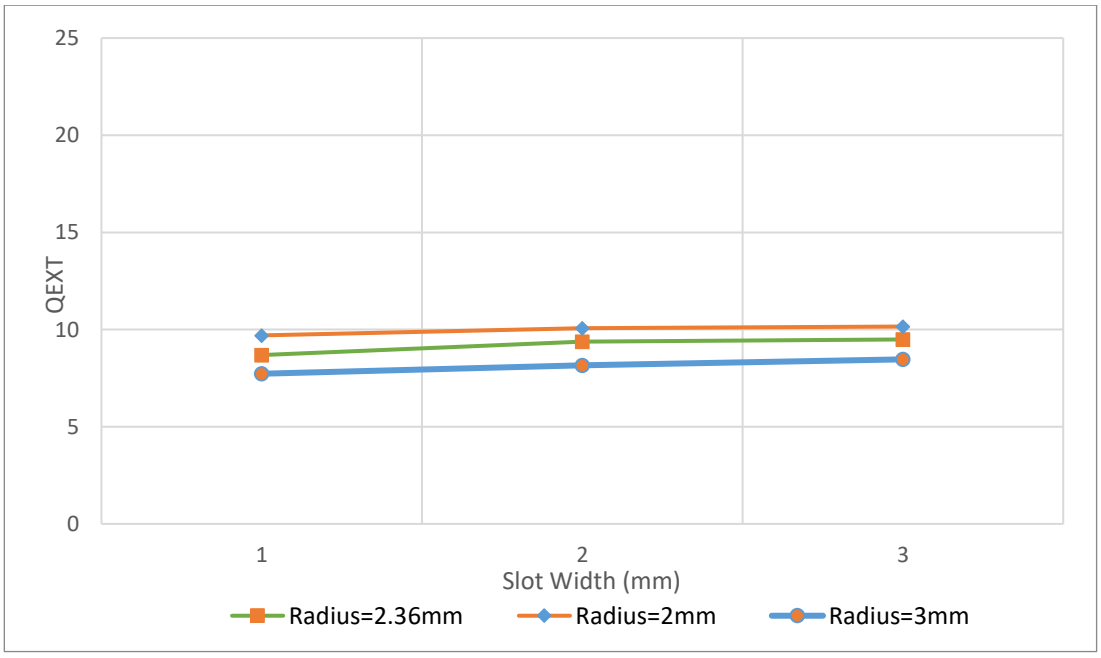

Figure 3-7 The impact of slot width variation on Q_{EXT}, where DRA height = 14.2mm, slot length = 8.5mm and radius of post = 2mm, 2.36mm and 3mm

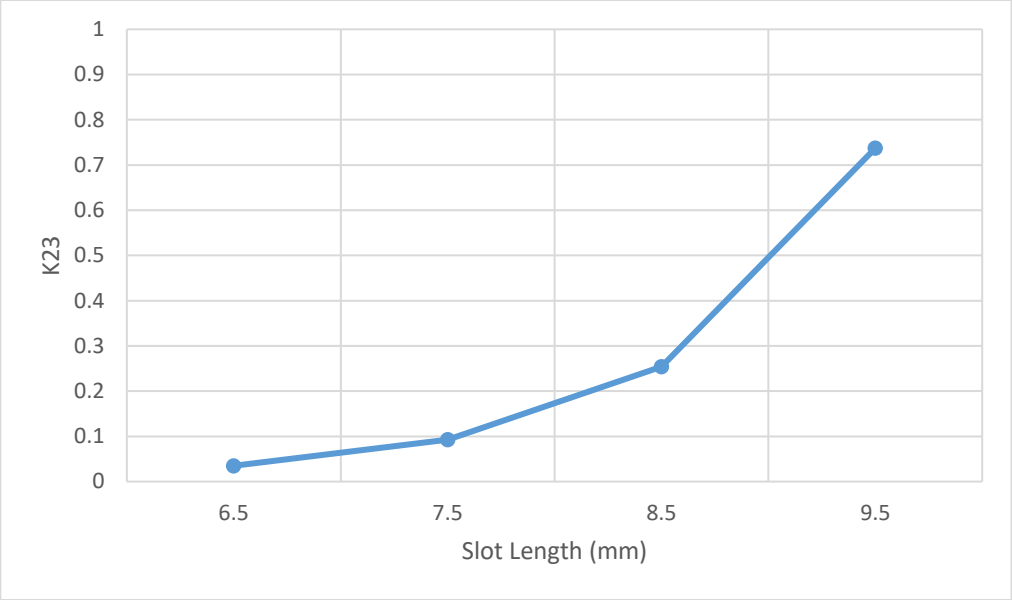

Figure 3-8 The impact of slot length variation on K_{23}, where slot width = 2.35mm, DRA height = 14.2mm and post radius = 2.36mm

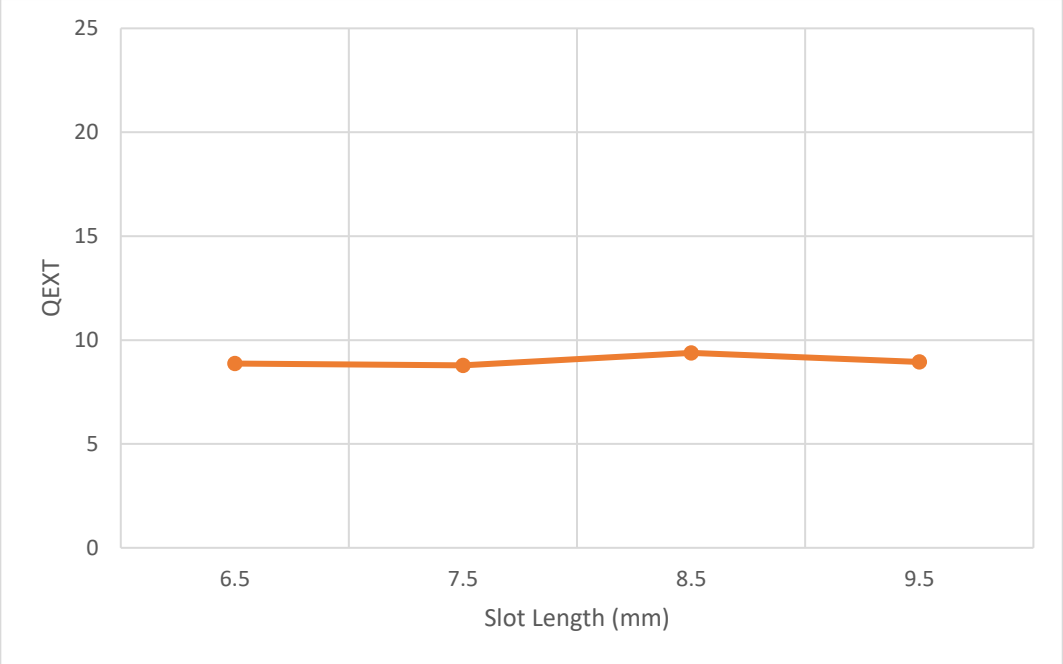

Figure 3-9 The impact of slot length variation on Q_{EXT}, where slot width = 2.35mm, DRA height = 14.2mm and post radius = 2.36mm

Based on the analysis presented above, as the DRA height increases, Q_{EXT} and K_{23} decreases. And then, when slot width increases, Q_{EXT} is barely affected and K_{23} increases. More importantly, the DRA height and post radius have the most significant effects on the bandwidth. As expected, the slot width and length mostly affect K_{23}.

Design 2:

Design of DRA with four corner air posts is shown in Figure 3-10. The parametric study results are presented in Figures 3-11 to 3-16.

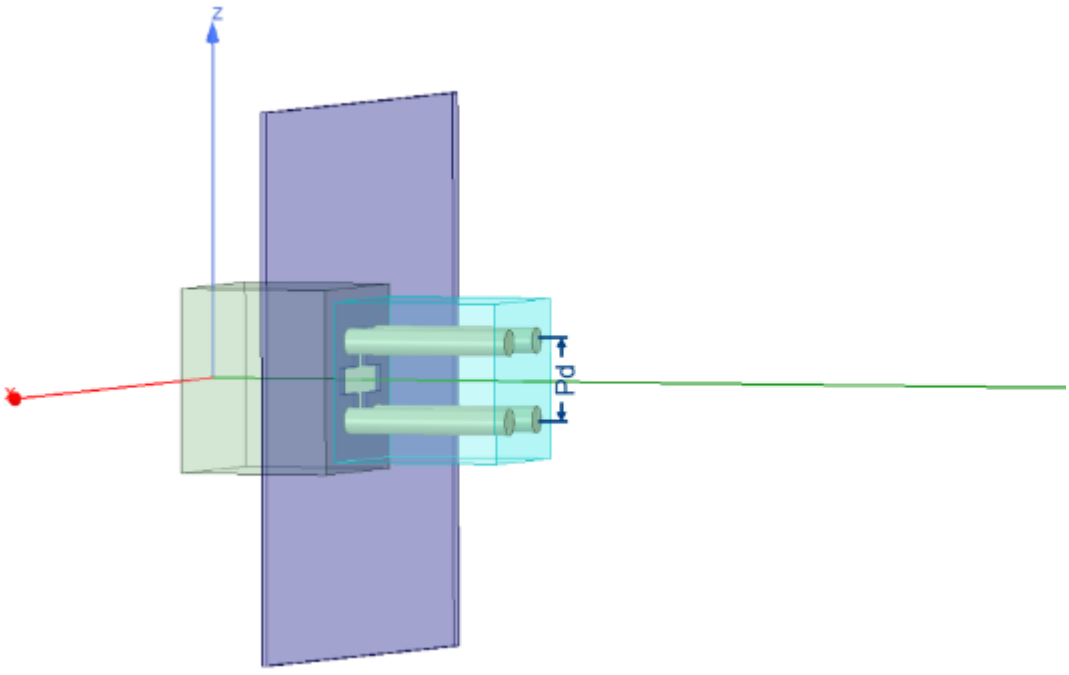

Figure 3-10 DR antenna with four corner air posts (DRA_a = 12.15mm; DRA_b = 12.15mm; DRA_d = 14.2mm; $L_3 = 11.66mm$; a = 13.98mm; Iris_d = 0.016in; Iris_w = 2.35 mm; Iris_l = 7.8mm; r_p =1mm; L_p = 14.2mm; P_d =6.15mm)

In the first case, slot length of 7.8 mm, and slot width of 2 mm and posts radius of 0.75 mm are selected, and the impact of varying DRA height on K_{23} and Q_{EXT} is studied. The analysis is shown in Figures 3-11 and 3-12. In second case, DRA height of 14.2 mm, slot length of 7.8 mm and posts radius of 0.75 mm are selected, and the impact of varying slot width on K_{23} and Q_{EXT} is studied. The analysis is shown in Figure 3-13 and 3-14. In the third case, DRA height of 14.2 mm, slot length of 7.8 mm and posts radius of 1 mm are selected and the impact of varying slot width post radius on K_{23} and Q_{EXT} is studied. The results are also presented in Figure 3-13 and 3-14. In the last case, DRA height of 14.2 mm, slot width of 2 mm and posts radius of 0.75 mm are selected and the impact of varying slot length on K_{23} and Q_{EXT} is studied. The analysis is shown in Figure 3.15 and 3.16.

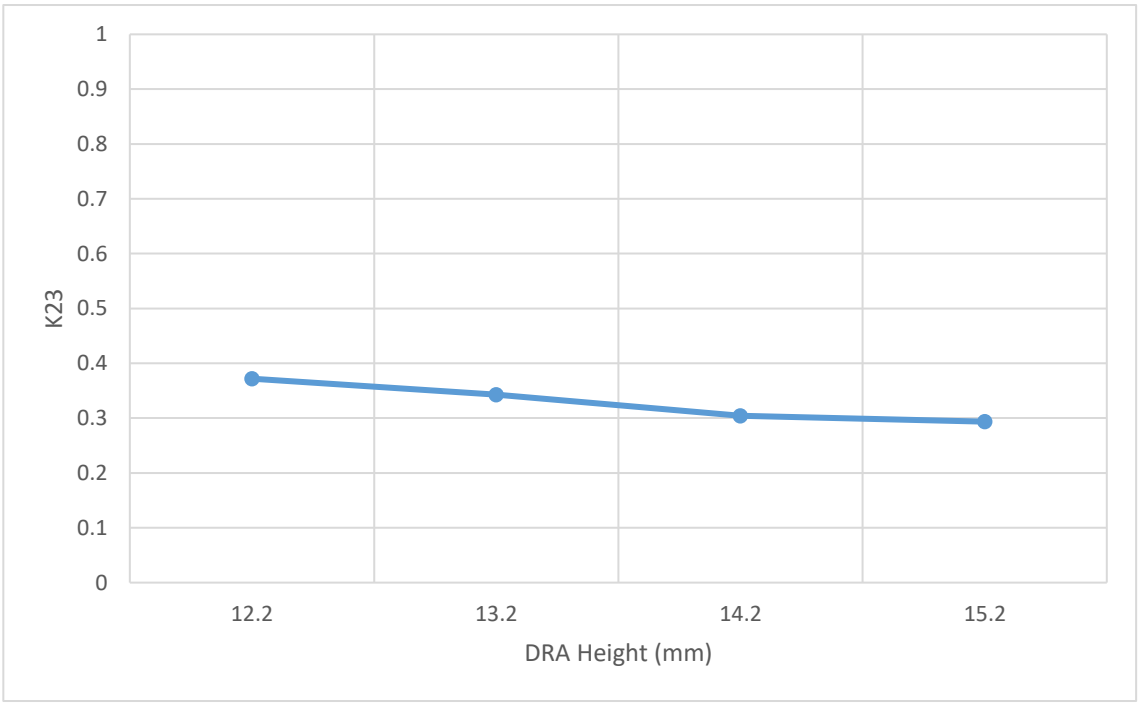

Figure 3-11 The impact of DRA height variation on K_{23}, where slot length = 7.8mm, slot width = 2mm and radius of posts = 0.75mm

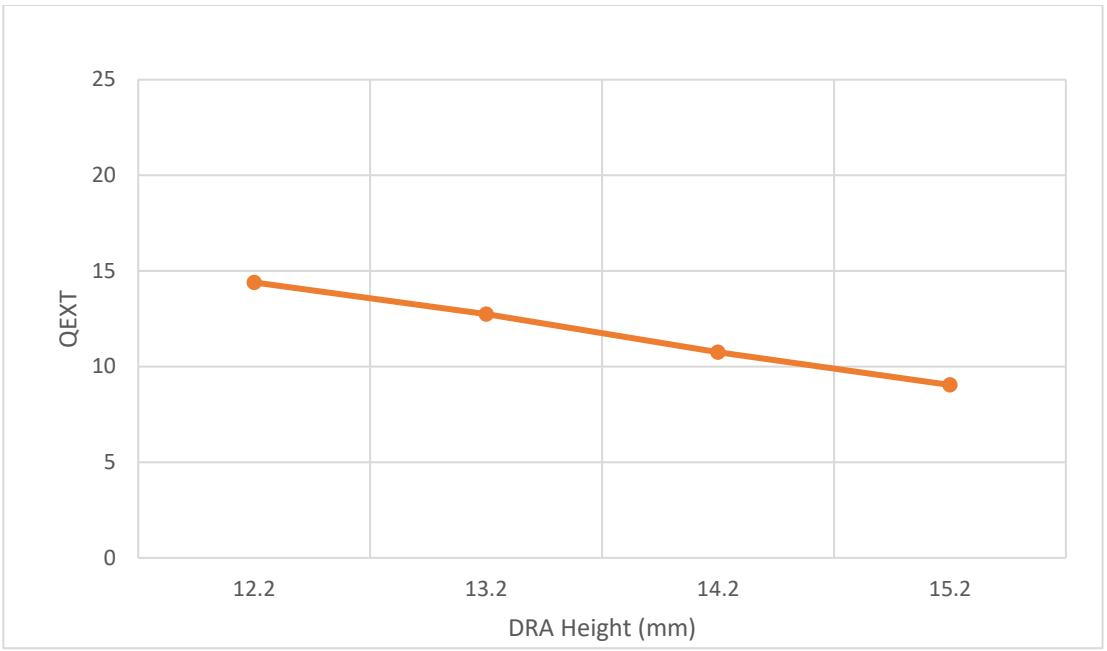

Figure 3-12 The impact of DRA height variation on Q_{EXT}, where slot length = 7.8mm, slot width = 2mm and radius of posts = 0.75mm

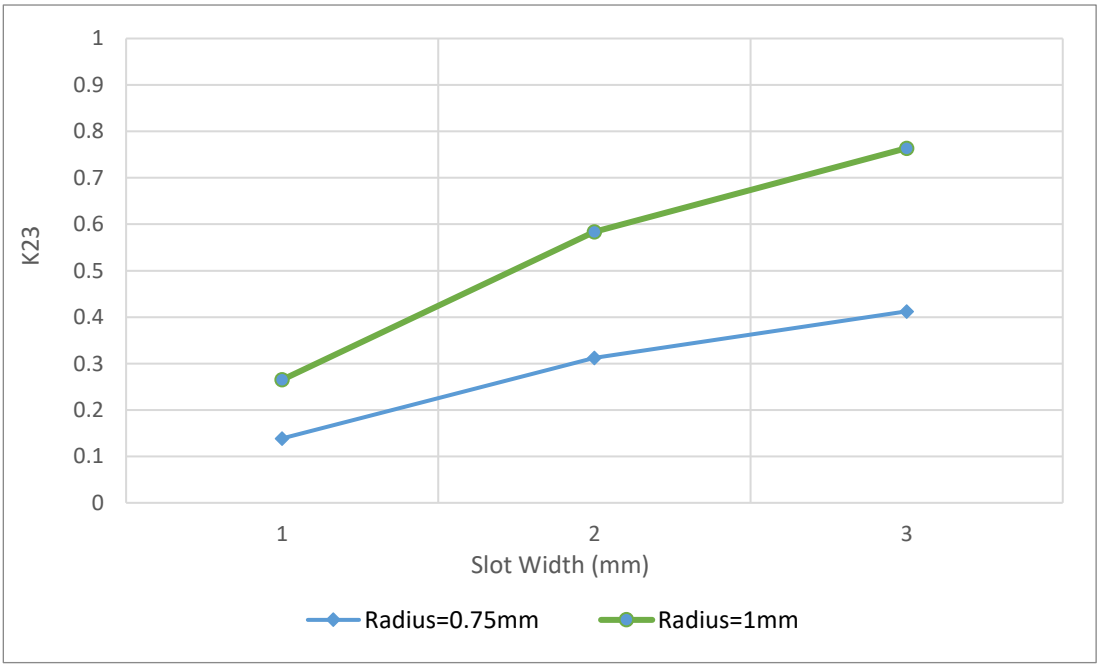

Figure 3-13 The impact of slot width variation on K_{23}, where slot length = 7.8mm, DRA height = 14.2mm and radius of posts = 0.75mm and 1mm

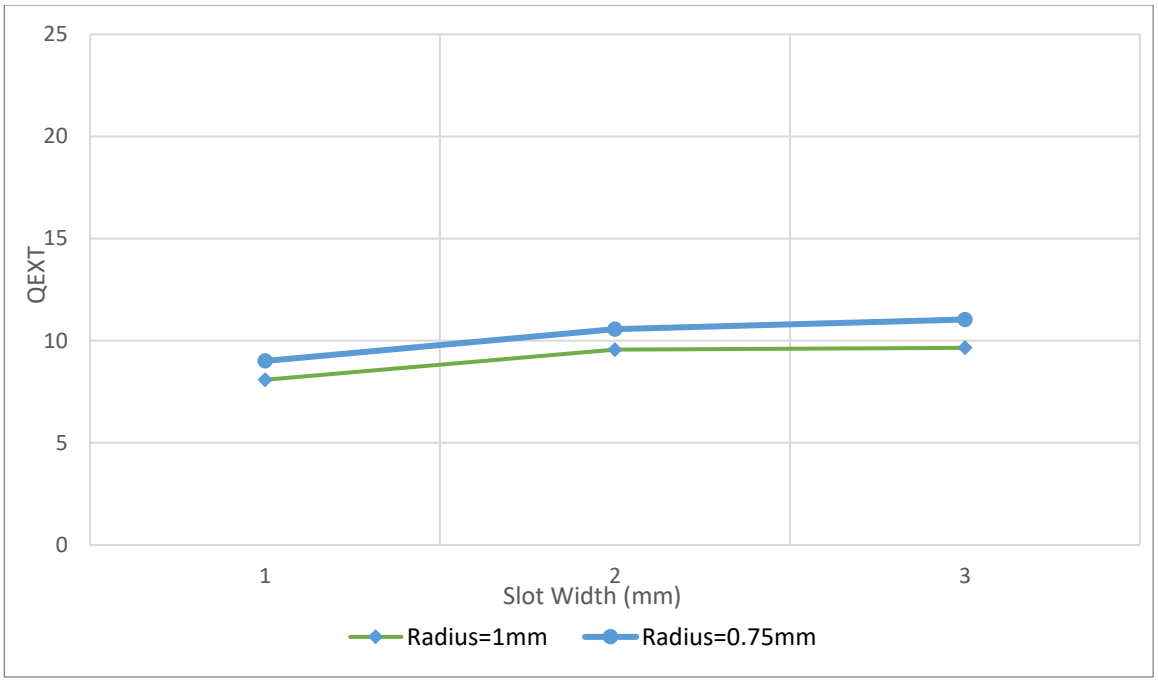

Figure 3-14 The impact of slot width variation on Q_{EXT}, where slot length = 7.8mm, DRA height = 14.2mm and radius of posts = 0.75mm and 1mm

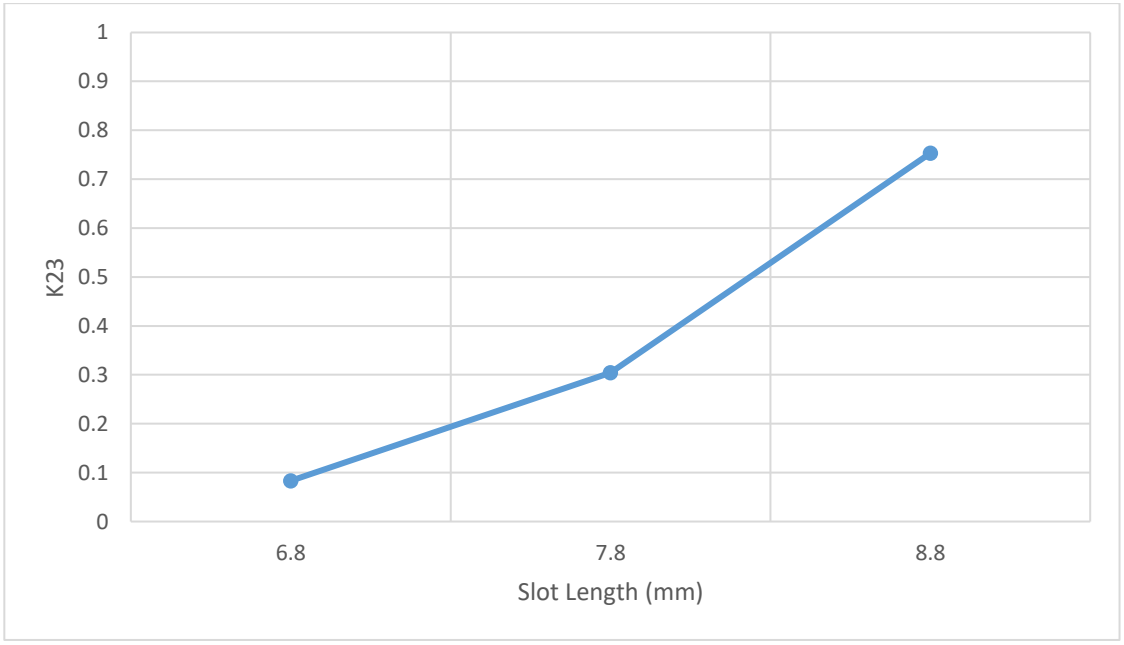

Figure 3-15 The impact of slot length variation on K_{23}, where slot width = 2mm, DRA height = 14.2mm and radius of posts = 0.75mm

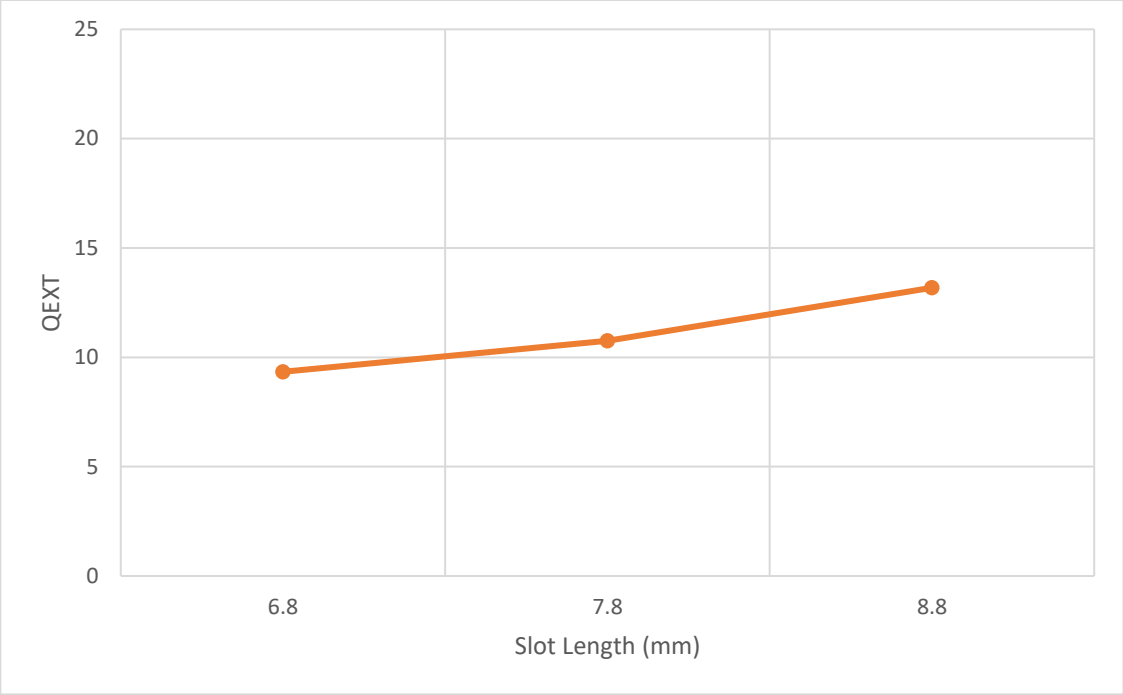

Figure 3-16 The impact of slot length variation on Q_{EXT}, where slot width = 2mm, DRA height = 14.2mm and radius of posts = 0.75mm

Based on the analysis presented above, as the DRA height increases, Q_{EXT} and K_{23} decrease. When slot width or slot length increases, Q_{EXT} and K_{23} increase.

Design 3:

Design of DRA with cross air posts is presented in Figure 3-17. The parametric study results are shown in Figures 3-18 to 3-23.

In the first case, slot width of 2 mm, slot length of 6.8 mm and radius of post of 0.5 mm are selected and the impact of varying DRA height on K_{23} and Q_{EXT} is studied. The analysis is shown in Figure 3-18 and 3-19. In the second case, slot length of 6.8 mm and DRA height of 14 mm are selected, and the impact of varying slot width and post radius on K_{23} and Q_{EXT} is studied. The analysis is shown in Figure 3-20 and 3-21. In the third case, slot length of 6.8 mm, post radius of 1 mm and DRA height of 14 mm are selected and impact of varying slot width on K_{23} and Q_{EXT} is analyzed. The study is shown in Figure 3-20 and 3-21. In the last case, slot width of 2 mm, DRA height of 14 mm and post radius of 0.75 mm are used and the impact of varying slot length is studied. The analysis is presented in Figure 3-22 and 3-23. Once again, post radius and DRA height have the strongest influence on the bandwidth.

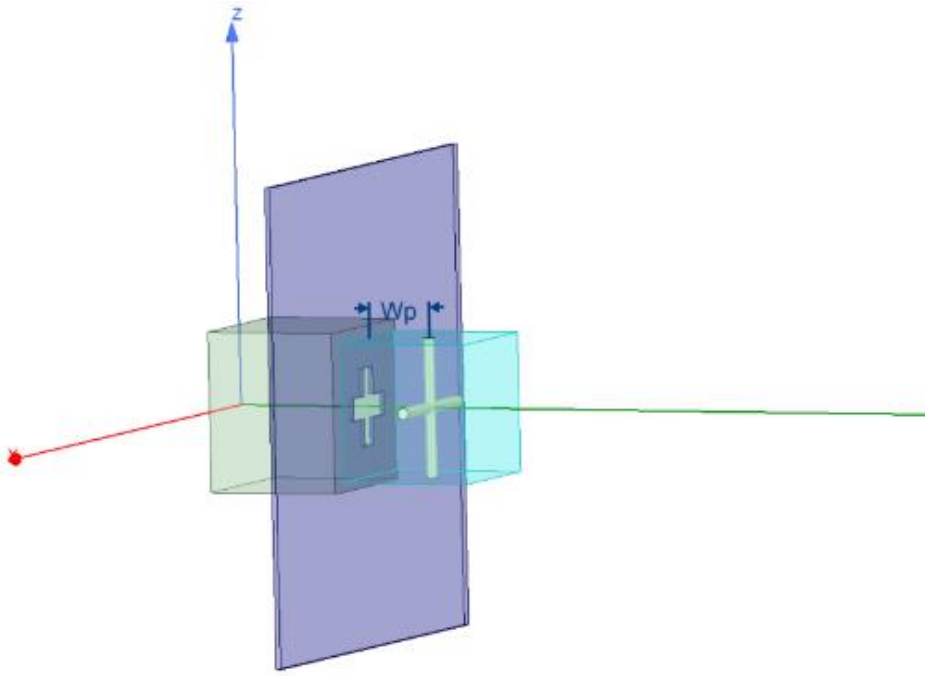

Figure 3-17 DR antenna with cross air post (DRA_a = 12.15mm; DRA_b = 12.15mm; DRA_d = 11.6mm; $L_3 = 11.66mm$; a = 13.98mm; Iris_d = 0.016in; Iris_w = 2 mm; Iris_l = 6.8mm; r_p =0.5mm; L_p = 14.2m; W_p =5.8mm)

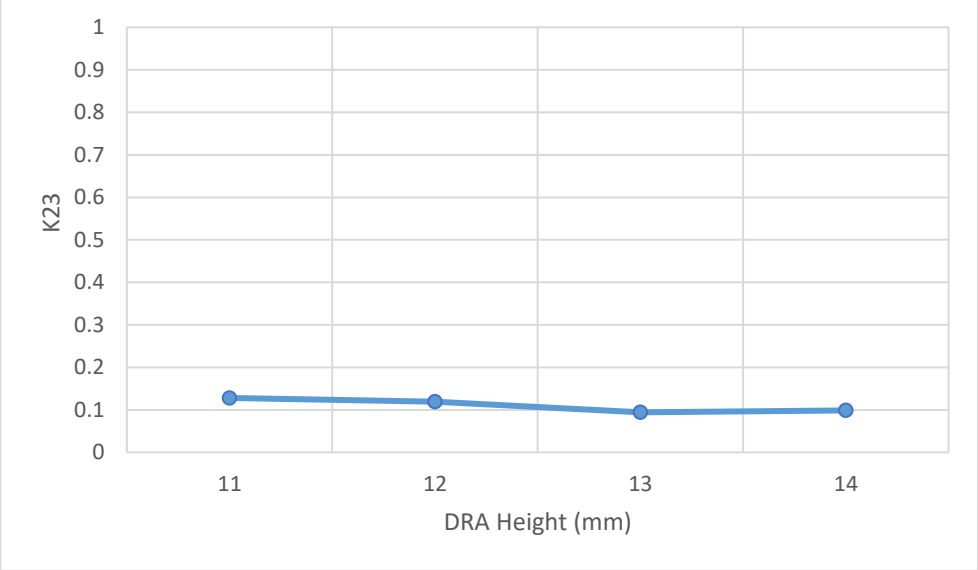

Figure 3-18 The impact of DRA height variation on K_{23}, where slot width = 2mm, slot length = 6.8mm and radius of posts = 0.5mm

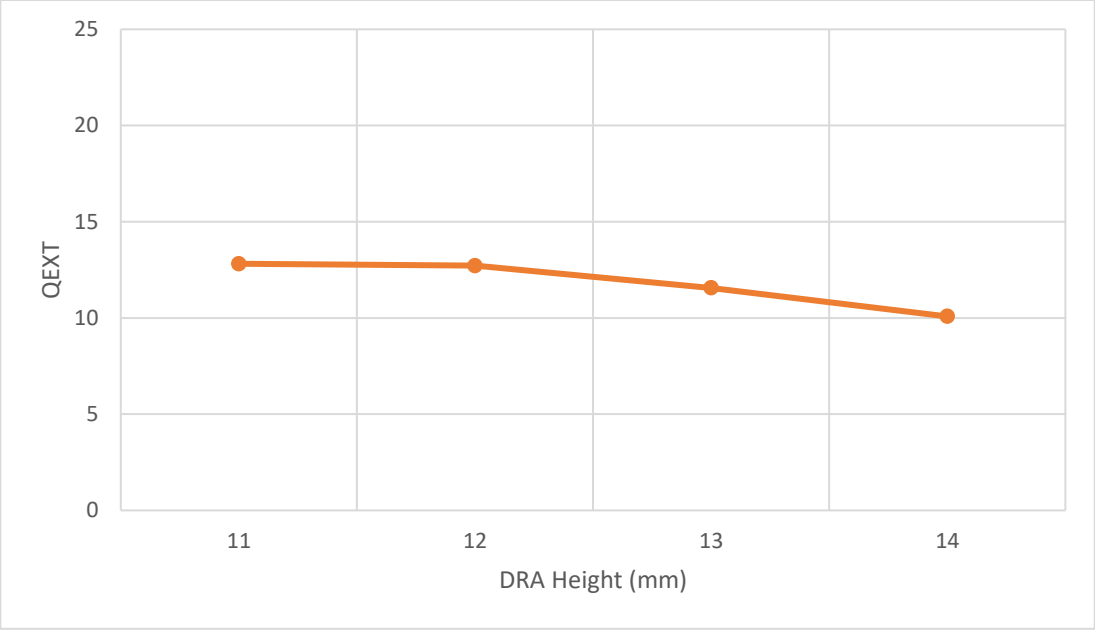

Figure 3-19 The impact of DRA height variation on Q_{EXT}, where slot width = 2mm, slot length = 6.8mm and radius of posts = 0.5mm

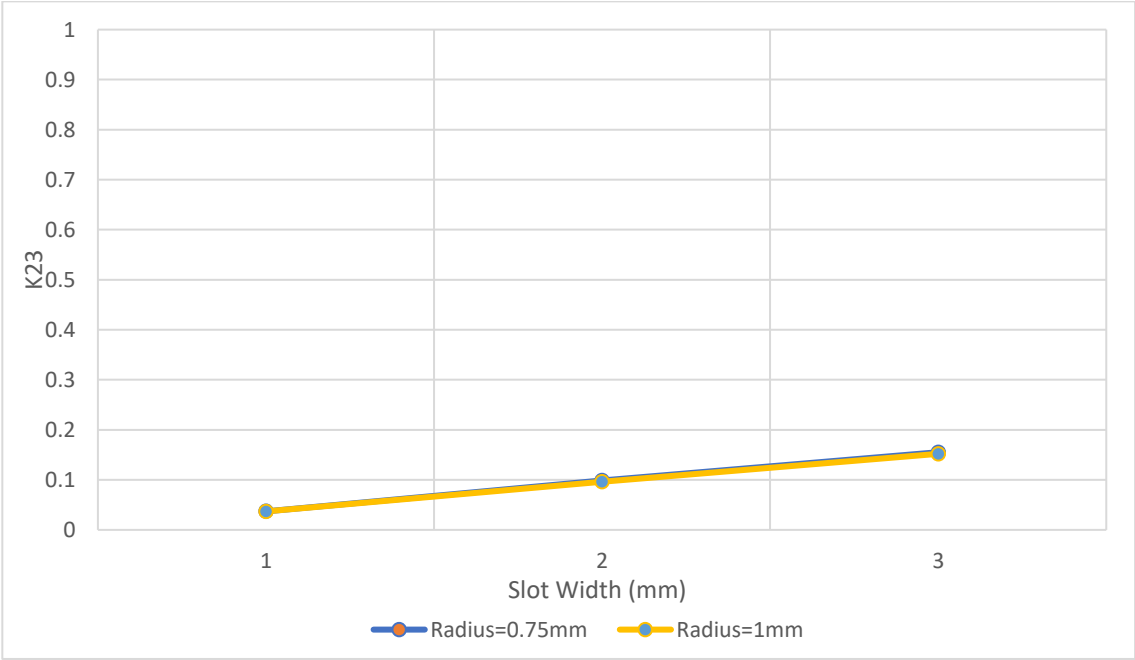

Figure 3-20 The impact of slot width variation on K_{23}, where slot length = 6.8mm, DRA height = 14mm and post radius = 0.75mm, 1mm

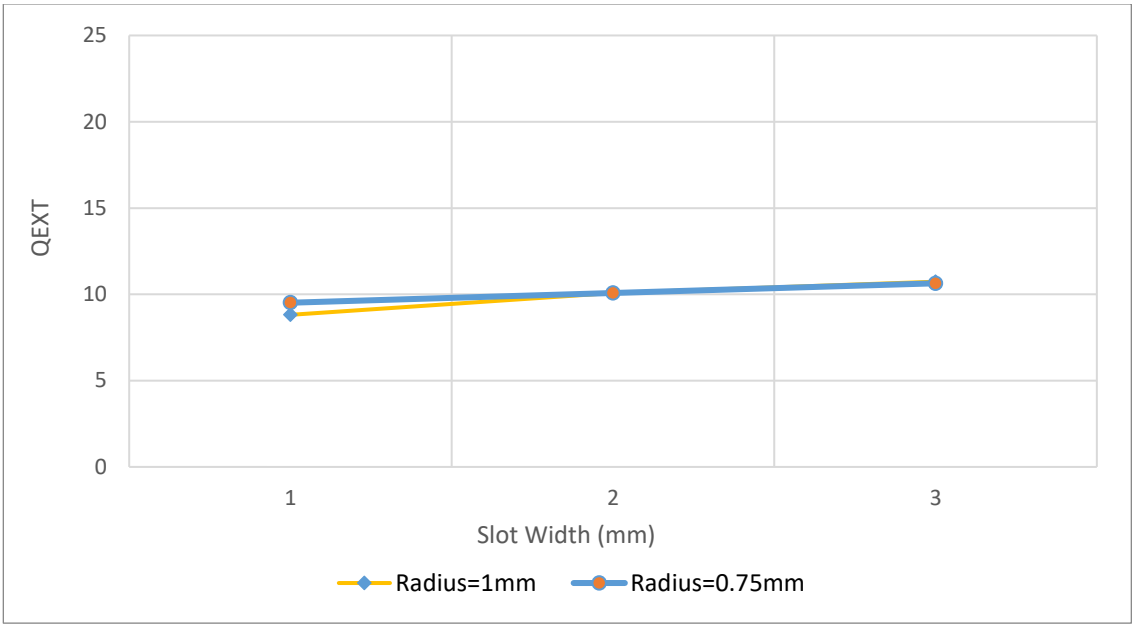

Figure 3-21 The impact of slot width variation on Q_{EXT}, where slot length = 6.8mm, DRA height = 14mm and post radius = 0.75mm, 1mm

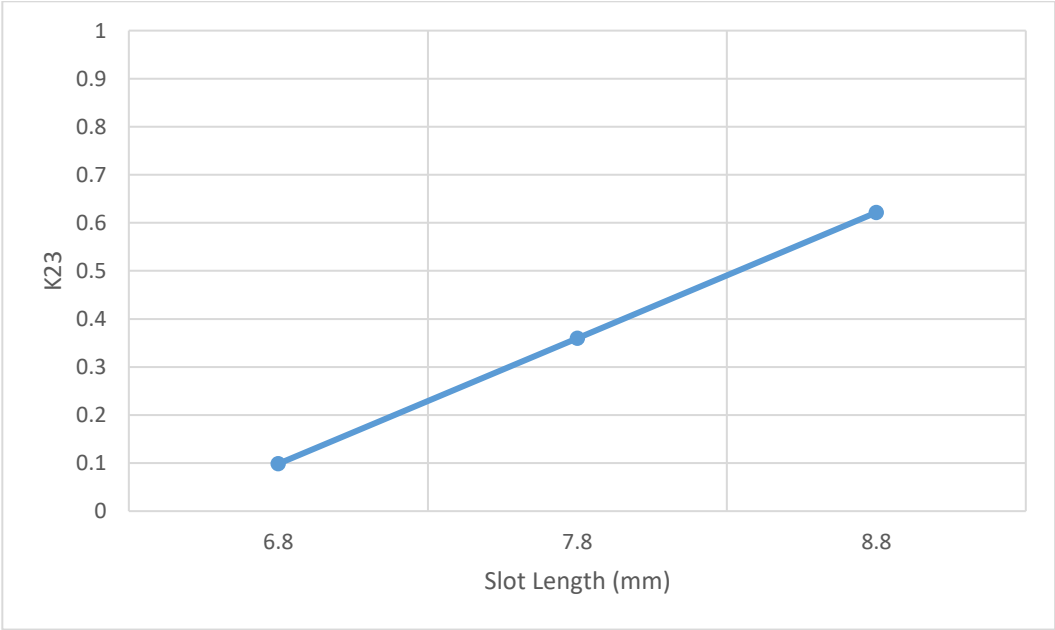

Figure 3-22 The impact of slot length variation on K_{23}, where slot width = 2mm, DRA height = 14mm and post radius = 0.75mm

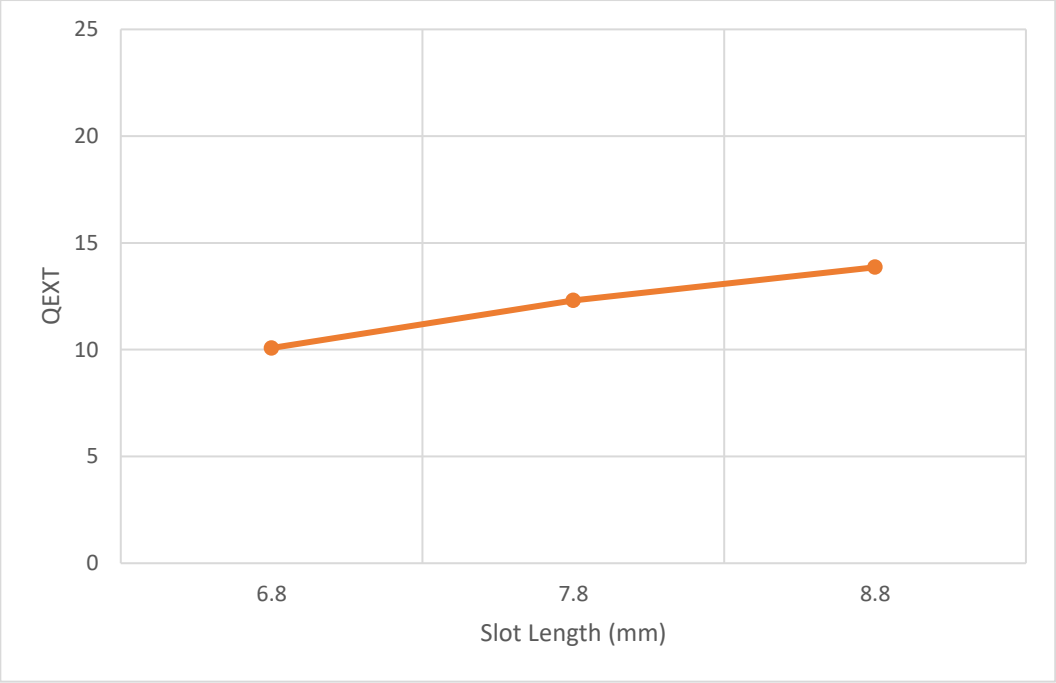

Figure 3-23 The impact of slot length variation on Q_{EXT}, where slot width = 2mm, DRA height = 14mm and post radius = 0.75mm

Design 4:

Design of DRA with intersecting parallel air posts is shown in Figure 3-24. The parametric studies are shown in Figures 3-25 to 3-30.

In the first case, slot width of 2 mm, slot length of 7 mm and radius of post of 0.75 mm are selected and the impact of varying DRA height on K_{23} and Q_{EXT} is studied. The analysis is shown in Figure 3-25 and 3-26. Then in the second case, DRA height of 13 mm, slot length of 7 mm and radius of posts of 0.75 mm are selected and the impact of varying slot width on K_{23} and Q_{EXT} is studied. The analysis is shown in Figure 3-27 and 3-28. In the third case, slot length of 7 mm, post radius of 1 mm and DRA height of 13 mm are selected

and the impact of varying slot width on K_{23} and Q_{EXT} is studied. The analysis is shown in Figure 3-27 and 3-28. In the last case, slot width of 2 mm, DRA height of 13 mm and radius of post of 0.75 mm are selected and the impact of varying slot length is studies. The analysis is shown in Figure 3-29 and 3-30.

Similar to previous cases, most significant influences on the bandwidth are caused by the post radius and DRA height.

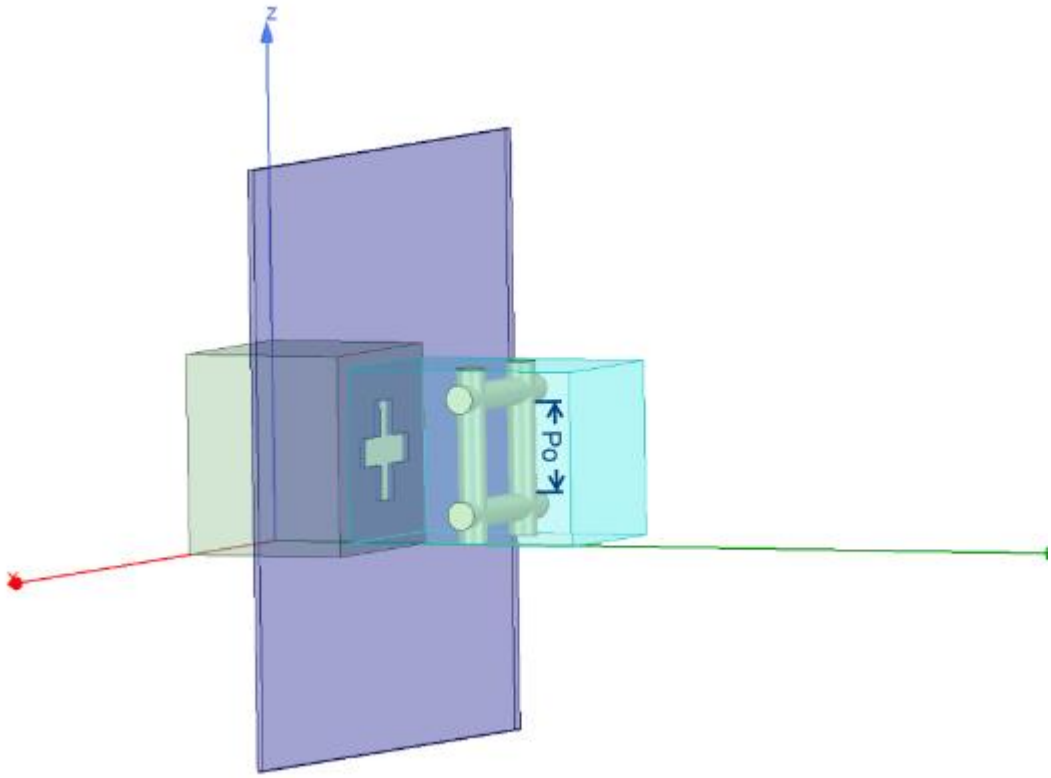

Figure 3-24 DR antenna with cross air post (DRA_a = 12.15mm; DRA_b = 12.15mm; DRA_d = 16mm; $L_3 = 11.66mm$; a = 13.98mm; Iris_d = 0.016in; Iris_w = 2 mm; Iris_l = 7mm; r_p =1mm; L_p = 14.2mm; W_p =5.8mm; P_o=9.15mm)

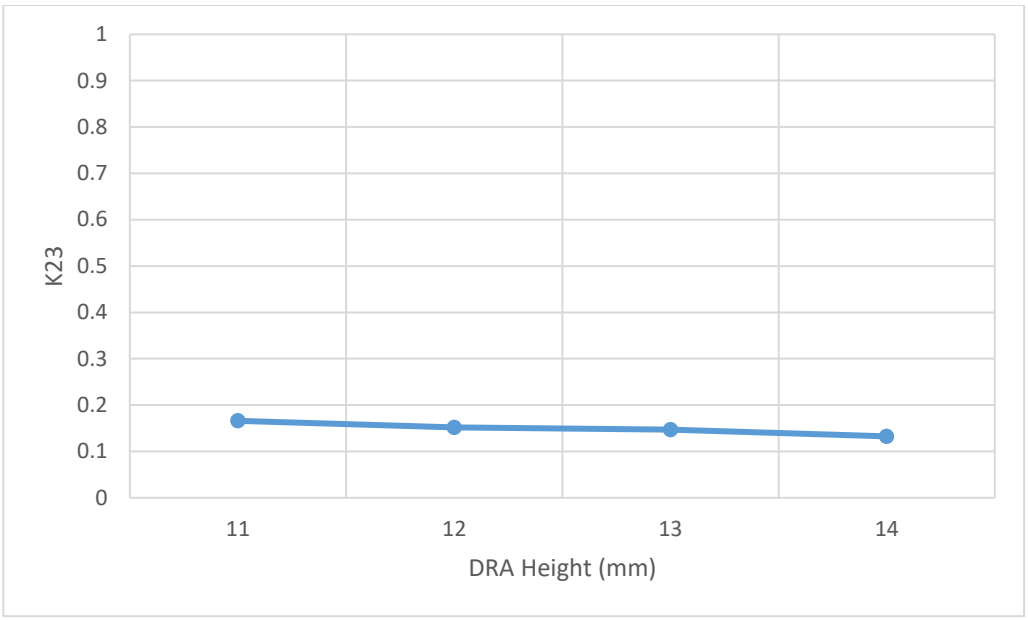

Figure 3-25 The impact of DRA height variation on K_{23}, where slot width = 2mm, slot length = 7mm and radius of posts = 0.75mm

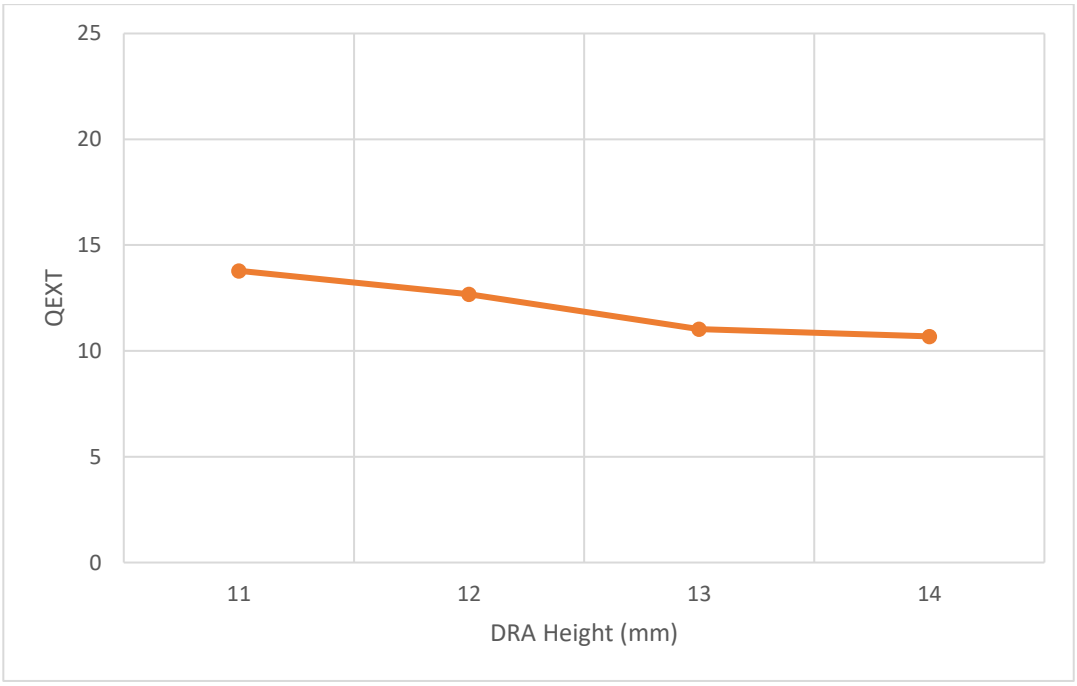

Figure 3-26 The impact of DRA height variation on Q_{EXT}, where slot width = 2mm, slot length = 7mm and radius of posts = 0.75mm

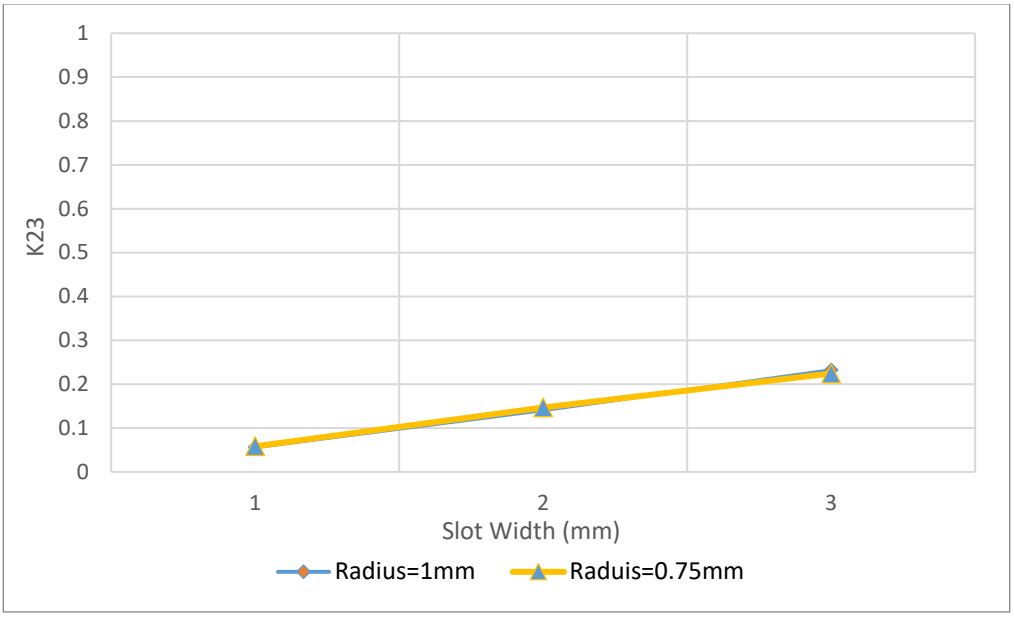

Figure 3-27 The impact of slot width variation on K_{23}, where DRA height = 13mm, slot length = 7mm and radius of posts =0.75mm and 1mm

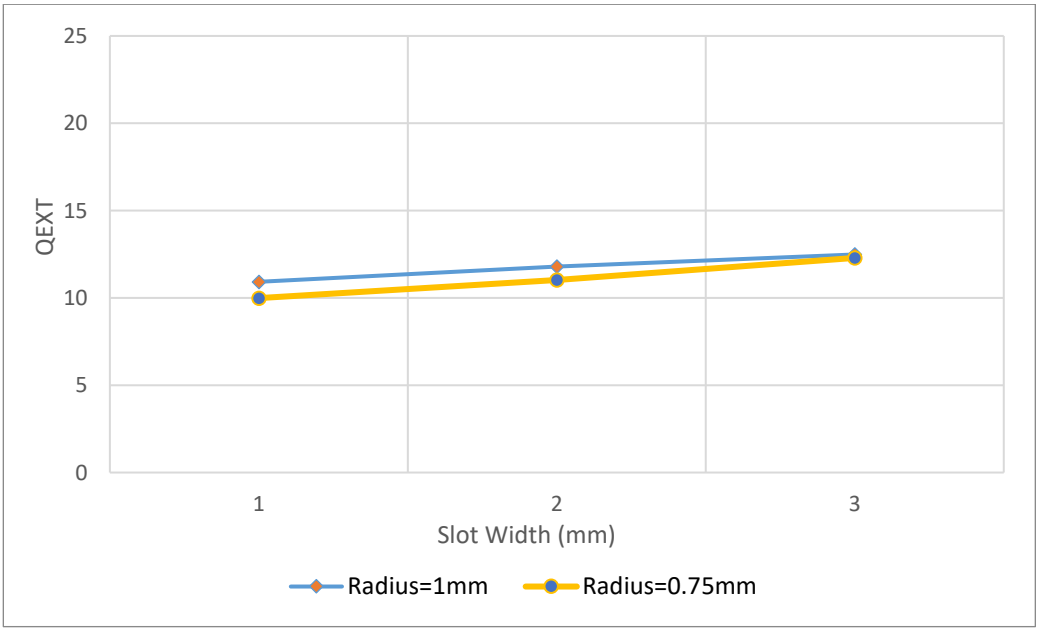

Figure 3-28 The impact of slot width variation on Q_{EXT}, where DRA height = 13mm, slot length = 7mm and radius of posts =0.75mm and 1mm

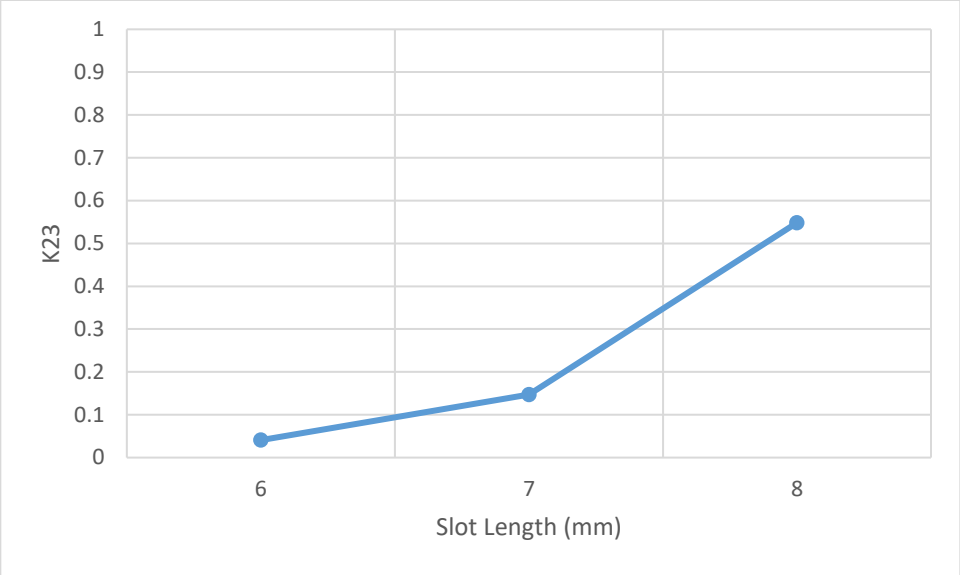

Figure 3-29 The impact of slot length variation on K_{23}, where DRA height = 13mm, slot width = 2mm and radius of post = 0.75mm

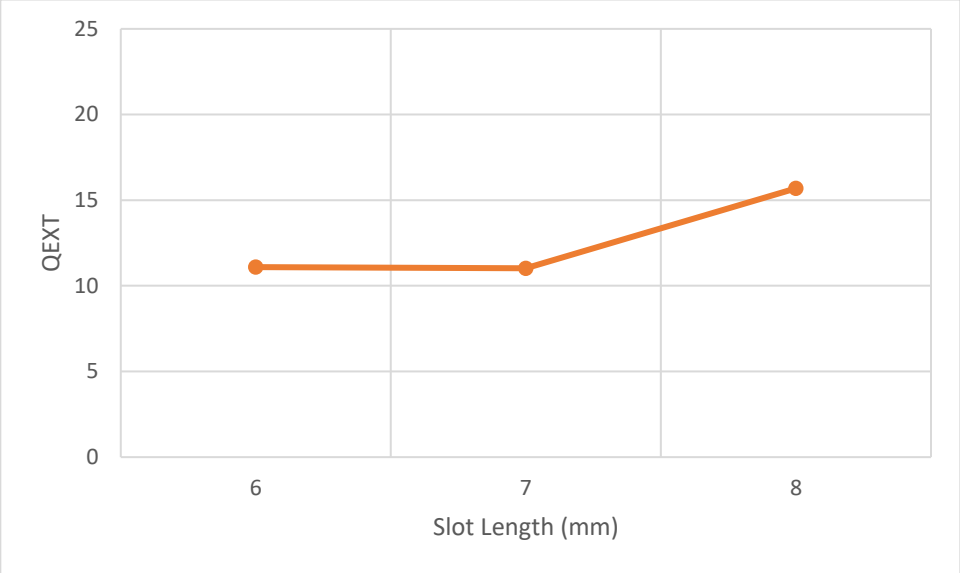

Figure 3-30 The impact of slot length variation on Q_{EXT}, where DRA height = 13mm, slot width = 2mm and radius of post = 0.75mm

In this section, four different DRA designs with increased bandwidth have been proposed.

The first design with one air post has been chosen to be used in the integrated filter antenna

design example in the next section. This is because it offers the largest tuning range of Q_{EXT} and K_{23} and is easy to fabricate comparing with other designs.

3.3 Integrated Design Example

To validate the analysis above, an integrated design of DR filter and DRA is presented in this section. The center frequency is 3.6 GHz and the dielectric constant ε_r is 20 with tanδ 5.625×10^{-5}.

Figure 3-31 shows the circuit model for the last resonator of the standalone 3-pole filter. $|S_{11}|$ from the circuit model and HFSS simulation results for the DRA with an air post in Figure 3-3 are compared in Figure 3-32. Based on equations (3.5) and (3.6), coupling coefficient to the DRA is 0.254, which is consistent with K_{23} = 0.245 of the filter.

The complete design is shown in Figure 3-33. The return loss in Figure 3-34 shows that a bandwidth of 300MHz is achieved after inserting an air post, which is significant wider comparing with the design in [44] with 200 MHz bandwidth. Good isolation (greater than 21.5 dB) between two ports is observed in Figure 3-35. The E-plane and H-plane radiation patterns at the center frequency when port 1 is excited are shown in Figure 3-36 and Figure 3-37, respectively. The realized gain is shown in Figure 3-38, showing filtering response, while the gain of the antenna is flat as shown in Figure 3-39. The gain is 6.73 dB. Figures 3-40 to 3-43 show similar results when port 2 is excited.

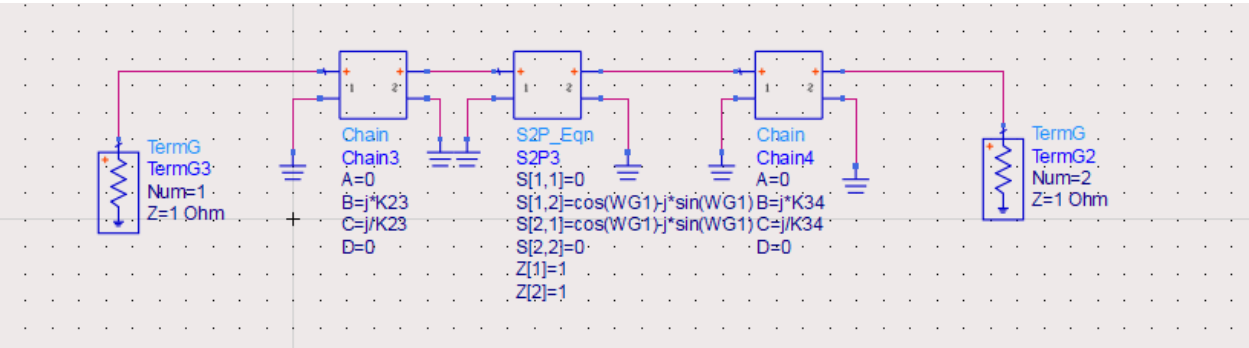

Figure 3-31 Filter last resonator equivalent circuit model when the bandwidth is 300MHz.

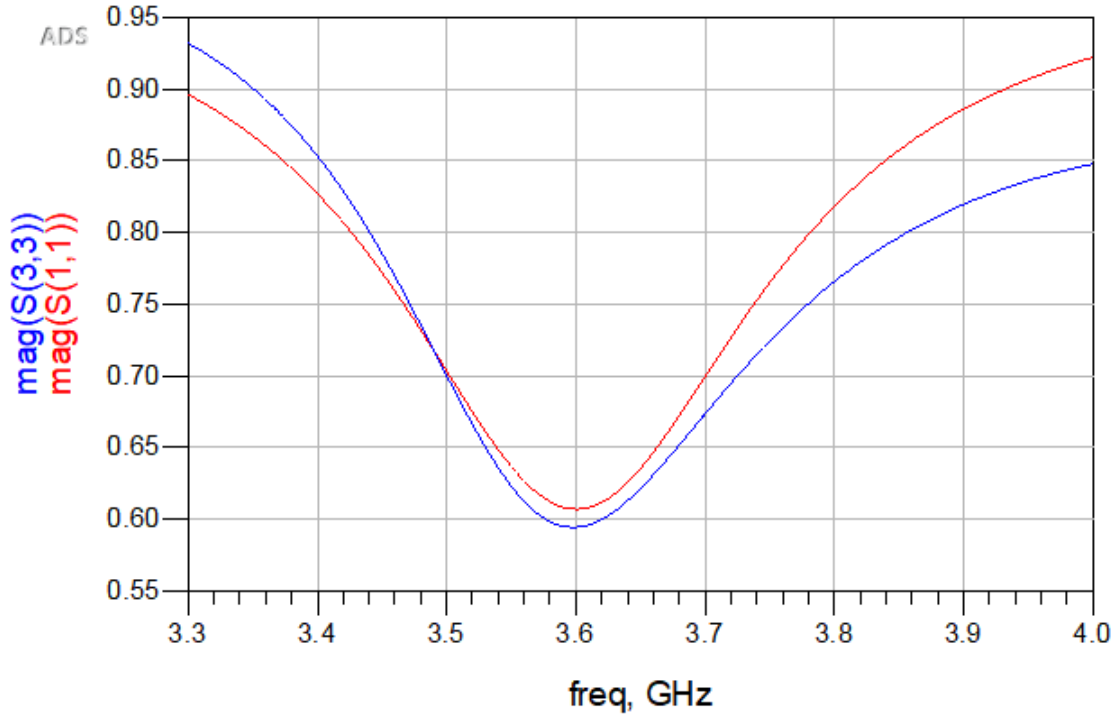

Figure 3-32 Filter last resonator and design of DRA with one air post

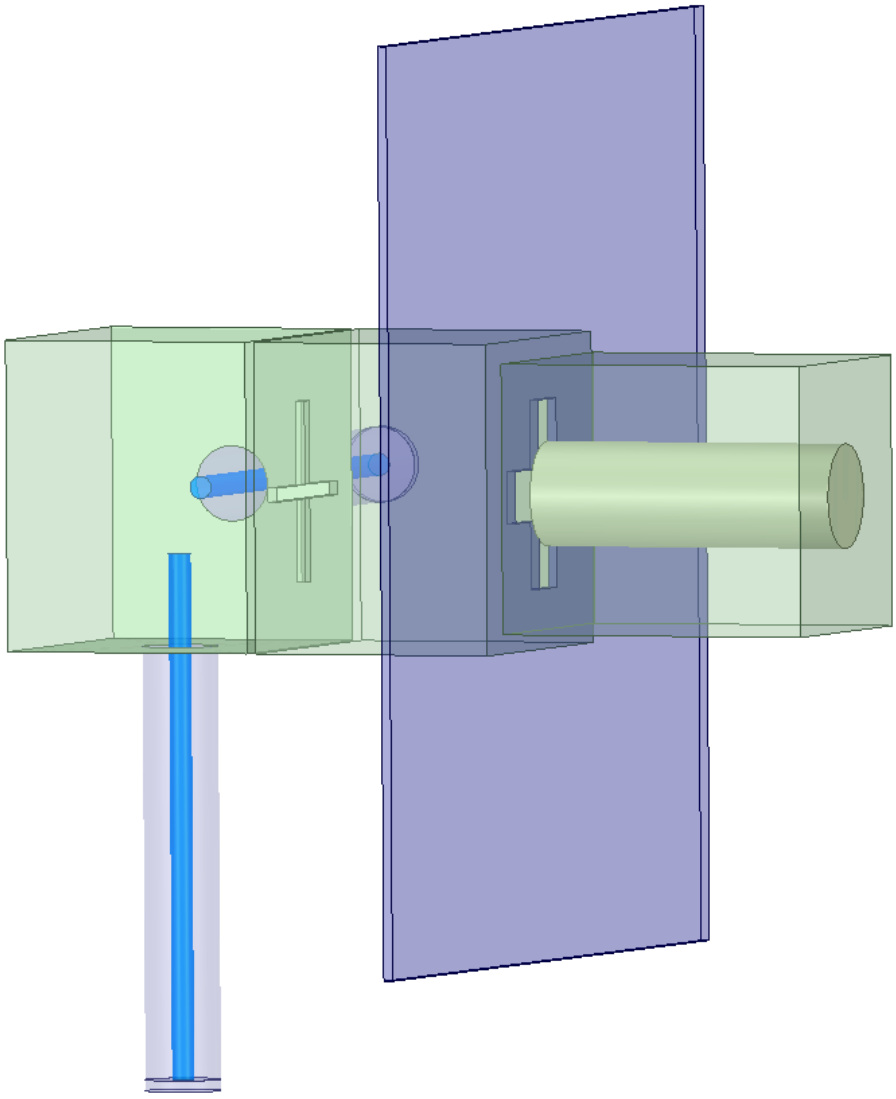

Figure 3-33 Filtering DR antenna with one air post (DRA_a = 12.15mm; DRA_b = 12.15mm; DRA_d = 14.2mm; L_1=11.055mm; w = 13.98mm; h = 13.98mm; slot_d = 0.016in; Iris_w_2 = 2.35mm; Iris_l_2 =7mm, Iris_w_1 = 0.4064mm; Iris_l_1 = 7.97mm; L_p =11.41mm;)

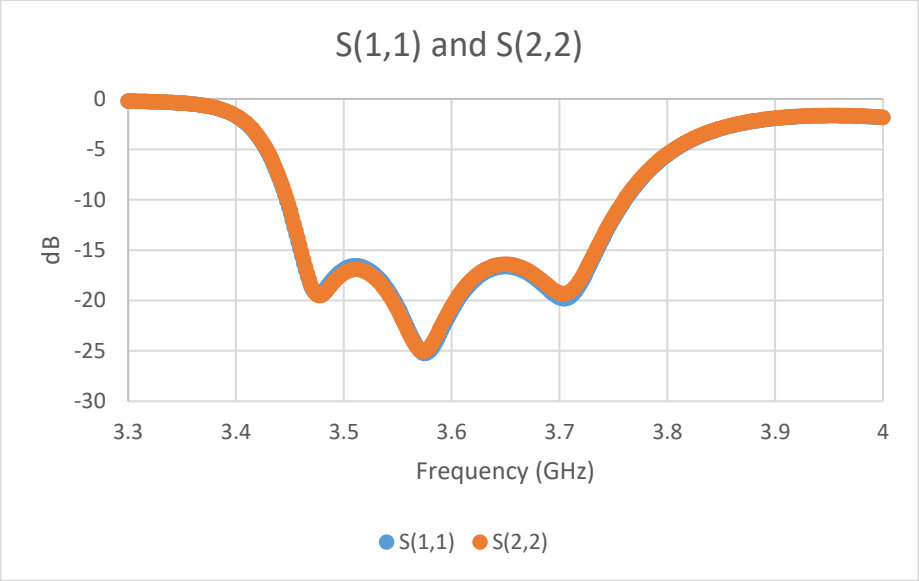

Figure 3-34 $|S_{11}|$ and $|S_{22}|$ responses of the DR filtering antenna

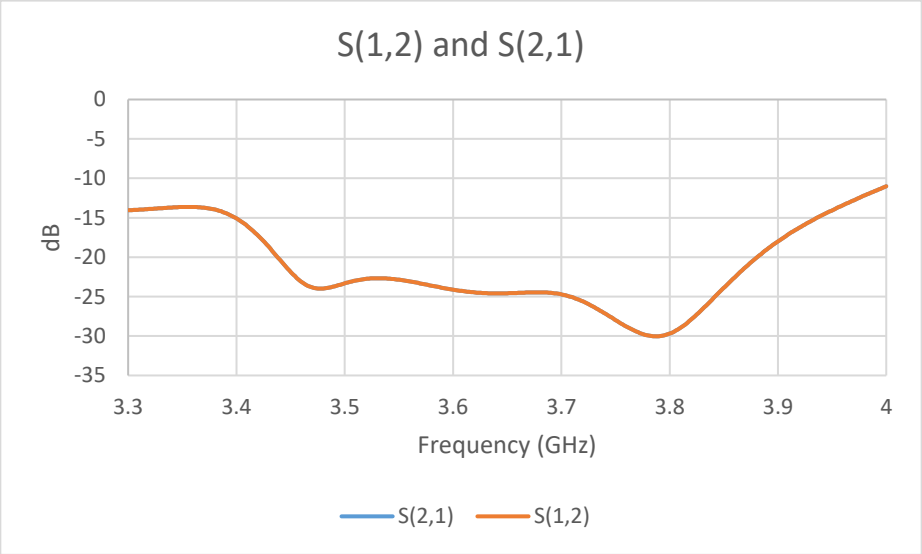

Figure 3-35 $|S_{12}|$ and $|S_{21}|$ responses of the DR filtering antenna

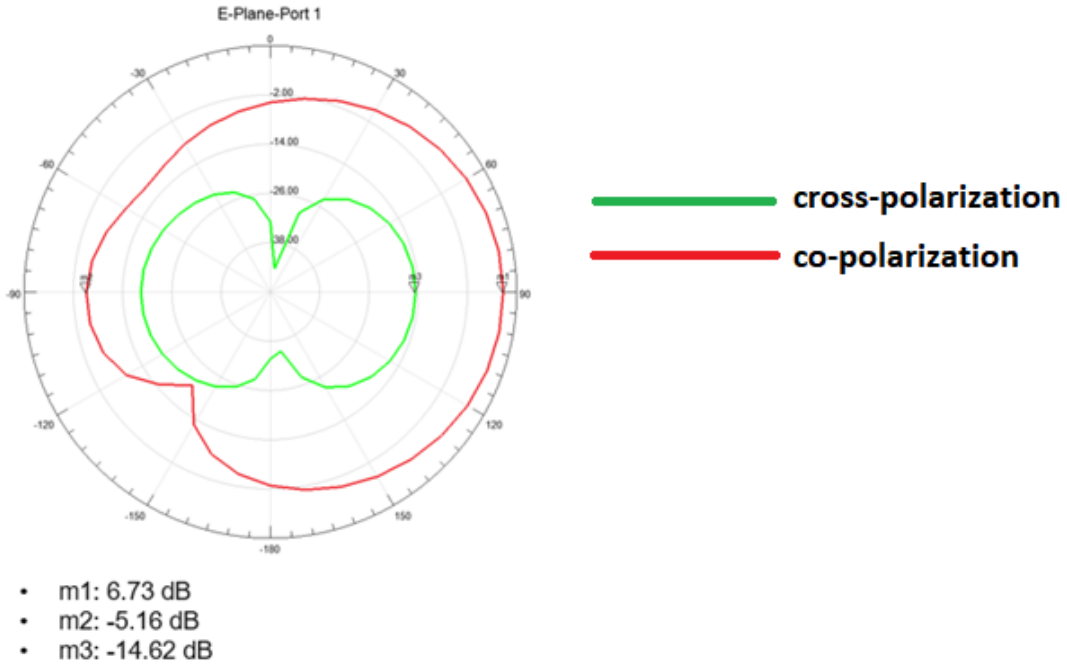

Figure 3-36 DR Filtering Antenna Radiation Pattern E-Plane when Port 1 is excited

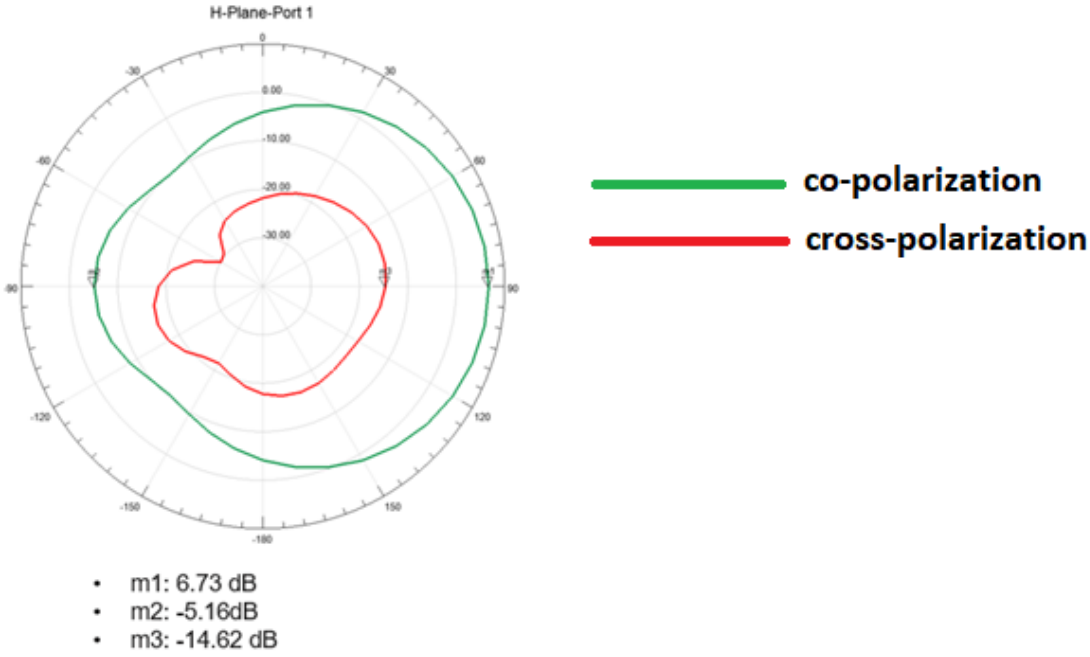

Figure 3-37 DR Filtering Antenna Radiation Pattern H-Plane when Port 1 is excited

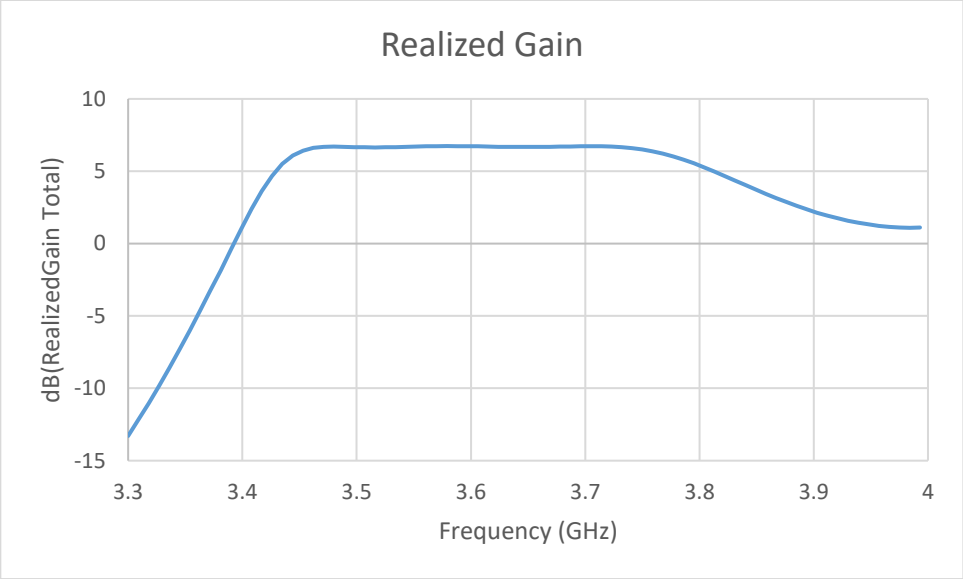

Figure 3-38 Realized Gain of 300MHz DR filtering antenna when Port 1 is excited

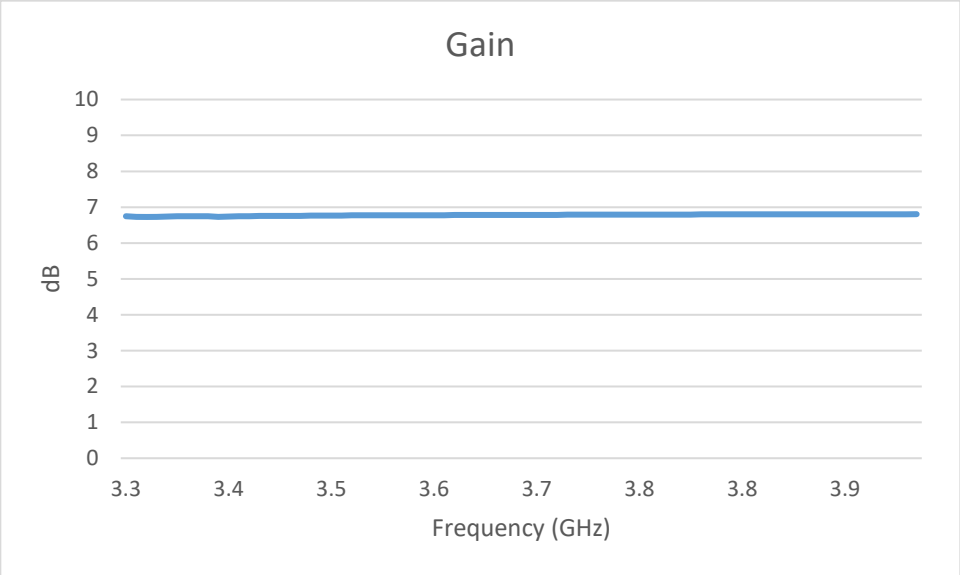

Figure 3-39 Gain of 300MHz DR filtering antenna when Port 1 is excited

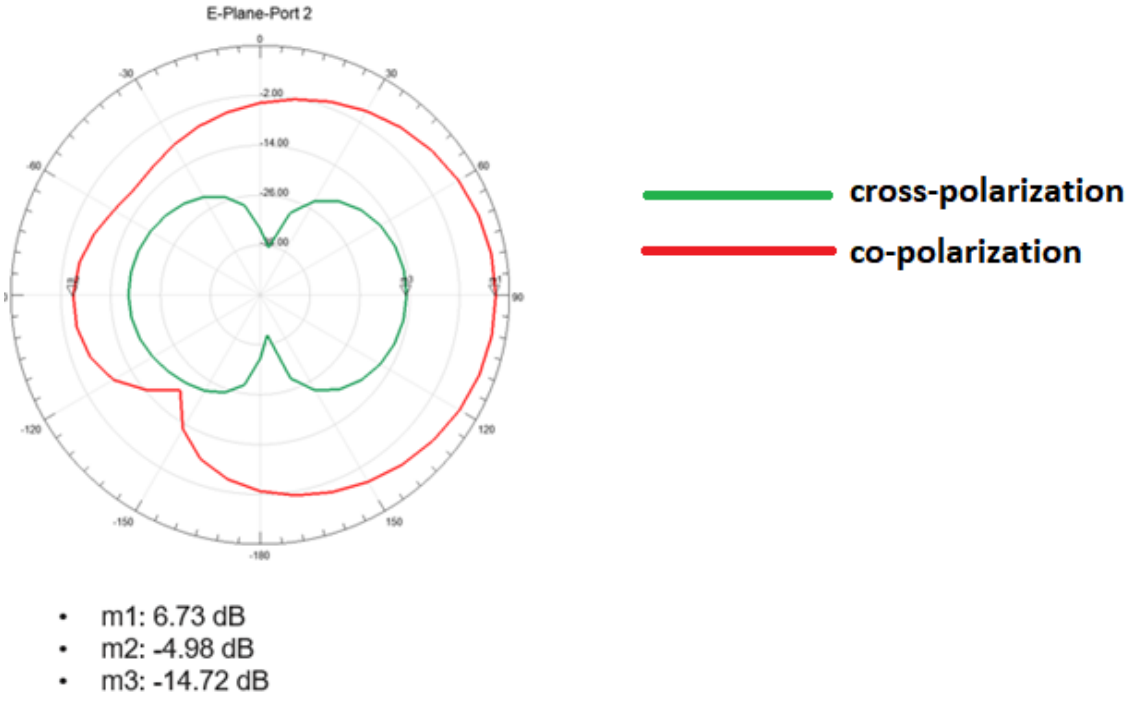

Figure 3-40 DR Filtering Antenna Radiation Pattern E-Plane when Port 2 is excited

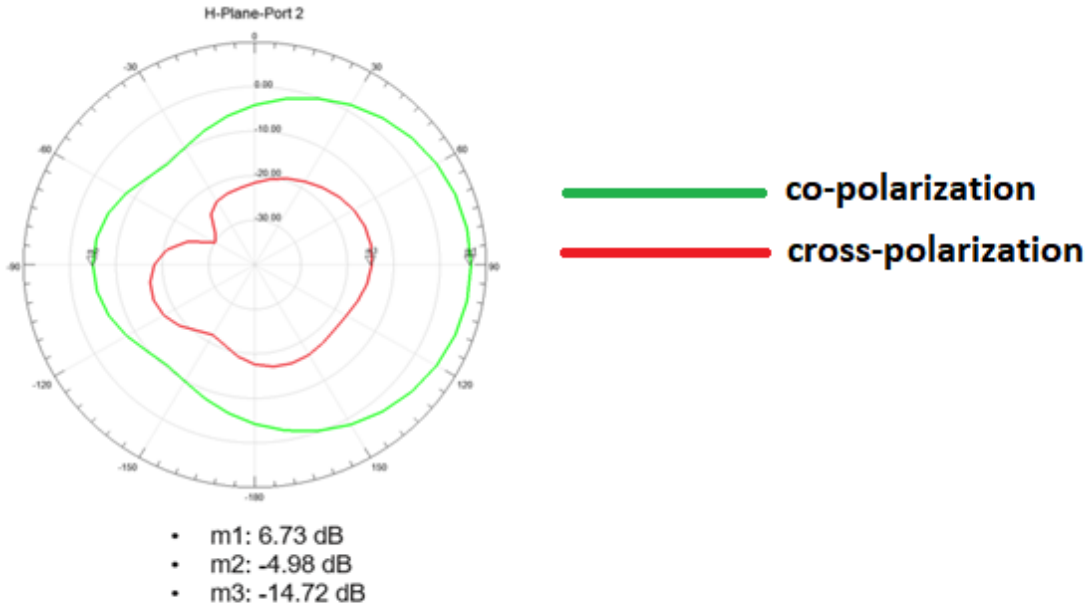

Figure 3-41 DR Filtering Antenna Radiation Pattern H-Plane when Port 2 is excited

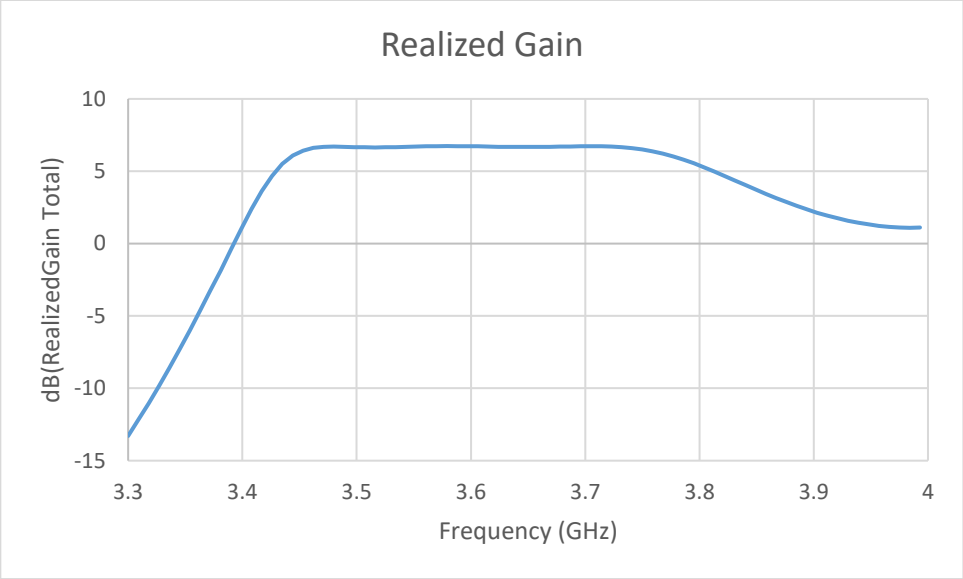

Figure 3-42 Realized Gain of 300MHz DR filtering antenna when Port 2 is excited

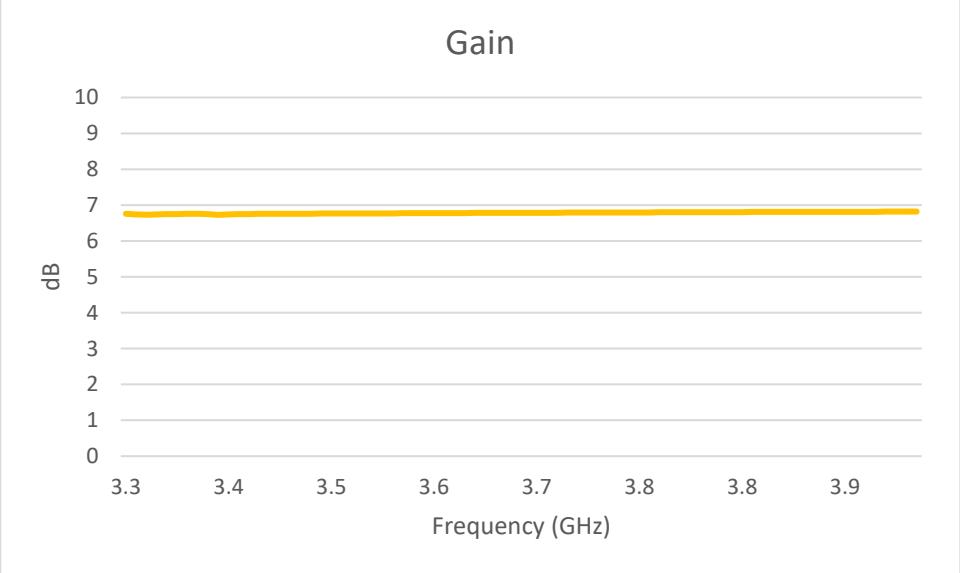

Figure 3-43 Gain of 300MHz DR filtering antenna when Port 2 is excited

3.4 Summary

In this chapter, different approaches of increasing bandwidth of filter antenna integration by inserting air posts in the DRA have been proposed. Parametric studies are performed on design variables. It has been shown that these methods not only effectively increase the bandwidth of the integrated design, but also allow ease in the tuning of Q_{EXT}.

The concept is verified by an integrated design of DRA with a 3-pole waveguide filter. The 10 dB impedance bandwidth after inserting an air post in the antenna is 300 MHz. The return loss is 15 dB within the passband. Isolation between two ports is greater than 21.5 dB. Both gain and realized gain are greater than 6.7 dB.

Chapter 4

Filtering Rectangular Dielectric Resonator Antenna

In this chapter, another approach to design filtering antennas is investigated, namely the fusion method [34]. Different from the integration of filter and antenna in the previous chapter, the fusion method mainly focuses on the modification of the antenna and does not require additional filtering circuits. In this chapter, designs of filtering rectangular dielectric resonator antenna (RDRA) fed by microstrip lines are presented. Both linearly polarized and dual polarized filtering RDRAs are shown. The comparison of results using the synthesis method and the fusion method is also discussed.

4.1 Linearly Polarized Filtering Rectangular DRA

In this section, a rectangular DRA without filtering function is designed as the first step. The antenna dimensions are calculated using equation (3.1) – (3.4). Microstrip line is used as the feed method to activate the antenna. As shown in figure 4-1, a rectangular DRA with length of dra_x, width of dra_y, height of dra_z and dielectric constant, ε_r, is placed on the square ground plane with length *s*. The substrate thickness is *t* and dielectric constant is ε_{rs}. The rectangular slot with length s_l and width s_w on the ground plane is used to excite the antenna. The distance between center of the DRA and the center of square ground is

offset by l_{off}. On the other side of the square substrate plane is a 50 Ω microstrip line with length L_s and w_s.

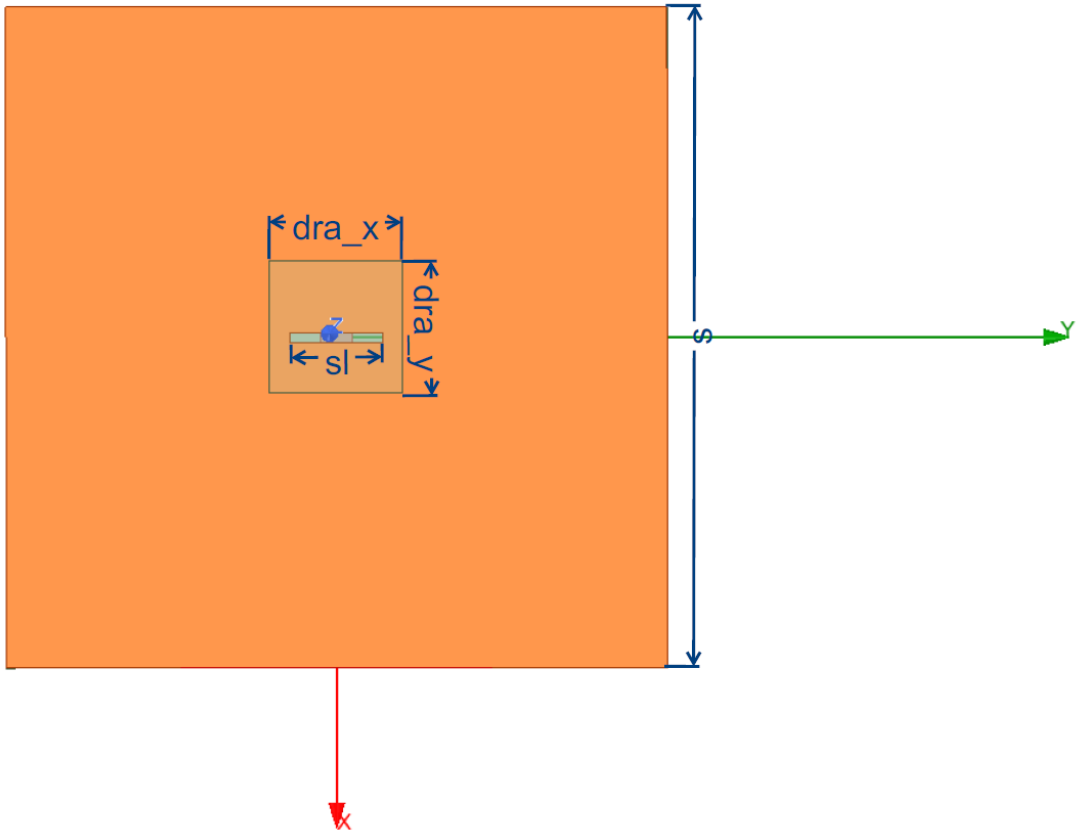

(a) Top View

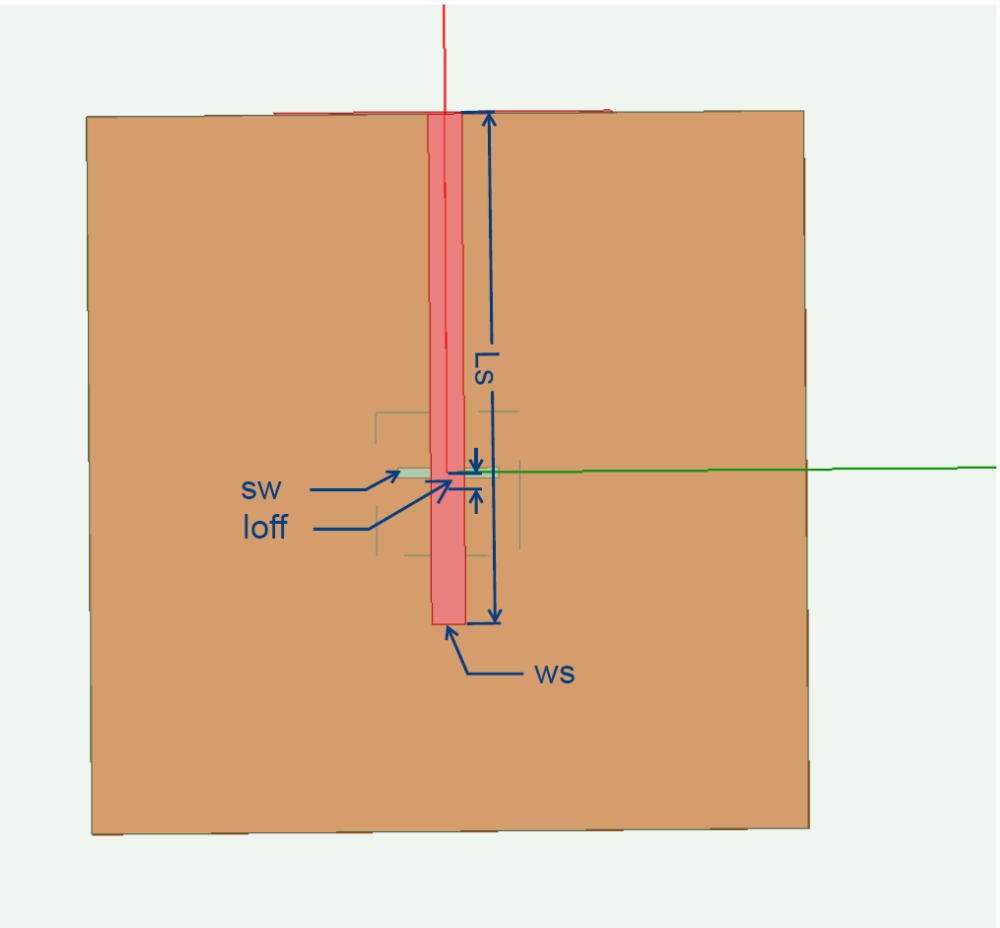

(b) Bottom View

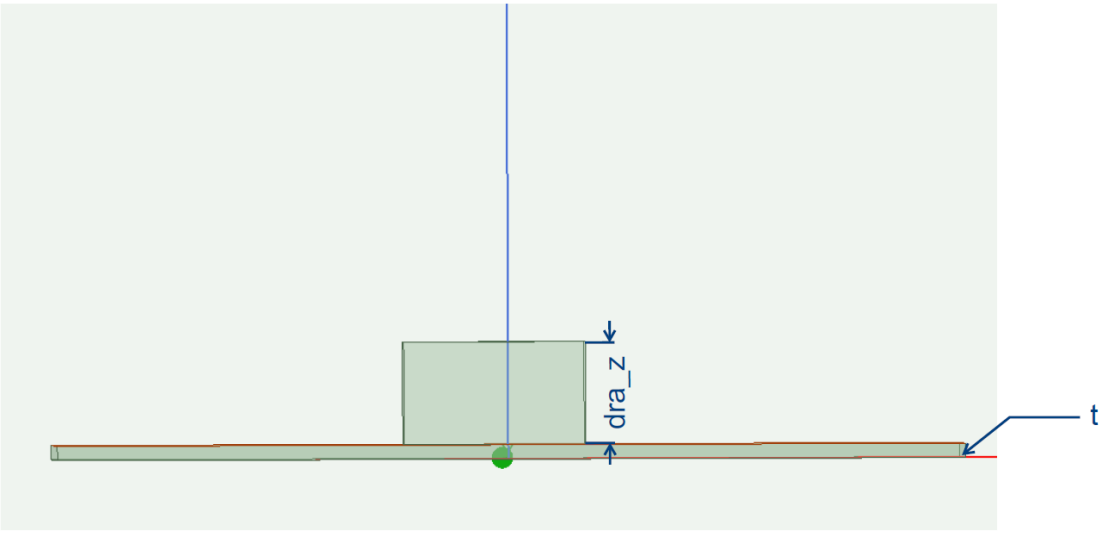

(c) Side view

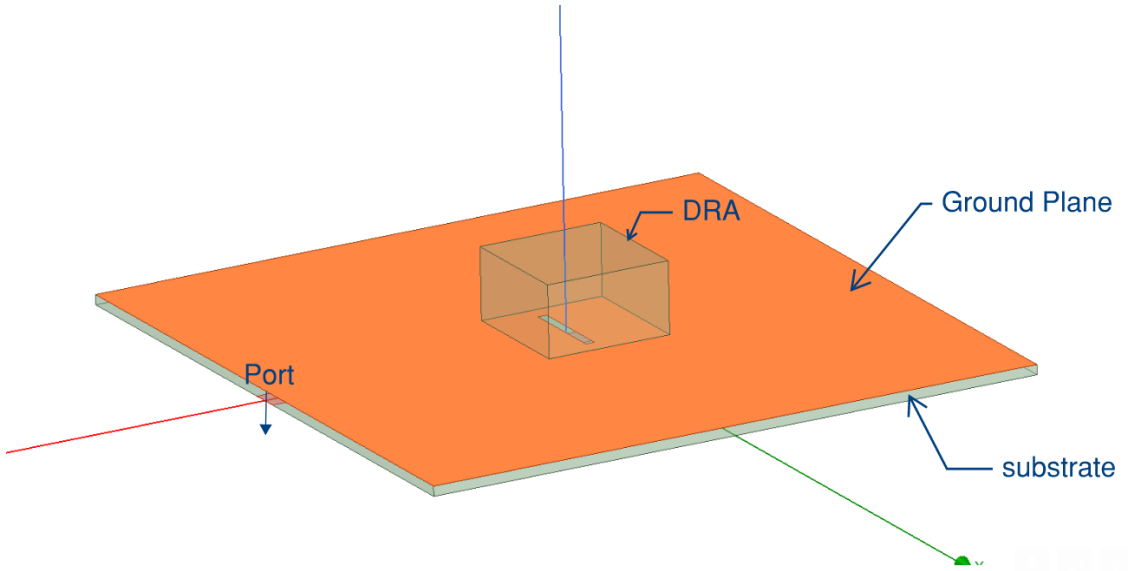

(d) Isometric view

Figure 4-1 Design of RDRA: (s=100mm, t=1.57mm, Ls=71.2mm, ws=4.7mm and loff=1.556mm, ε_r=10, ε_{rs}=2.33, sl=14.14mm, sw=1.41mm, dra_x=20mm, dra_y=20mm, dra_z=11.3mm)

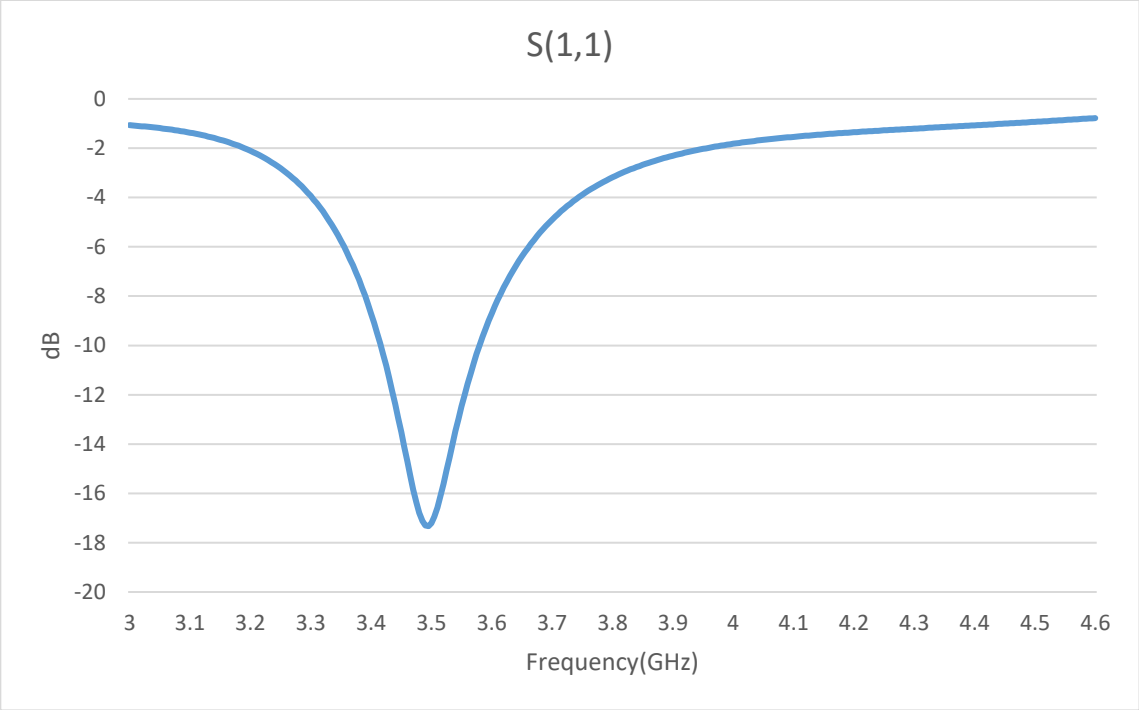

Figure 4-2 Return loss of RDRA.

Figure 4-2 shows the central frequency of antenna is 3.35 GHz. The return loss is 25 dB. The DRA design is the initial design for Design 1 and Design 2 to apply the fusion method, which cancels radiation and achieves transmission zero(s) by inserting posts in the DRA. In the following, two designs of filtering antenna are presented. The two designs use the same method and concept except that the dielectric constant of the DRA $\varepsilon_r = 10$ for Design 1 and $\varepsilon_r = 20$ for Design 2. The dielectric constant of the substrate is 2.33 in both cases.

Design 1:

Based on DRA design in Figure 4-1, the configuration of filtering rectangular DRA is presented in Figure 4-3. Instead of using the rectangular slot, a circular slot with radius R_s is applied to facilitate the addition of conducting posts. Three copper posts with radius $R_{p,}$ are inserted to the DRA. Post spacing, D_1, is equally divided from middle post. The left and the right posts are attached to ground plane and the middle post passes through circular slot and connects to the microstrip feedline. The copper strip with length *Strip_l* and width *Strip_w* connects the posts horizontally on top of the DRA surface. Therefore, the design has three loops, namely the left loop, the right loop, and the big loop. Currents in these loops generate magnetic fields that are in the opposite direction of the magnetic field of the TE^{y}_{111} mode of the DRA. The cancelling effect results in transmission zeros (radiation null).

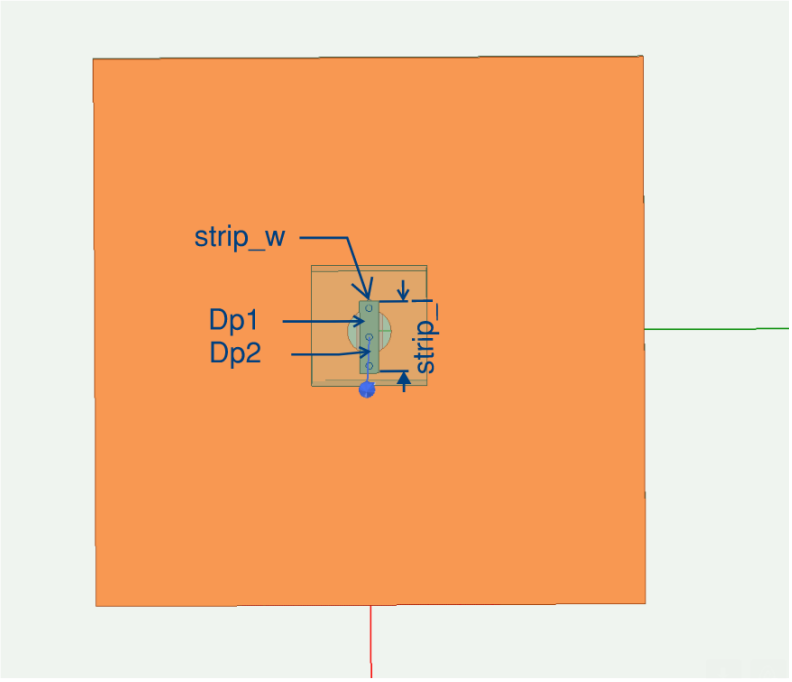

(a) Top view of filtering RDRA with three posts

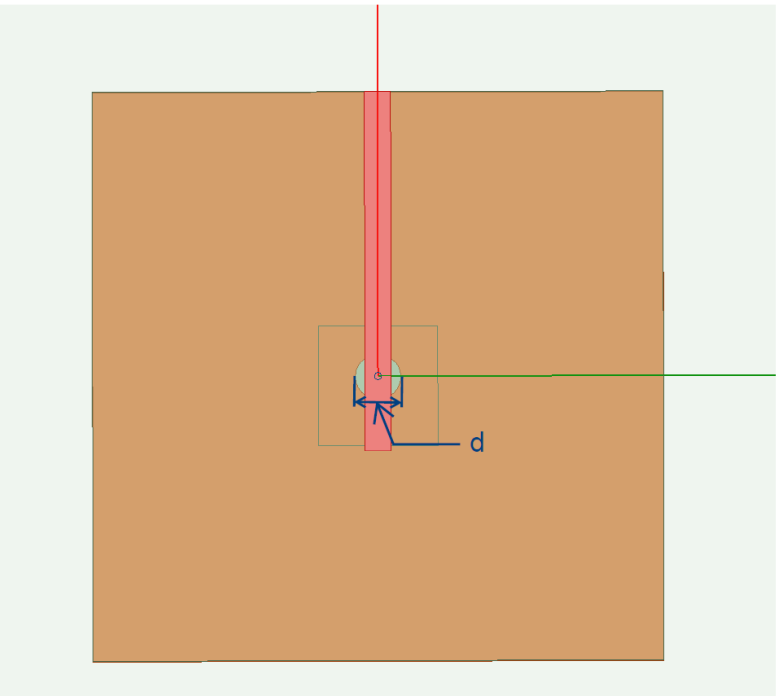

(b) Bottom view of filtering RDRA with three posts

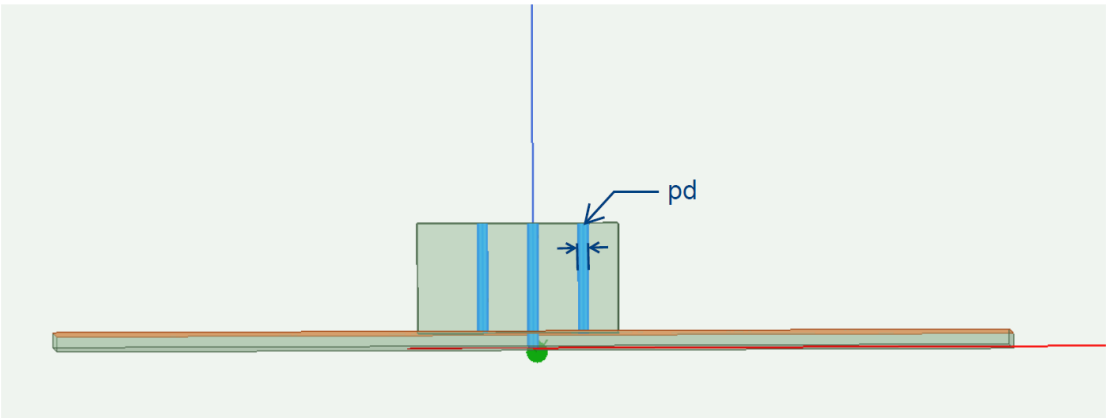

(c) Side view of filtering RDRA with three posts

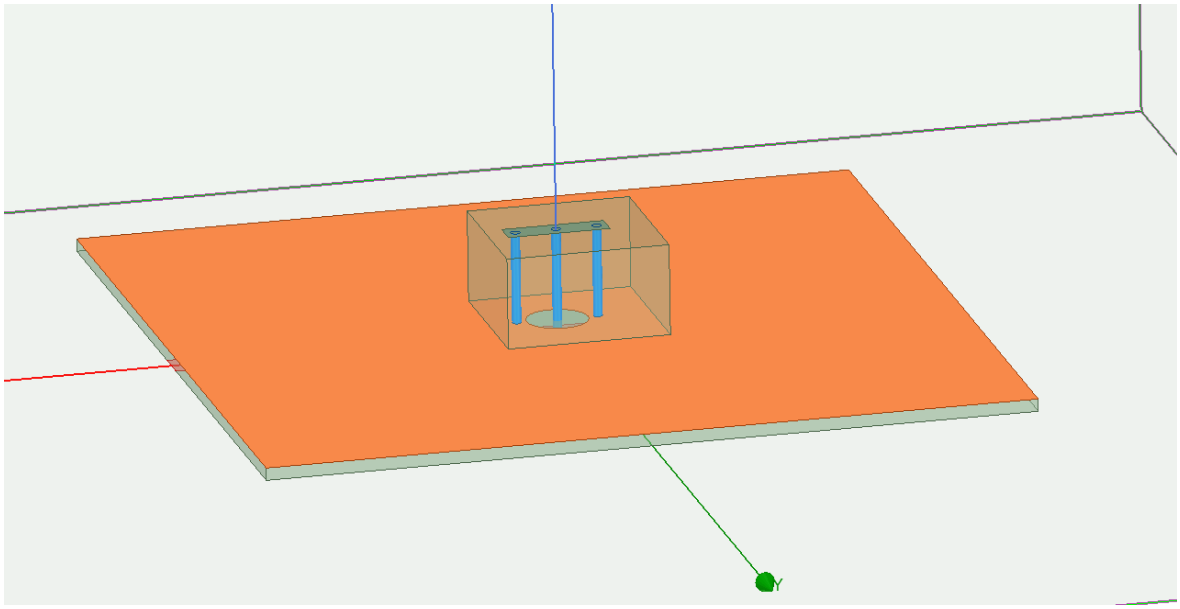

(d) Isometric view of filtering RDRA with three posts

Figure 4-3 Design of filtering RDRA with 3posts (s=100mm, t=1.57mm, Ls=63.182mm, ws=4.7mm and loff=1.576mm, ε_r=10, ε_{rs}=2.33, d=8mm, dra_x=21mm, dra_y=21mm, dra_z=11.46mm, pd=1.1954mm, strip_l= 13.182mm, strip_w=3.5mm, Dp_1=Dp_2= 5.266mm)

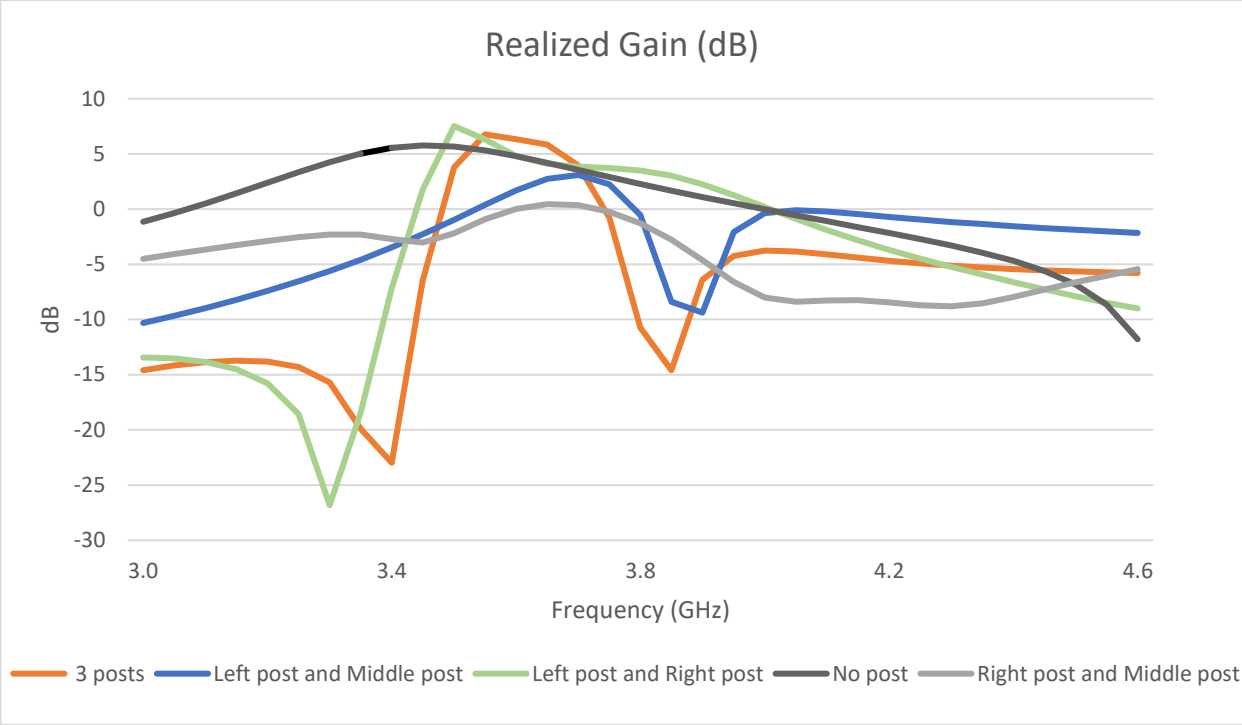

Figure 4-4 Realized gain of filtering RDRA with different loops.

Figure 4-4 presents the comparison of realized antenna gain with different loops. When the antenna does not have any posts (the original DRA in Figure 4-1), the realized gain is relatively flat with no transmission zeros. When the left and middle posts are added to the antenna, which excites the left loop, the upper passband transmission zero appears. When antenna has the left and right posts to excite the big loop, the lower passband transmission zero presents. The figure gives indication on how to control transmission zeros locations by adjusting the post distances.

Parametric Study

To achieve good antenna performance, parametric study has been performed for a number of design variables. A total of five different cases have been studied by adjusting the dimensions of strip length, post spacing, slot radius, post radius and offset. Based on the variable dimensions, figures of realized gain have been presented to show the differences.

In the first case, post spacing D_1 is 5.266 mm, slot radius is 4 mm, post radius is 0.6 mm and offset is 1.576 mm, and the impact of varying strip length is studied. The analysis is presented in Figure 4-5.

In the second case, the strip length is 13.182 mm, slot radius is 4 mm, post radius is 0.6 mm and offset is 1.576 mm, and the impact of varying post spacing is analyzed in Figure 4-6.

In the third case, the strip length is 13.182 mm, post spacing is 5.266 mm, post radius is 0.6 mm and offset is 1.576 mm, and the impact of varying slot radius is studied and shown in Figure 4-7.

In the fourth case, strip length is 13.182 mm, post spacing is 5.266 mm, slot radius is 4 mm and offset is 1.576 mm, and the impact of varying post radius is analyzed in Figure 4-8.

In the last case, strip length is 13.182 mm, post spacing is 5.266 mm, slot radius is 4 mm and post radius is 0.6 mm, and the impact of varying of offset is shown in Figure 4-9.

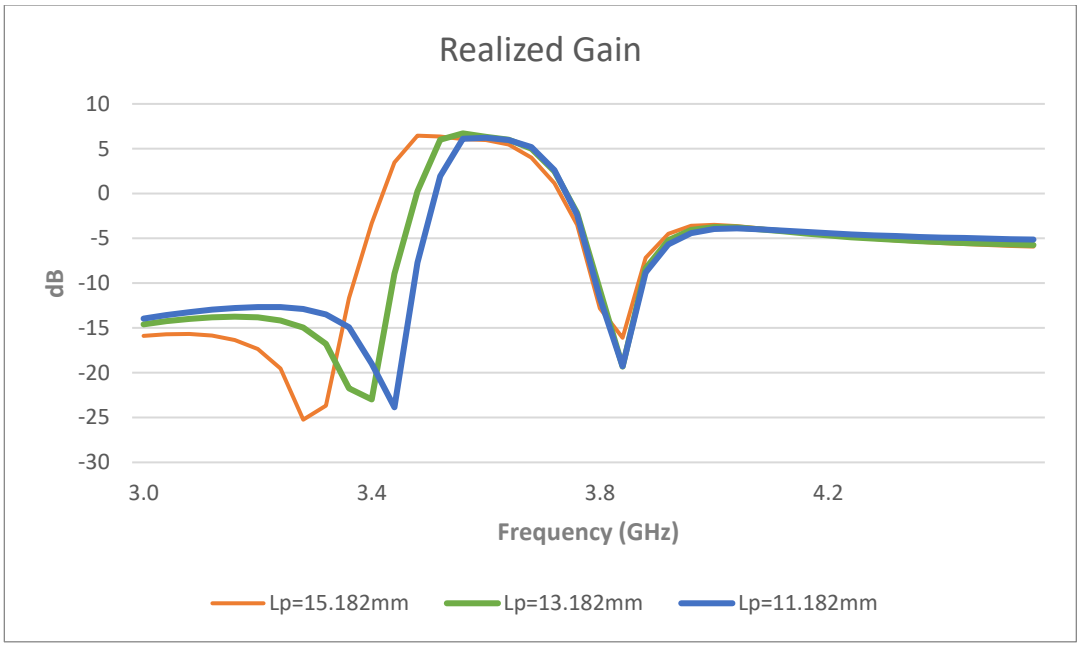

Figure 4-5 The impact of strip length on realized gain, where post spacing is 5.266 mm, slot radius is 4 mm, post radius is 0.6 mm and offset is 1.576 mm

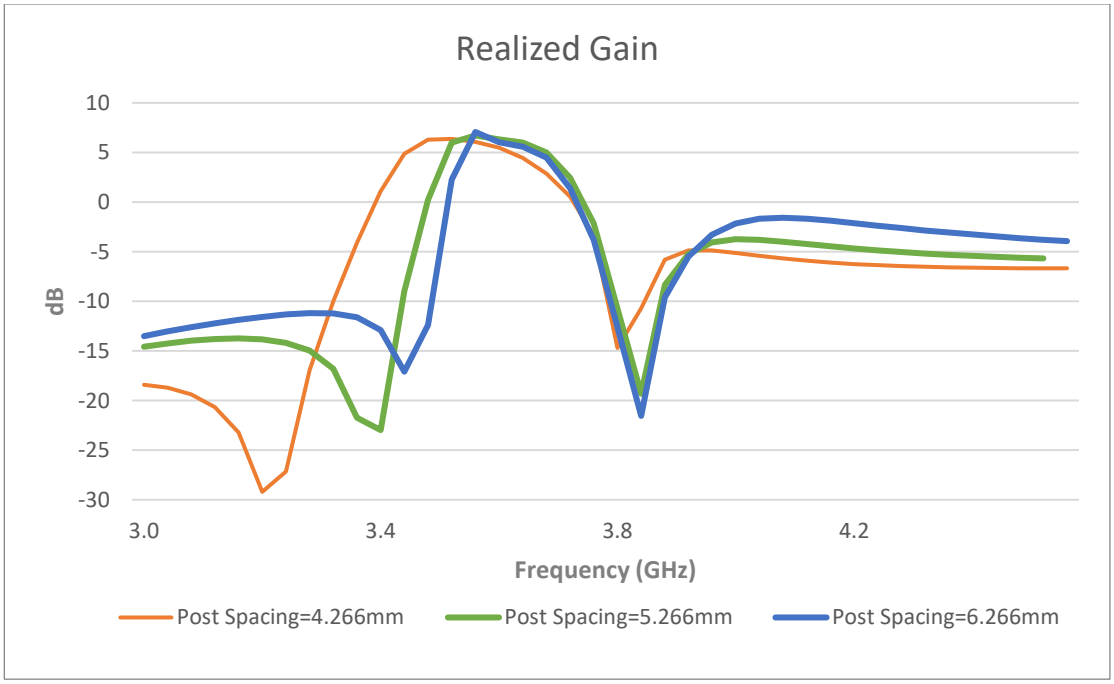

Figure 4-6 The impact of post spacing on realized gain, when strip length is 13.182 mm, slot radius is 4 mm, post radius is 0.6 mm and offset is 1.576 mm

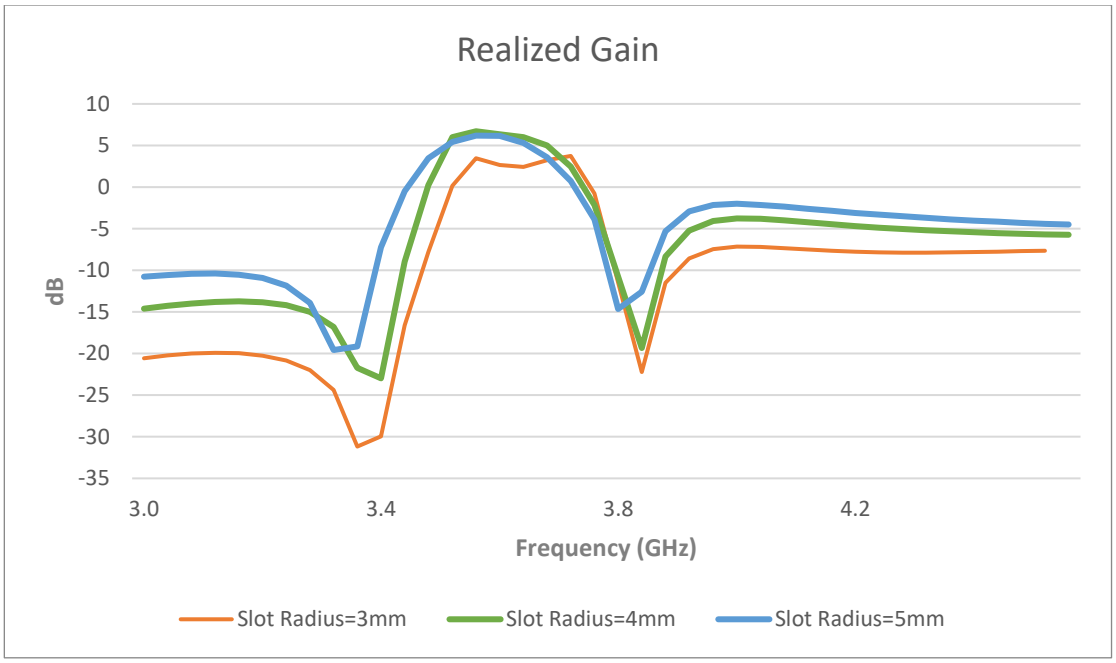

Figure 4-7 The impact of slot radius on realized gain, when the strip length is 13.182 mm, post spacing is 5.266 mm, post radius is 0.6 mm and offset is 1.576 mm

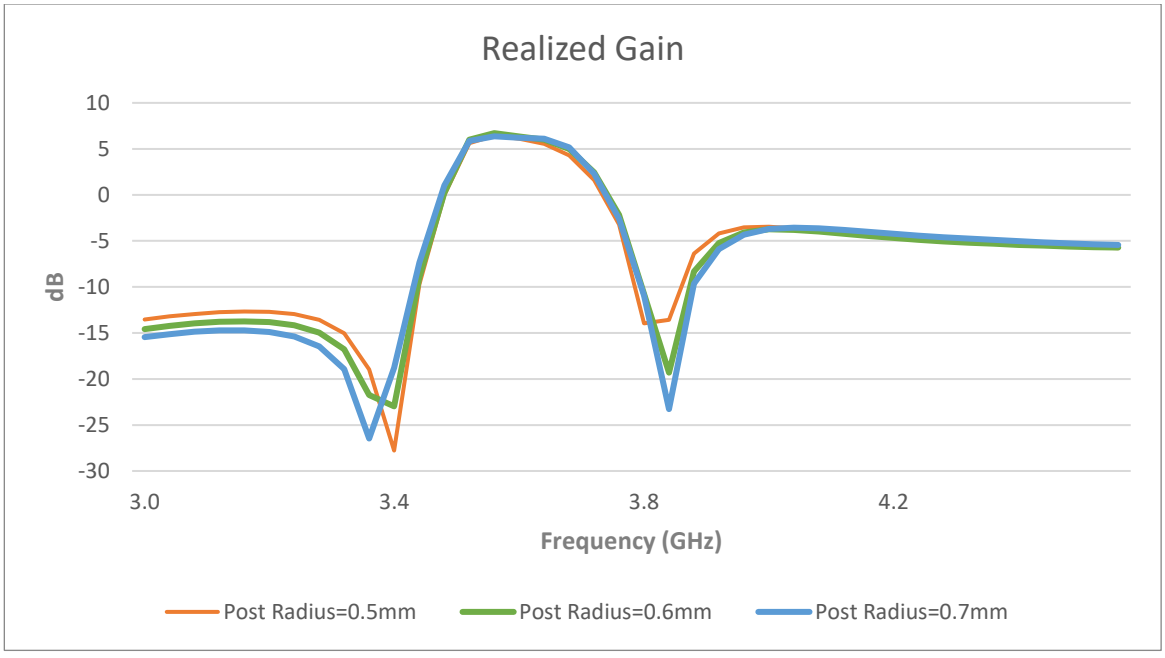

Figure 4-8 The impact of post radius on realized gain, strip length is 13.182 mm, post spacing is 5.266 mm, slot radius is 4 mm and offset is 1.576 mm

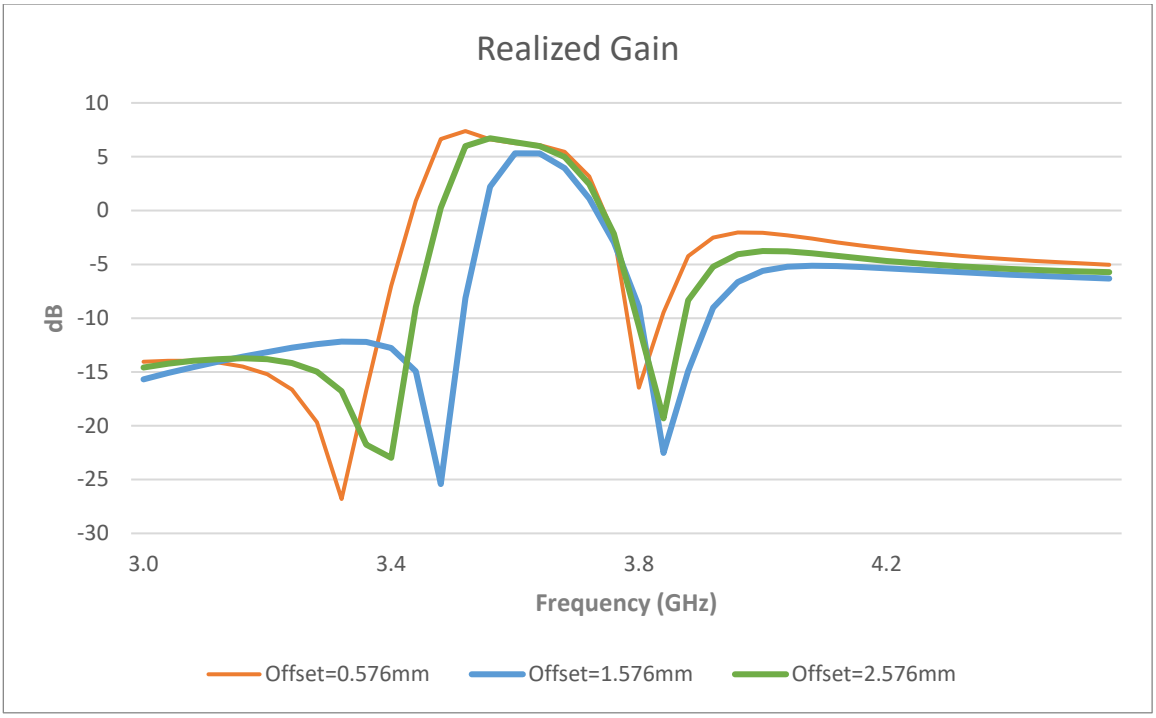

Figure 4-9 The impact of offset on realized gain, where strip length is 13.182 mm, post spacing is 5.266 mm, slot radius is 4mm and post radius is 0.6 mm

Based on parametric study, as strip length is increased from 11.182 mm to 15.182 mm, lower passband radiation null shifts downward in Figure 4-5. As the post spacing is increased from 4.266 mm to 5.266 mm, lower passband radiation null shifts upward in Figure 4-6. When slot radius increases from 3 mm to 5 mm, the responses shift down in frequency as shown in Figure 4-7. When post radius increases from 0.5 mm to 0.7 mm, the responses barely change in Figure 4-8. As offset increases from 0.576 mm to 2.576 mm, the whole curve shifts upward, which means both the lower radiation null and the upper radiation null shift upward, as shown in Figure 4-9. In the analysis, lower transmission zero is easier to control by adjusting post spacing and strip length. Upper transmission zero is mainly controlled by offset.

After optimization, the result of completed RDRA filtering antenna design is shown below. The center frequency is 3.6 GHz, and bandwidth is 200 MHz. Gain and realized gain are 6.78 dB.

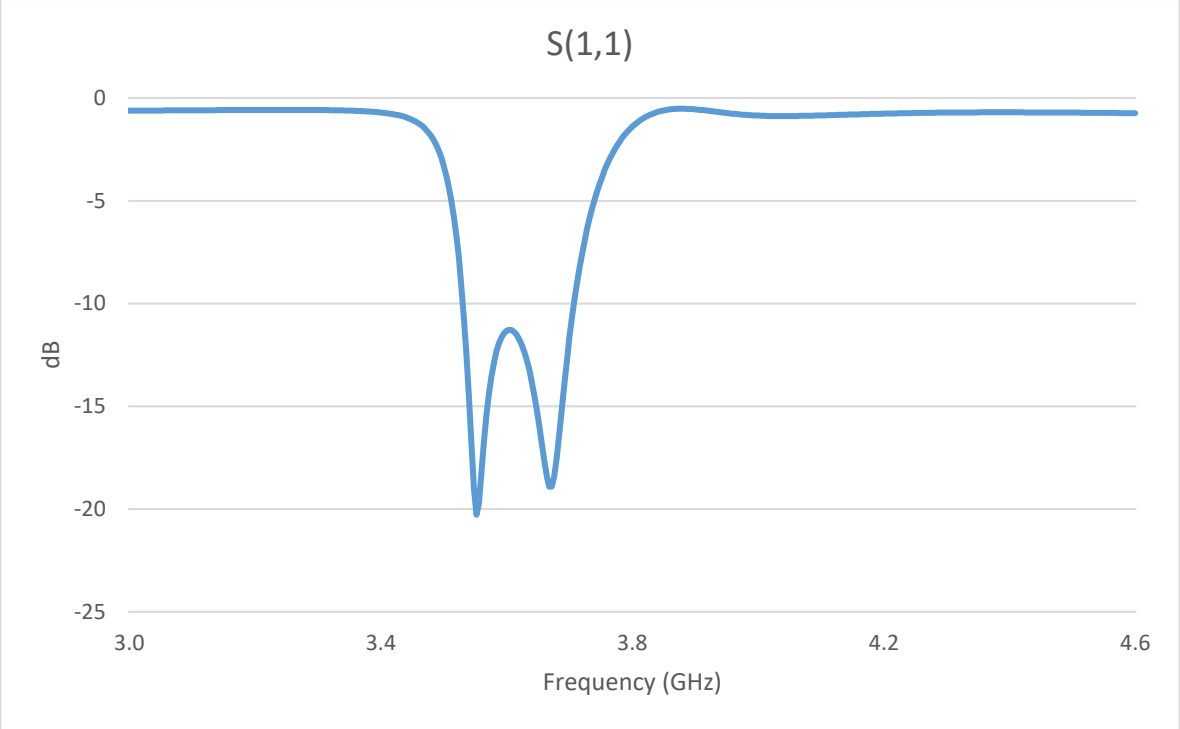

Figure 4-10 |S(1,1)| of filtering RDRA with 3 posts.

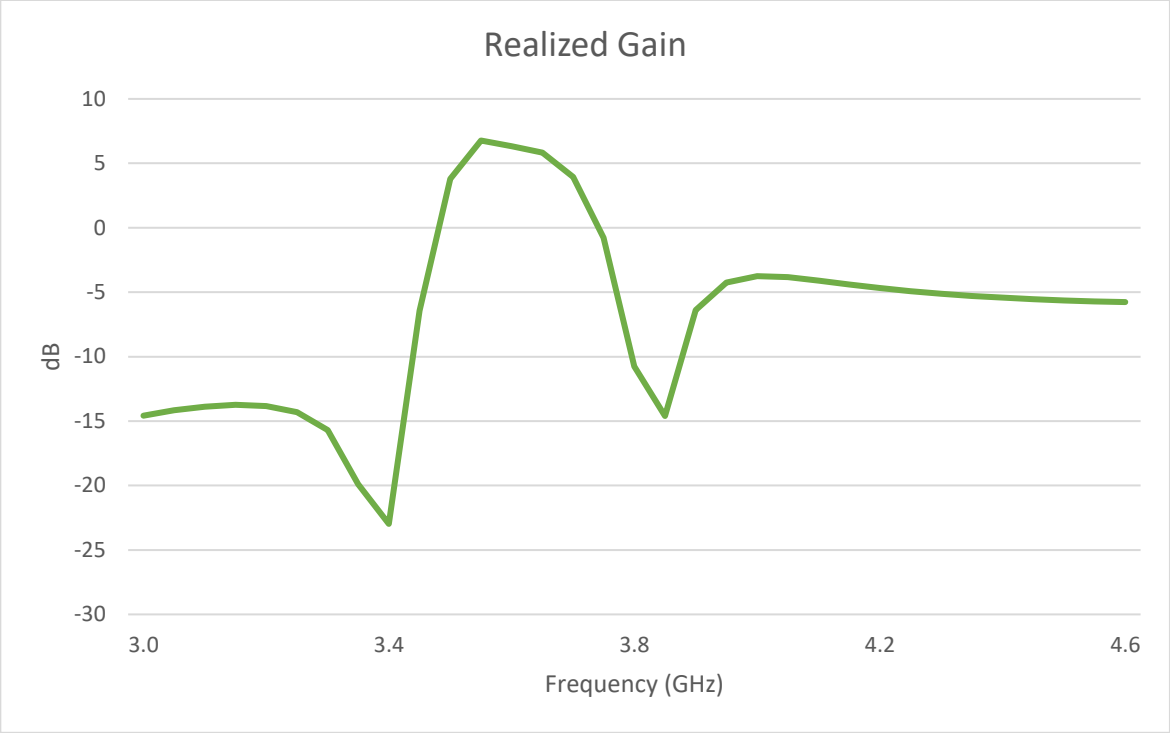

Figure 4-11 Realized gain of filtering RDRA with 3 posts.

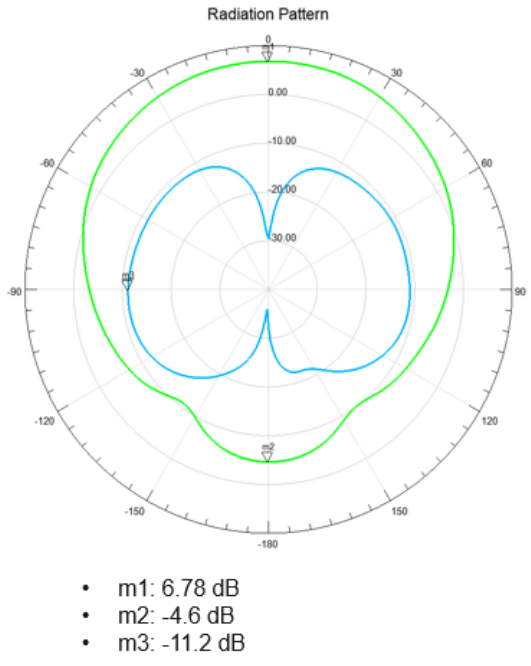

- m1: 6.78 dB
- m2: -4.6 dB
- m3: -11.2 dB

Figure 4-12 Gain radiation patterns of filtering RDRA at 3.6 GHz.

Design 2:

The structure of the filtering antenna is the same as design 1. The design parameters are shown in Figure 4-13. Since the dielectric constant is significantly higher (ε_r = 20), the structure is much more compact. As a result, tuning of the design is more difficult and there is limited range to adjust design variables. The return loss, realized gain, and radiation pattern are shown in Figures 4-14, 4-15, and 4-16, respectively. The center frequency is 3.6 GHz. The bandwidth is 60 MHz, which is much narrower comparing to design 1. Gain and realized gain are 4.85 dB.

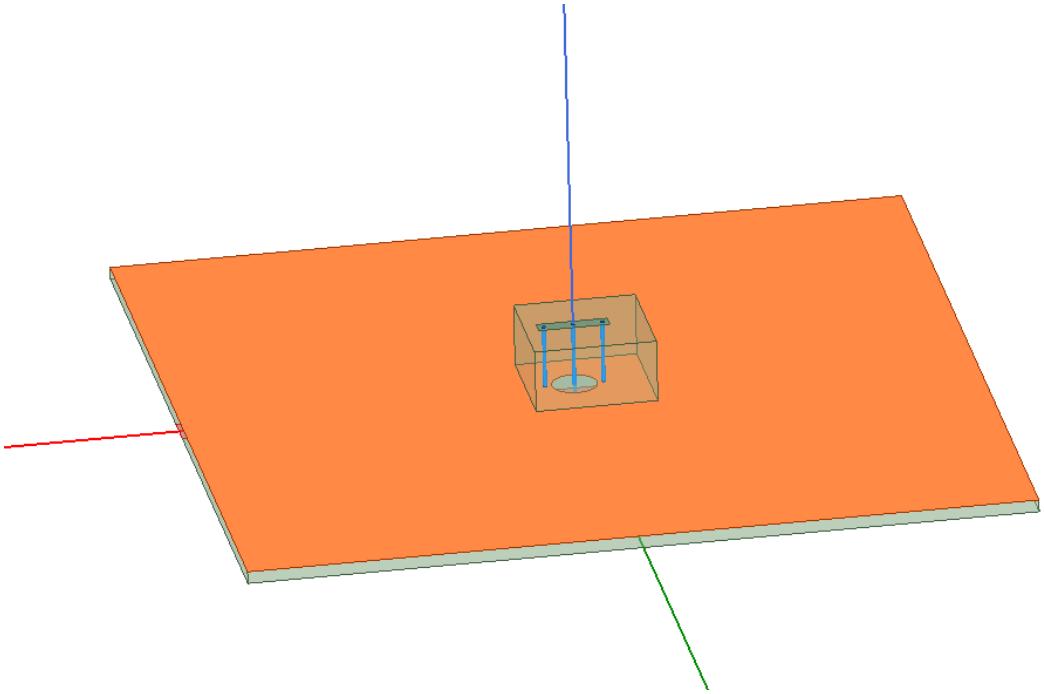

Figure 4-13 Design of filtering RDRA with 3 posts (s=100mm, t=1.57mm, Ls=63.182mm, ws=4.7mm and loff=1.52mm, ε_r=20, ε_{rs}=2.33, d= 5.8mm, dra_x=15.38mm,

dra_y=15.38mm, dra_z=8mm, pd=1.1954mm, strip_l= 9mm, strip_w=2mm, Dp_1=Dp_2=3.7mm)

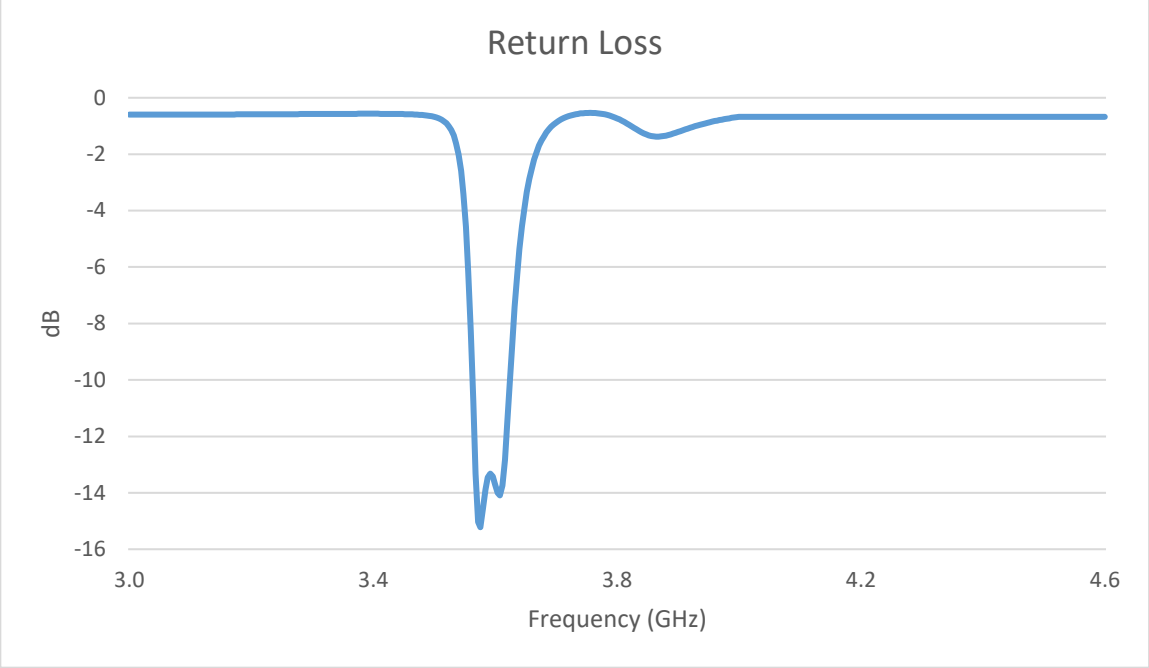

Figure 4-14 Return loss of linear polarized filtering RDRA with 3 posts.

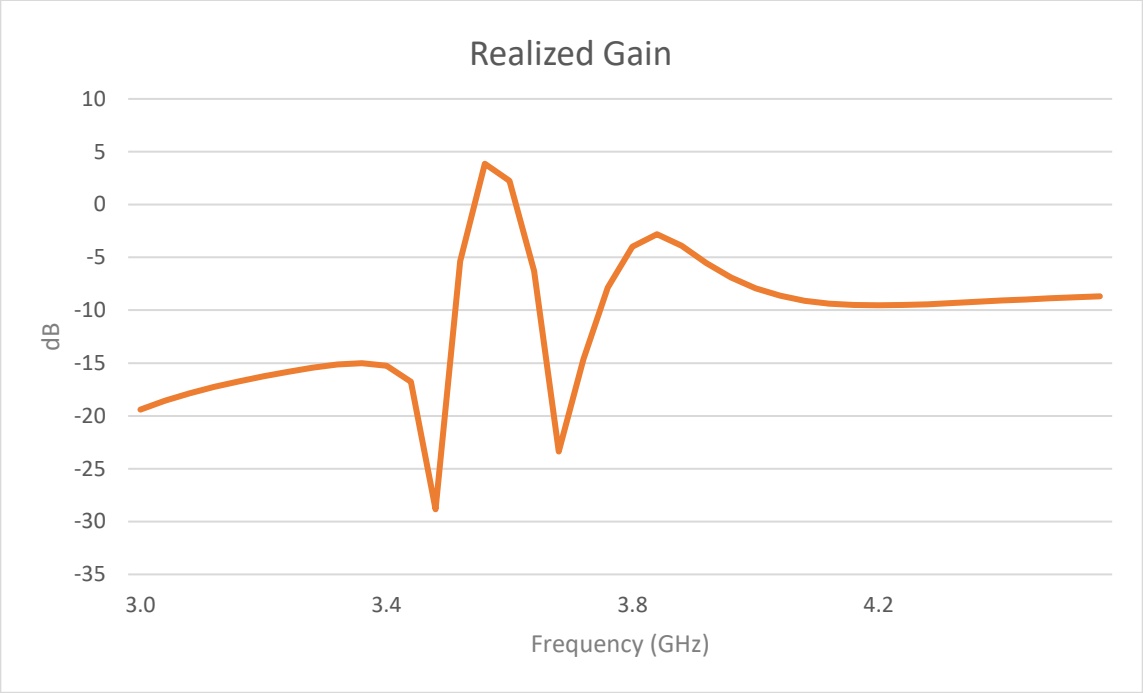

Figure 4-15 Realized gain of linear polarized filtering RDRA with 3 posts.

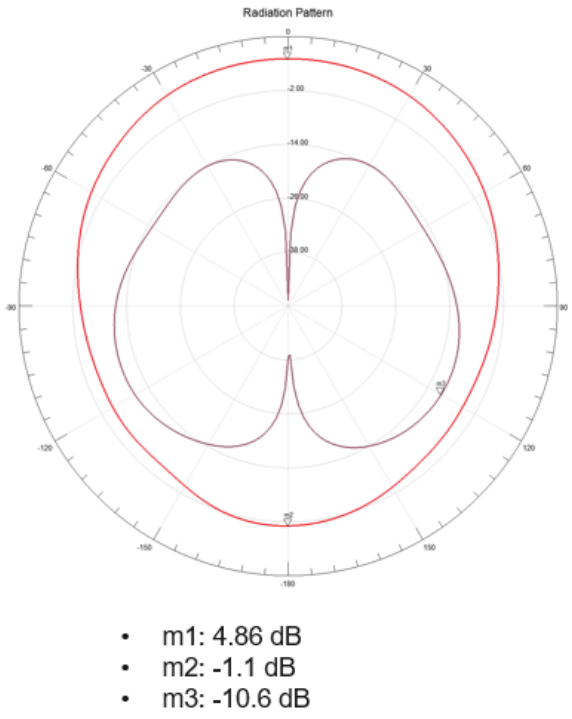

Figure 4-16 Gain radiation patterns of filtering RDRA at 3.6 GHz.

In this section, two designs of linearly polarized filtering RDRA designs are presented, which are based on radiation cancelation by the conducting loops inserted in the DRAs. The center frequencies for both designs are 3.6 GHz. Design 1, with DRA dielectric constant 10, can achieve a bandwidth of 200 MHz. Design 2, with DRA dielectric constant 20, has a much narrower bandwidth of 60 MHz, as a result of the high dielectric constant. The gain is also lower comparing to design 1.

4.2 Dual Polarized Filtering Rectangular DRA

In this section, the same concept and steps are applied to dual polarized filtering rectangular DRA. Frist a dual polarized RDRA with no filtering function is designed as shown in Figure 4-17. Posts are subsequently inserted to achieve the filtering antenna with dual polarizations.

In Figure 4-17, DRA is placed on the square ground plan with length *s*. The substrate has thickness *t* and substrate constant ε_{rs}. Rectangular slots are used to excite the dual polarized antenna. The distance between the center of the DRA and the center of square ground is offset by L_{off}. On the other side of the substrate, two 50 Ω microstrip lines are used to feed

the antenna with dual polarizations. The dielectric constant is 10 and the dielectric constant of the substrate is 2.33.

Simulation results are presented in Figures 4-18 to 4-22. Center frequency of the design is 3.6 GHz, and the bandwidth is 300 MHz. Gain is 5.32 dB.

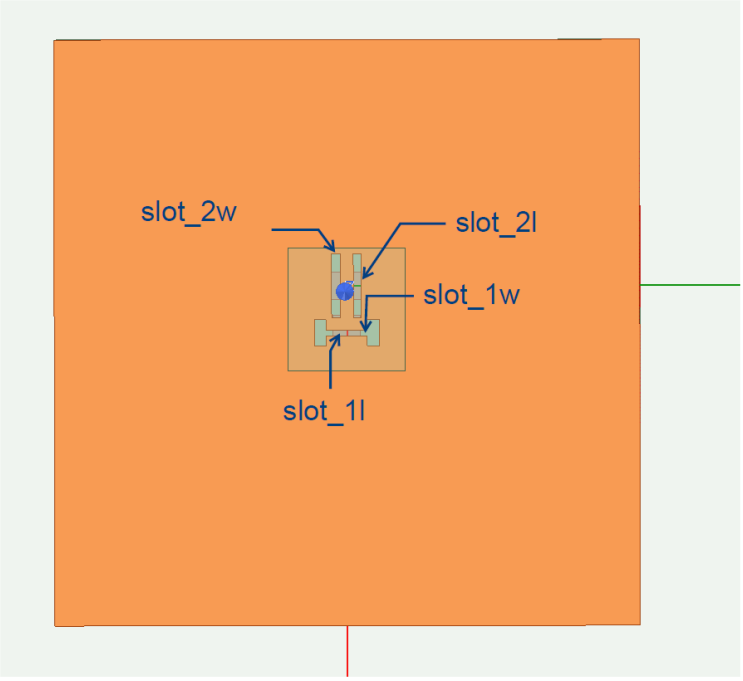

(a) Top view of RDRA

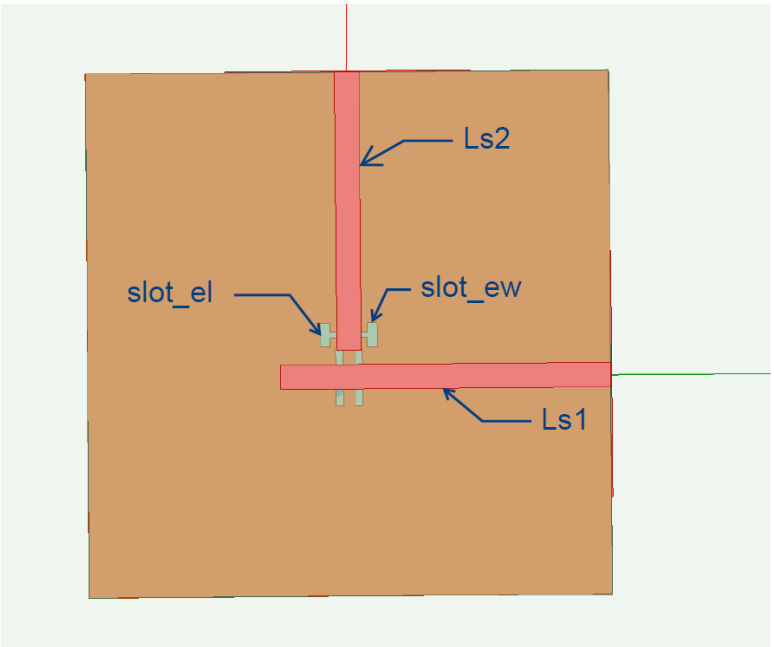

(b) Bottom view of RDRA

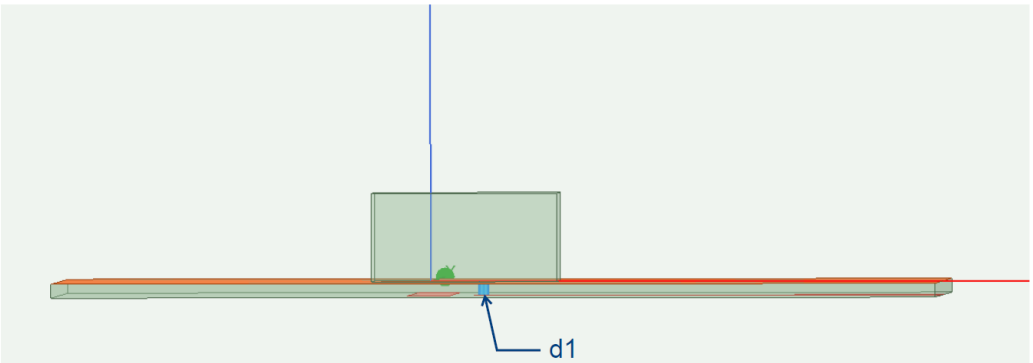

(c) Side view of filtering RDRA

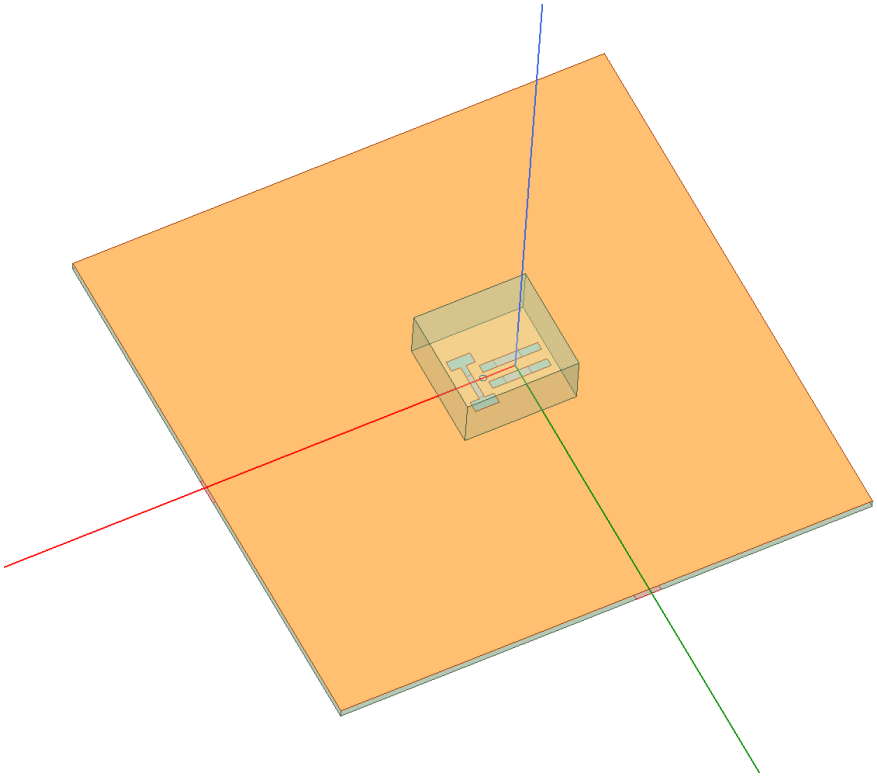

(c) Isometric view of filtering RDRA

Figure 4-17 Design of dual polarized RDRA(s=100mm, t=1.57mm, Ls2=53mm, Ls1= 63.1818mm, ws=4.7mm and loff=4mm, ε_r=10, ε_{rs}=2.33, pl=47mm, pw=10.99mm, dra_x=21mm, dra_y=20mm, dra_z=10mm, sl_1= 11mm, sl_1w=1mm, sl_2= 11mm, sl_2w= 1.5mm, sl_el=4.5mm, sl_ew=2mm)

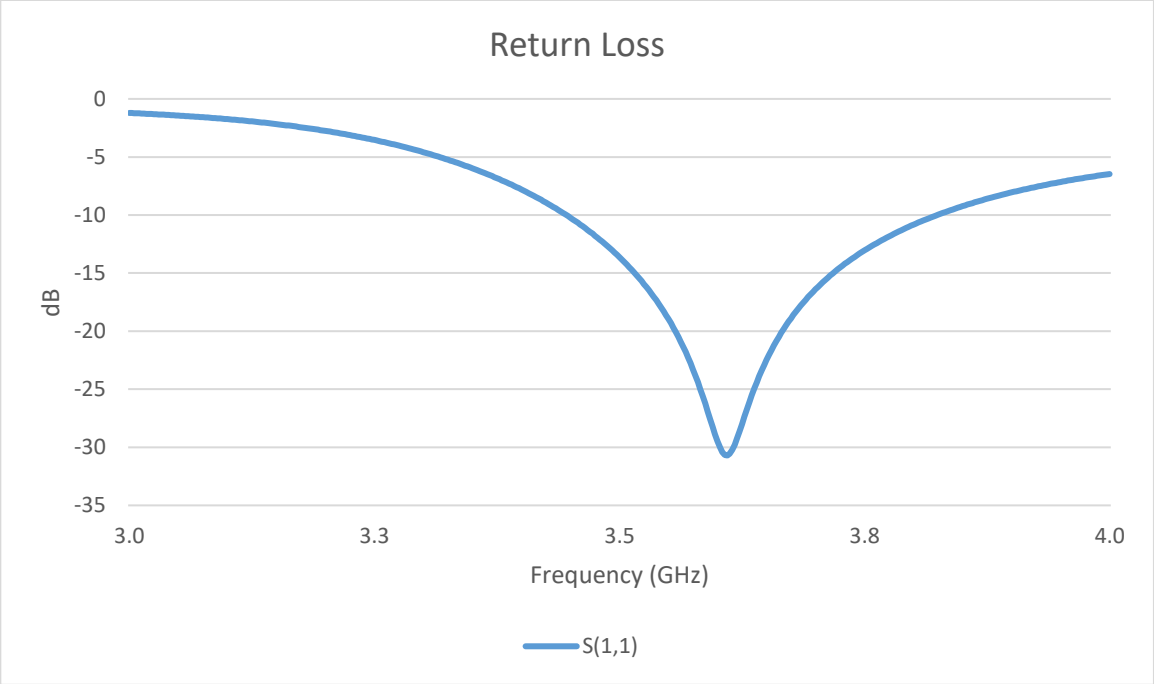

Figure 4-18 Return loss of filtering antenna port 1

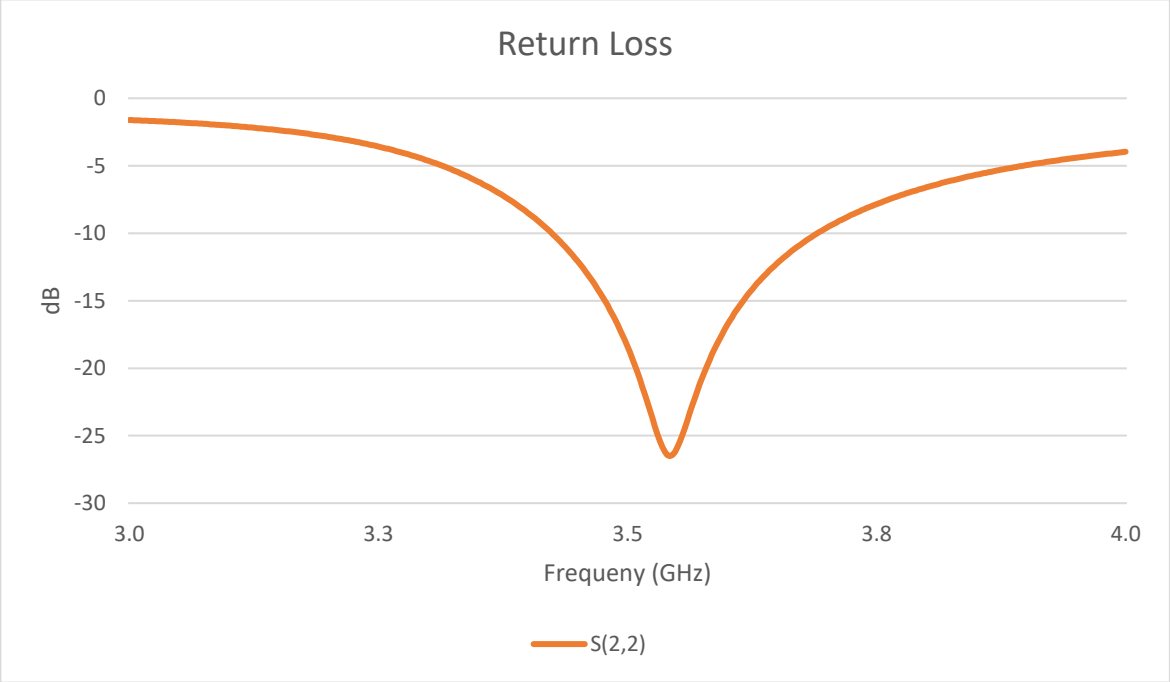

Figure 4-19 Return loss of filtering antenna port 2

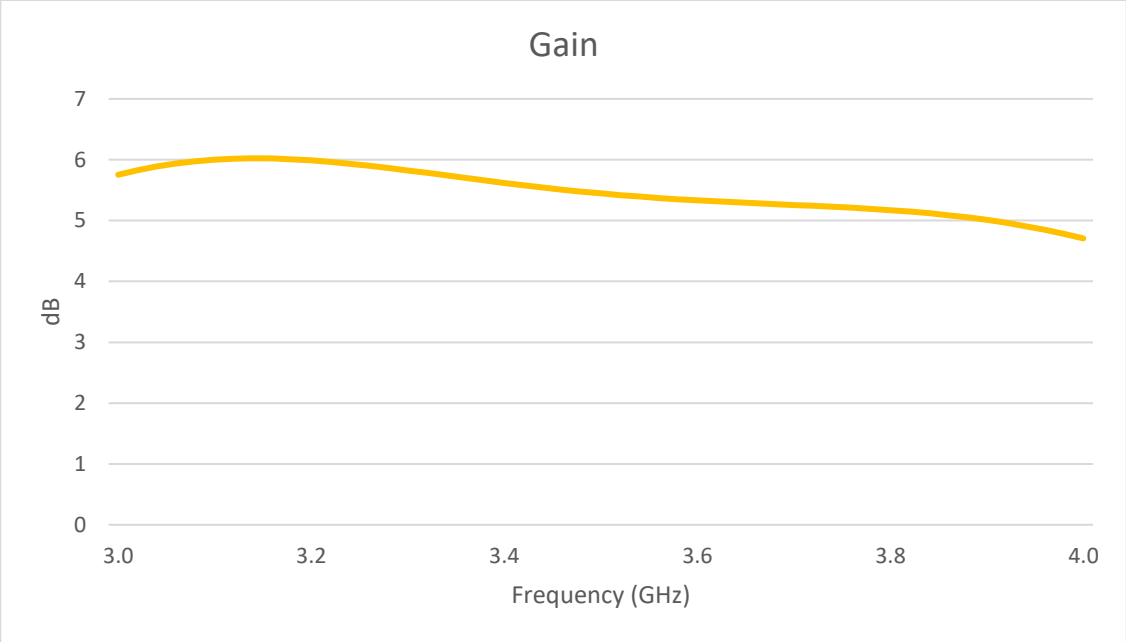

Figure 4-20 Gain of filtering antenna

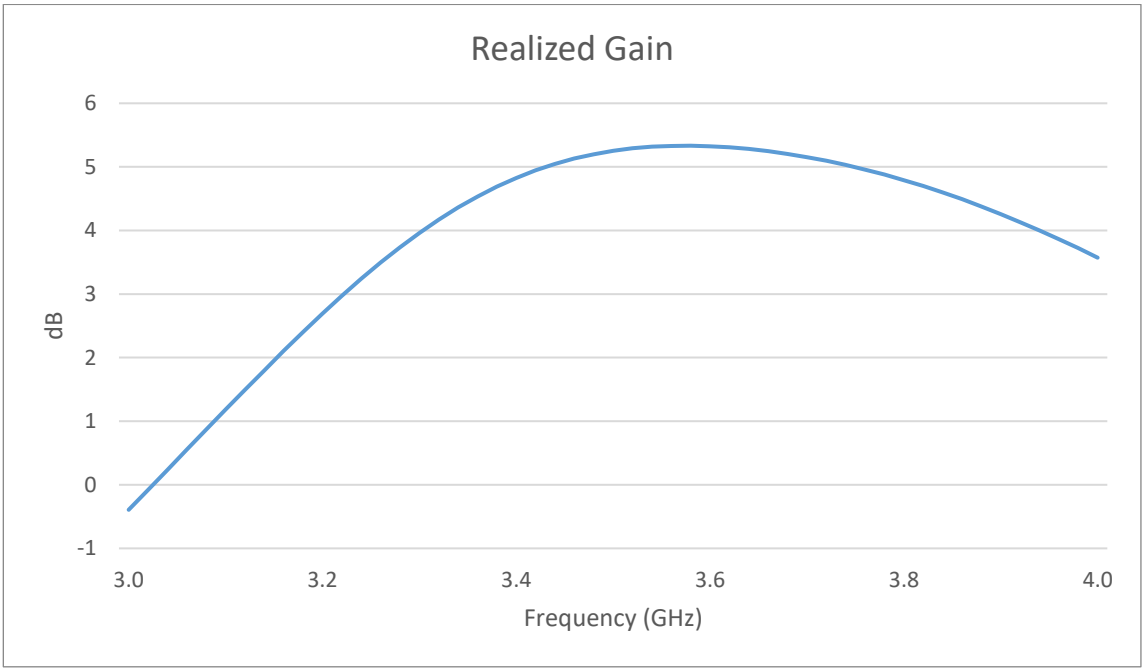

Figure 4-21 Realized gain of filtering antenna

Then dual polarized RDRA with filtering function is designed next. Similar method as in Section 4.1 is followed, using conducting posts and loops to achieve transmission zero. However, due to the complexity of the structure, the middle post is removed. As shown in Figure 4-23, there is only one loop for each polarization. Therefore, radiation nulls are only achieved on the lower side of the passband in the dual polarized filtering DRA.

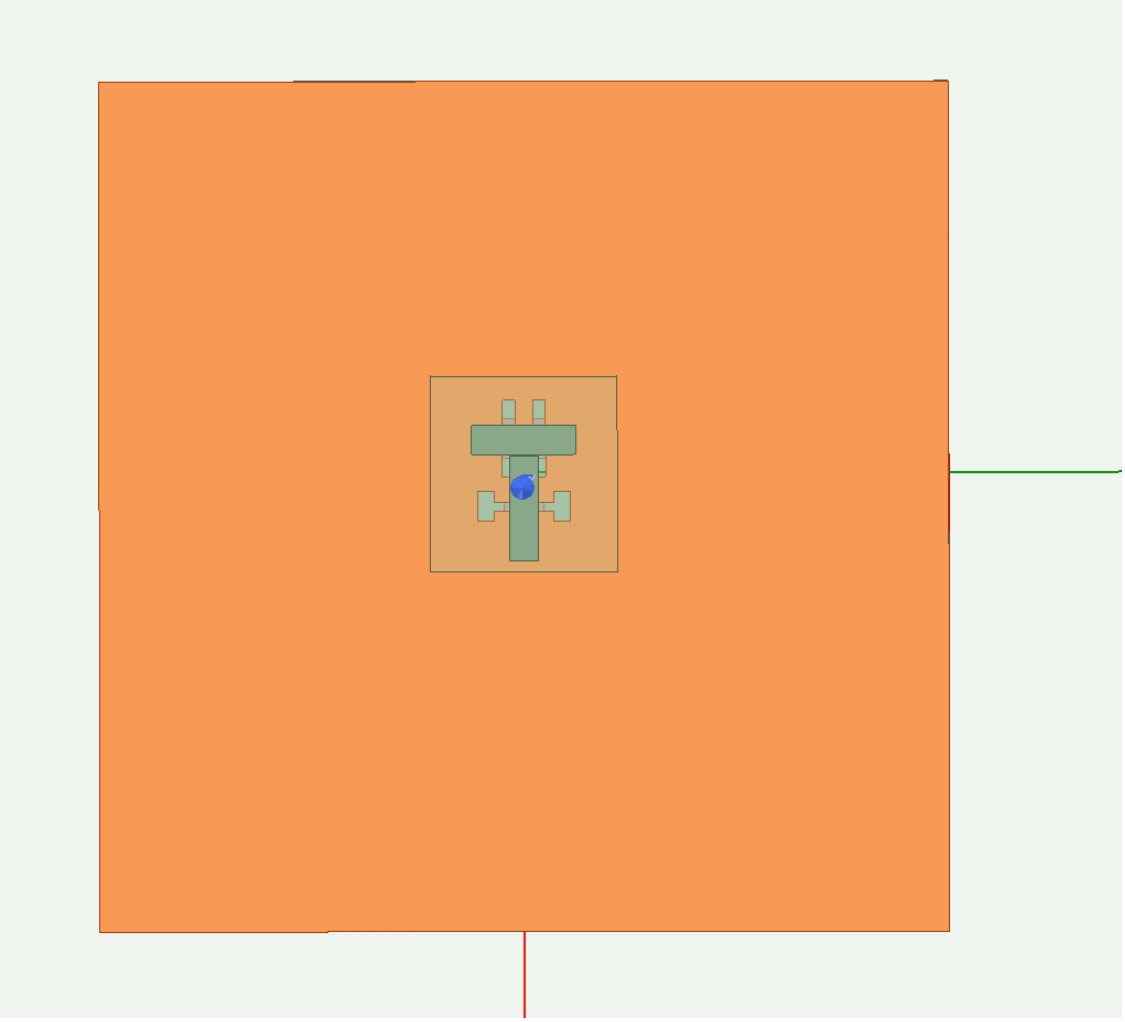

(a) Top view of filtering RDRA dual polarization

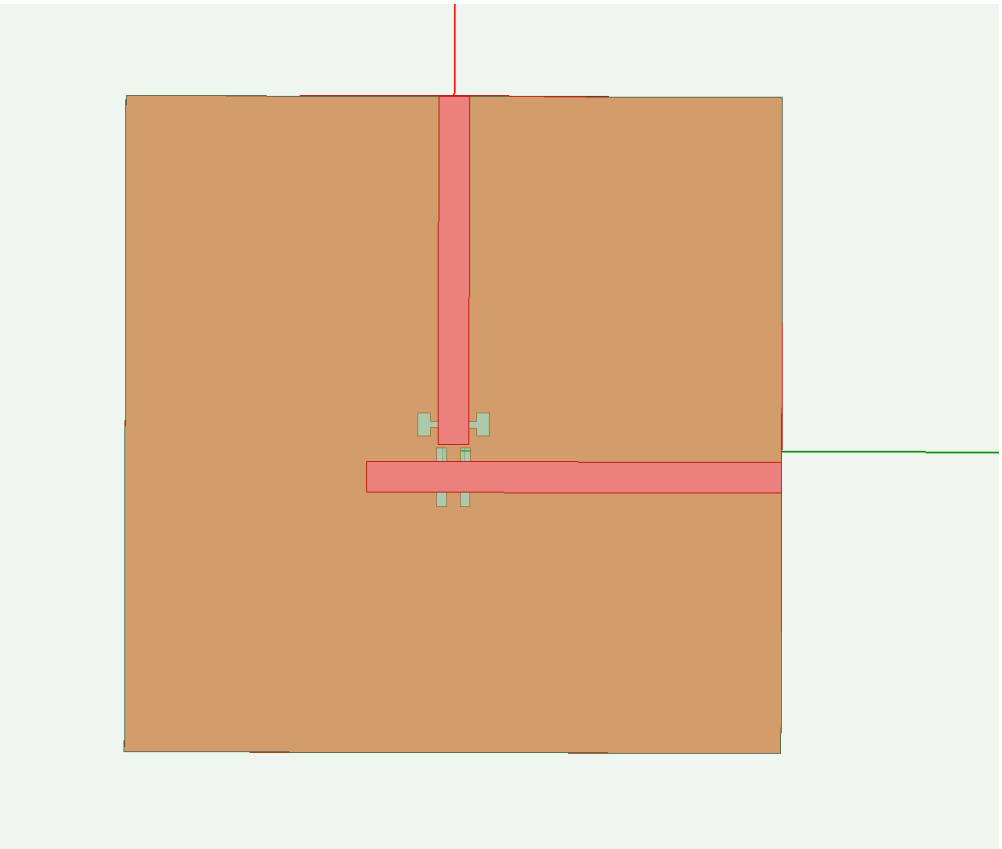

(b) Bottom view of filtering RDRA dual polarization

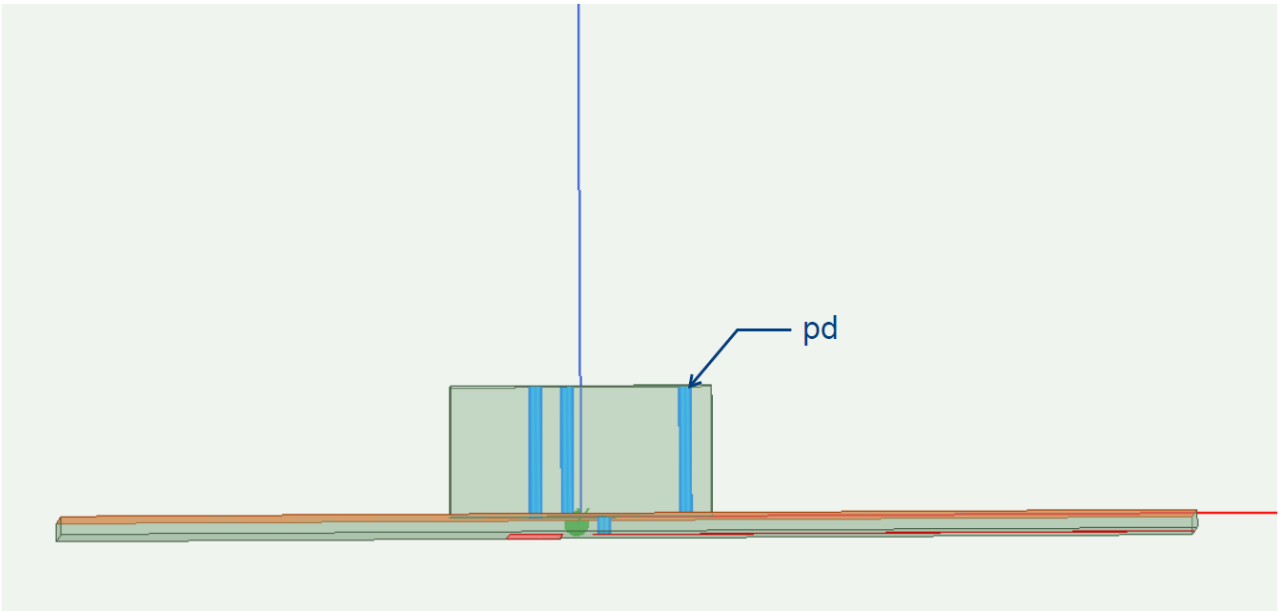

(c) Side view of filtering RDRA with no posts

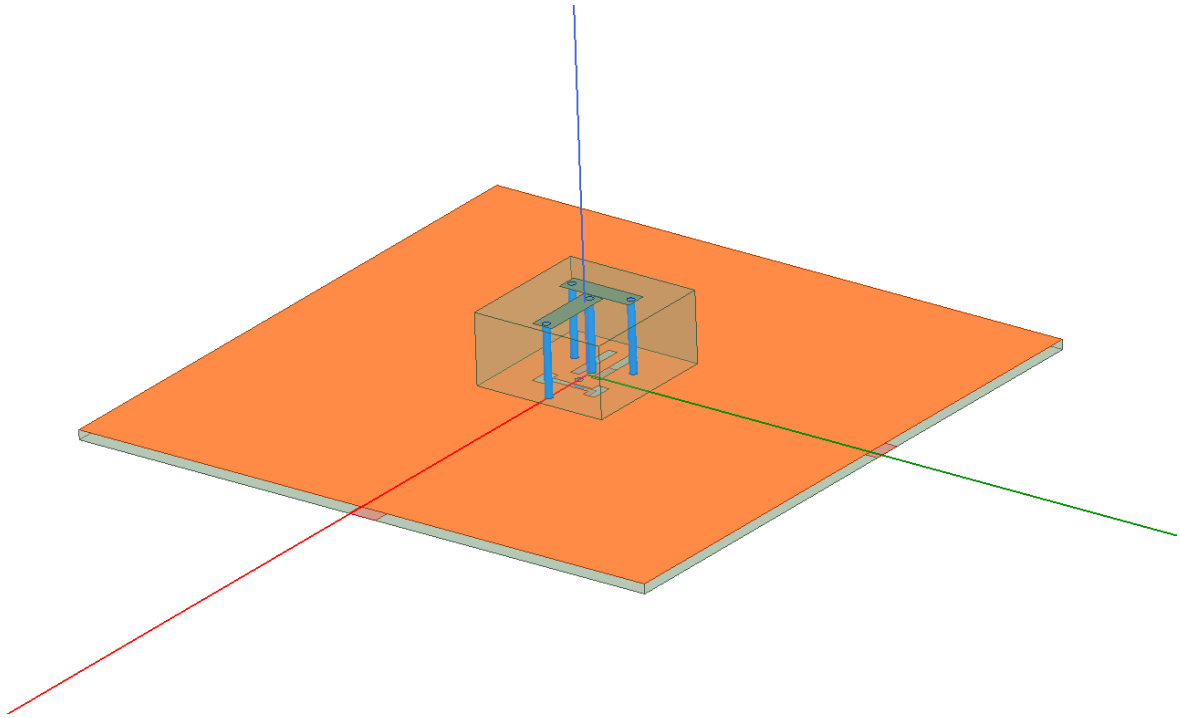

(d) Isometric view of filtering RDRA with no posts

Figure 4-22 Design of fileting RDRA dual polarization (s=100mm, t=1.57mm, Ls=53mm, ws=4.7mm and loff=4mm, ε_r=10, ε_{rs}=2.33, dra_x=23mm, dra_y=22mm, dra_z=11.46mm, sl_1= 11mm, sl_1w=1mm, sl_2= 9mm, sl_2w= 1.5mm, sl_el=3.5mm, sl_ew=2mm, strip_l=12.3mm, strip_w=3.4mm, pd =1.2mm, Dp_1 = Dp_2=5.2mm)

Parametric Study

Four different cases are studies in this section. Results of tuning the DRA height, slot lengths, and slot width are presented below.

In the first case, slot_1 length is 11 mm, slot_2 length is 9 mm, slot_2 width is 1.5 mm, slot_el length is 3.5 mm and slot_ew width is 2 mm, and the impact of varying DRA height is studied. The analysis is presented in Figure 4-23.

In the second case, DRA height is 23 mm, slot_2 length is 9 mm, slot_2 width is 2 mm, slot_e1 length is 3.5 mm and slot_ew width is 2 mm, and the impact of varying slot_1 length is analyzed in Figure 4-24.

In the third case, DRA height is 23 mm, slot _1 length is 11 mm slot_2 length is 9 mm, slot_2 width is 1.5 mm and slot_ew width is 2 mm, and the impact of varying slot_el length is shown in Figure 4-25.

In the last case, DRA height is 23 mm, slot _1 length is 11 mm slot_2 length is 9 mm, slot_2 width is 1.5 mm and slot_el length is 3.5 mm, and the impact of varying slot_ew width is shown in Figure 4-26.

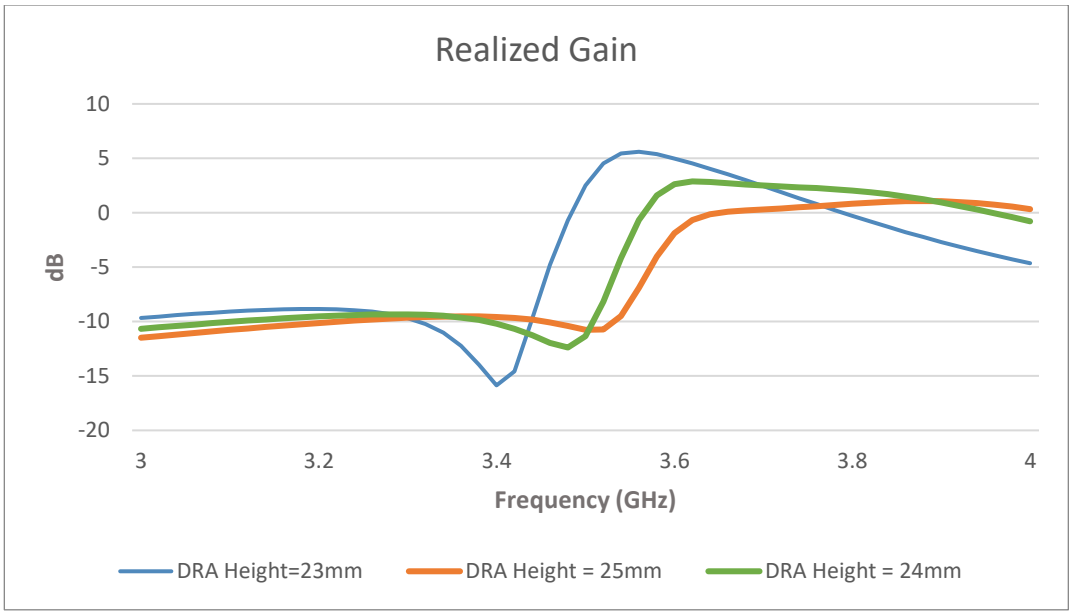

Figure 4-23 The impact of DRA height on realized gain, where slot_1 length is 11mm, slot_2 length is 9mm, slot_2 width is 1.5mm, slot_el length is 3.5mm and slot_ew width is 2mm

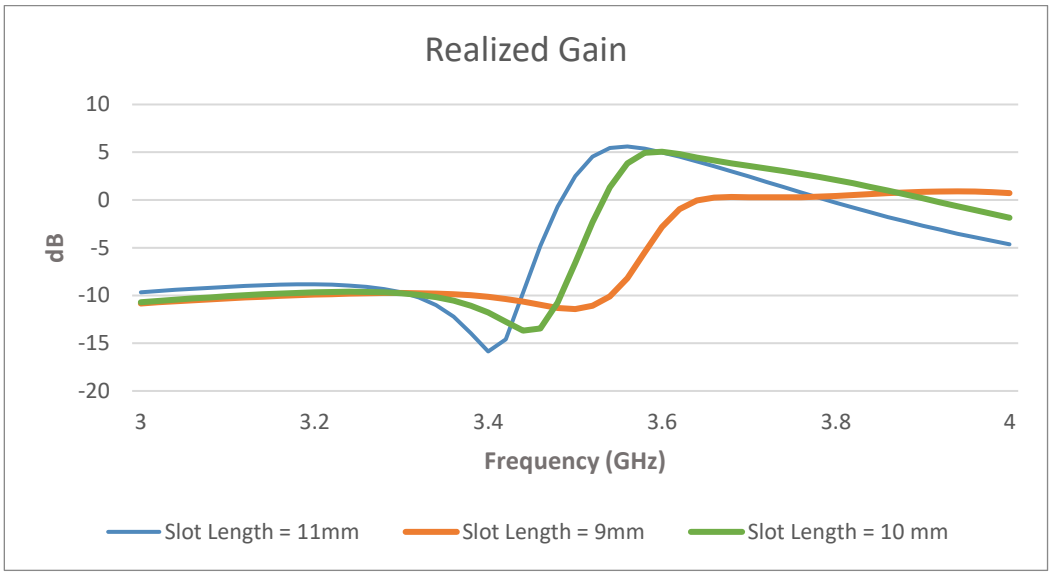

Figure 4-24 The impact of slot_1 length on realized gain, where slot_2 length is 9 mm, slot_2 width is 1.5mm, DRA height is 23mm, slot_el length is 3.5mm and slot_ew width is 2mm

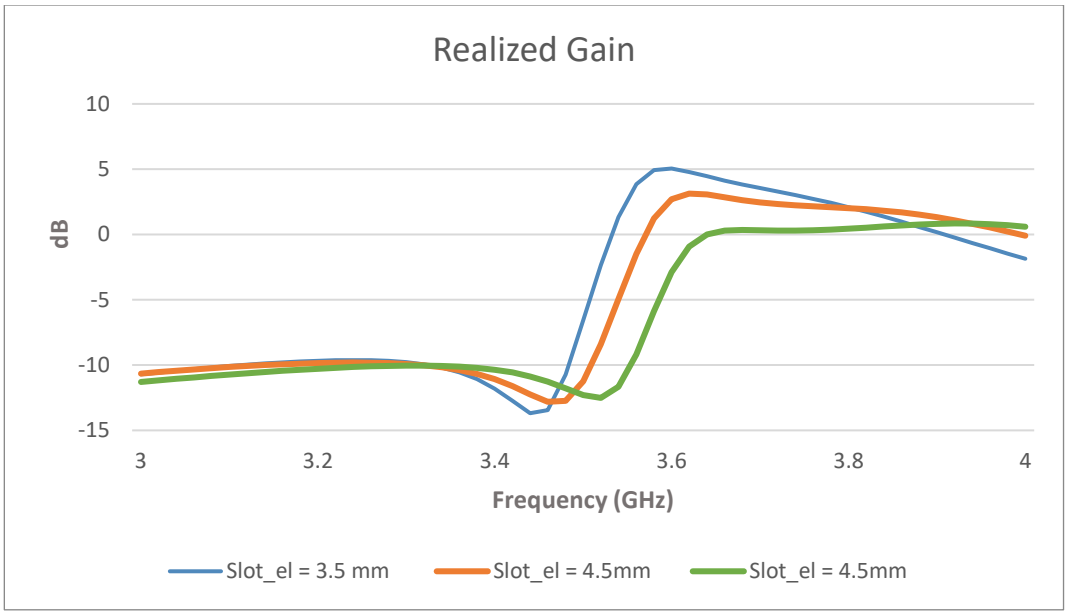

Figure 4-25 The impact of slot_el length on realized gain, where slot_1 length is 11 mm, slot_1 width is 2mm, DRA height is 23mm, slot_2 length is 9mm and slot_ew width is 2mm

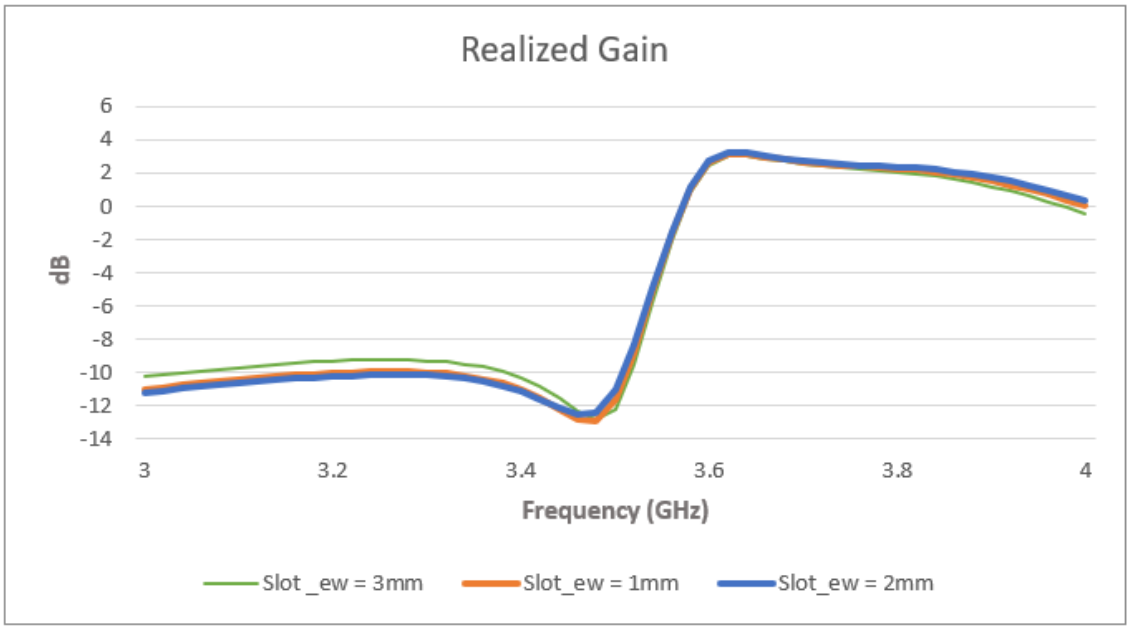

Figure 4-26 The impact of slot_ew width on realized, where slot_1 length is 11 mm, slot_1 width is 2mm, DRA height is 23mm, slot_2 length is 9mm and slot_el length is 3.5mm

Based on the parametric study, as DRA height increases, the transformer zero shifts upward. When slot length increases, the transformer zero shifts downwards. As slot_el increases, the transformer zero shifts upwards. As slot_ew increases, the realized gain barely changes. Therefore, to control the transmission zero, we need to tune DRA height and slot lengths.

Dual Polarized Filtering Antenna Example

After tuning the variables, the final dimensions are given in Figure 4-23. The dielectric constant of DRA is 10 and the dielectric constant of substrate is 2.33. The simulation results of the completed design are presented below in Figures 4-27 to 4-37. The center frequency of the design is 3.6 GHz and the bandwidth is 100 MHz. Good isolation is achieved, with greater than 24 dB isolation between two ports in Figure 4-29. The realized gain, gain, and radiation patterns when port 1 is excited are presented in Figures 4-30 to 4-33, showing a gain of 5.8 dB. Similar results are shown in Figures 4-34 to 4-37 when port 2 is excited.

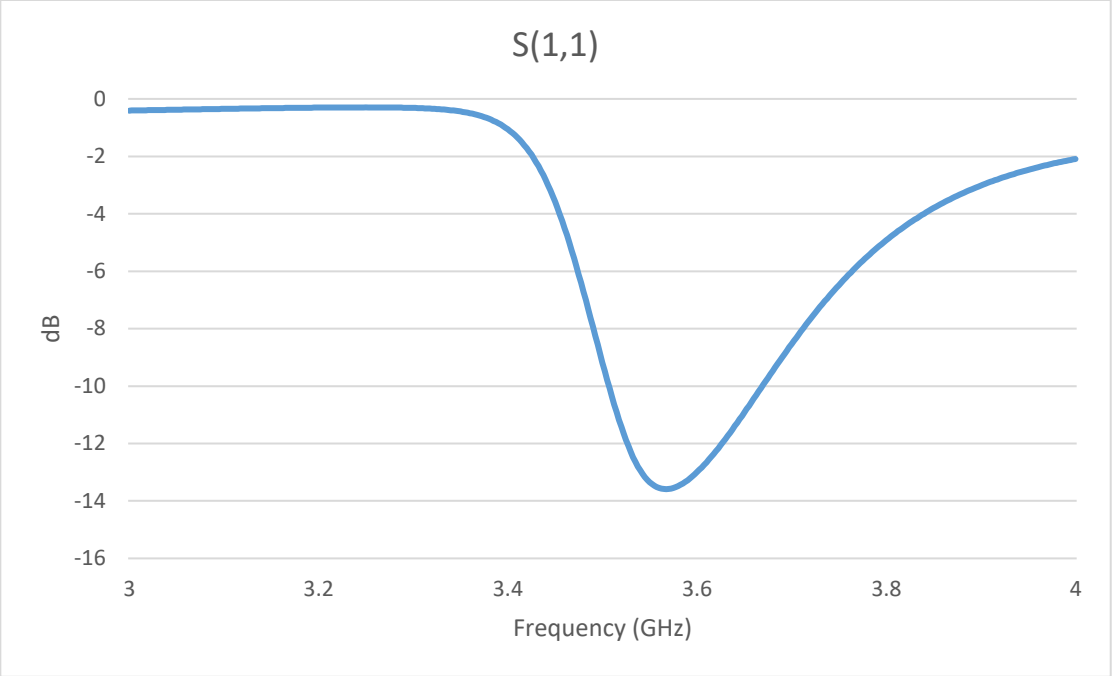

Figure 4-27 |S(1,1)| of dual polarized filtering antenna.

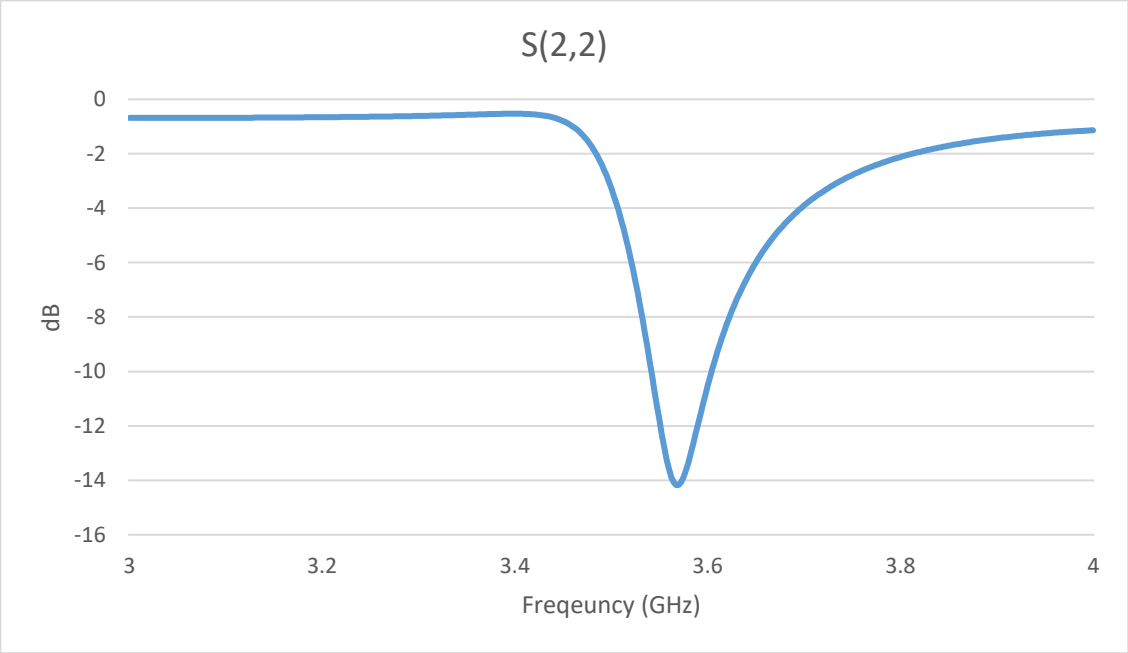

Figure 4-28 |S(2,2)| of dual polarized filtering antenna

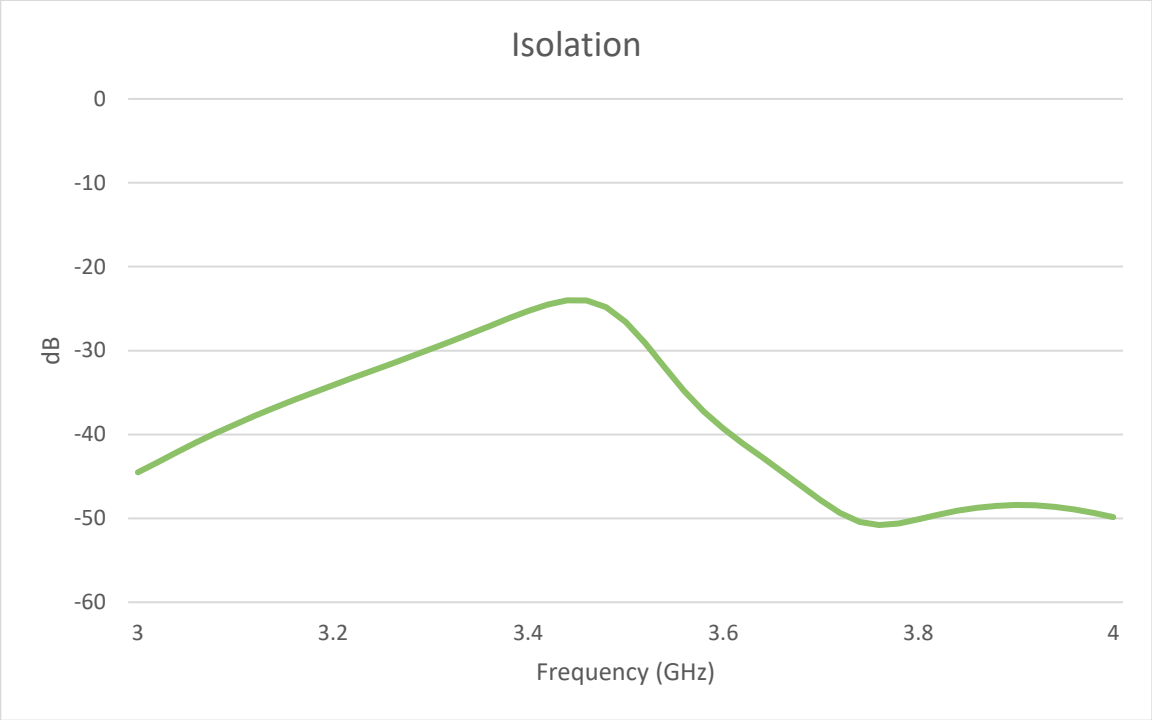

Figure 4-29 | S(2,1)| of dual polarized filtering antenna

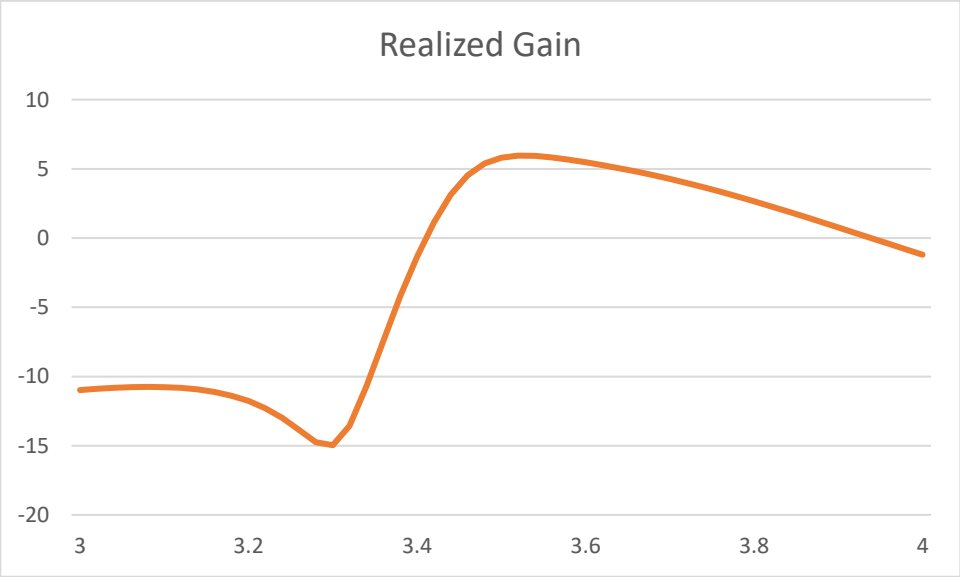

Figure 4-30 Realized Gain of dual polarized filtering antenna when Port 1 is excited

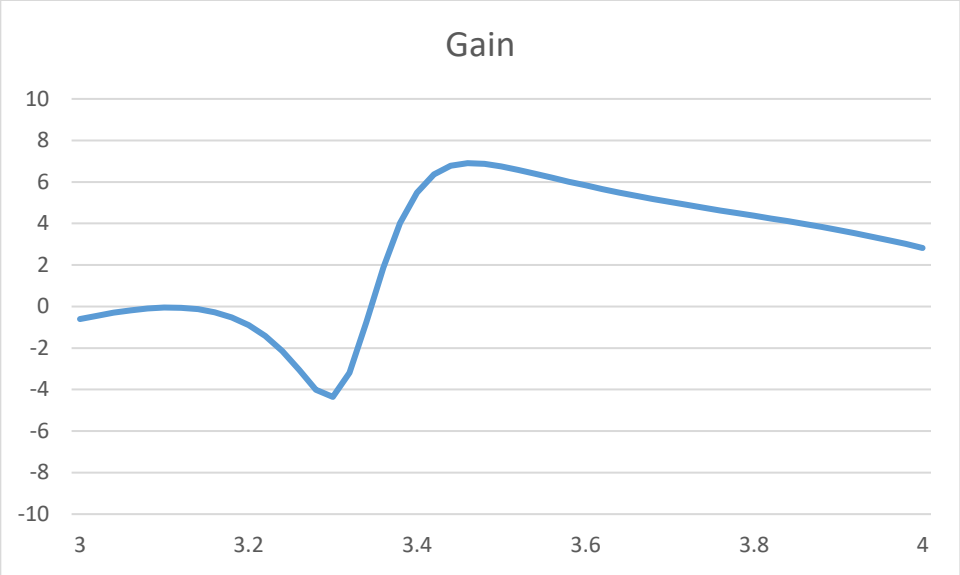

Figure 4-31 Gain of dual polarized filtering antenna when Port 1 is excited

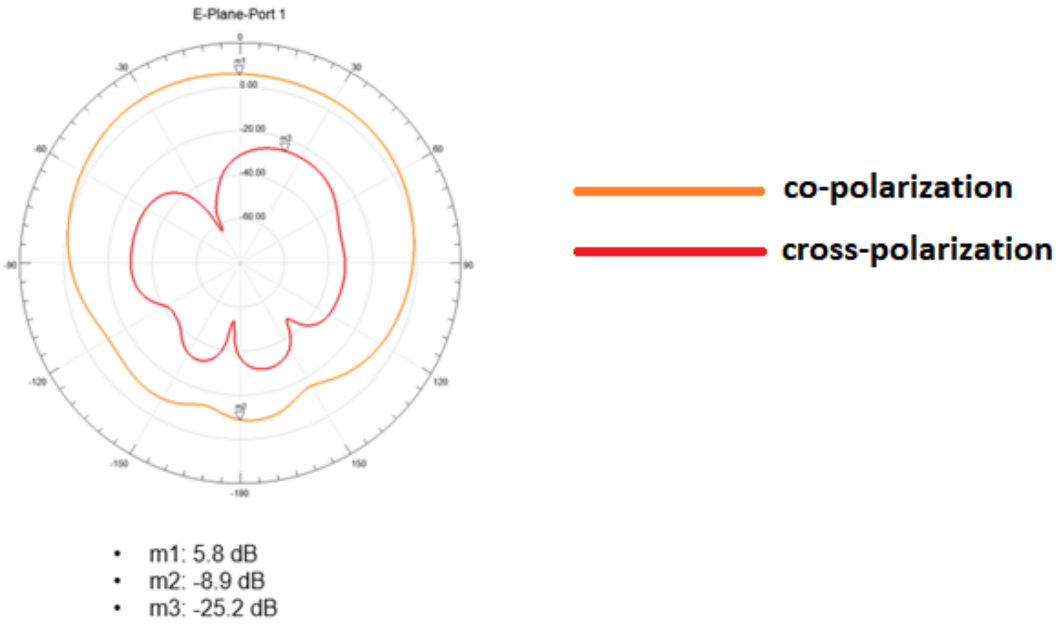

Figure 4-32 DR Filtering Antenna Radiation Pattern E-Plane when Port 1 is excited

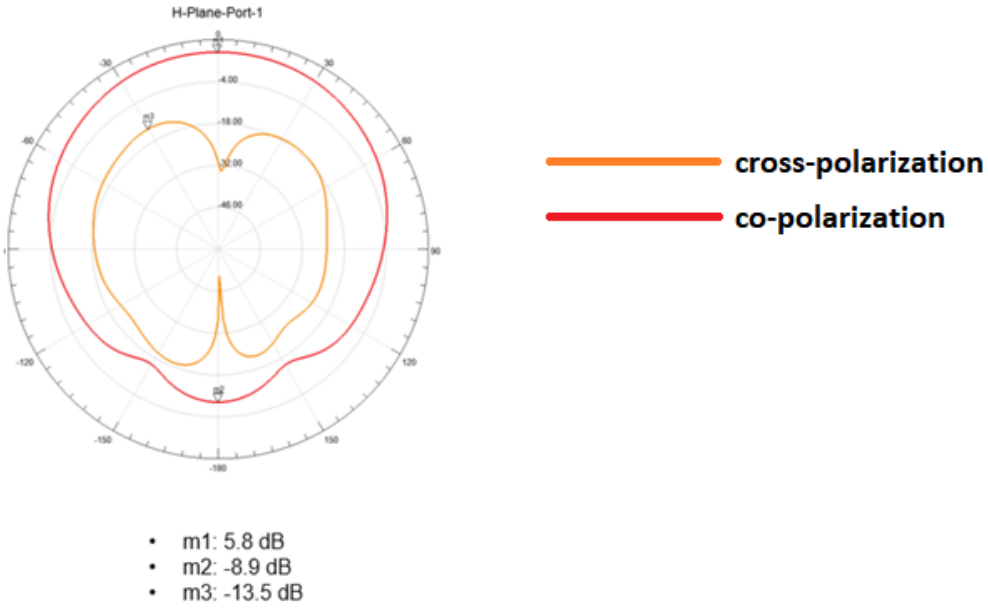

Figure 4-33 DR Filtering Antenna Radiation Pattern H-Plane when Port 1 is excited

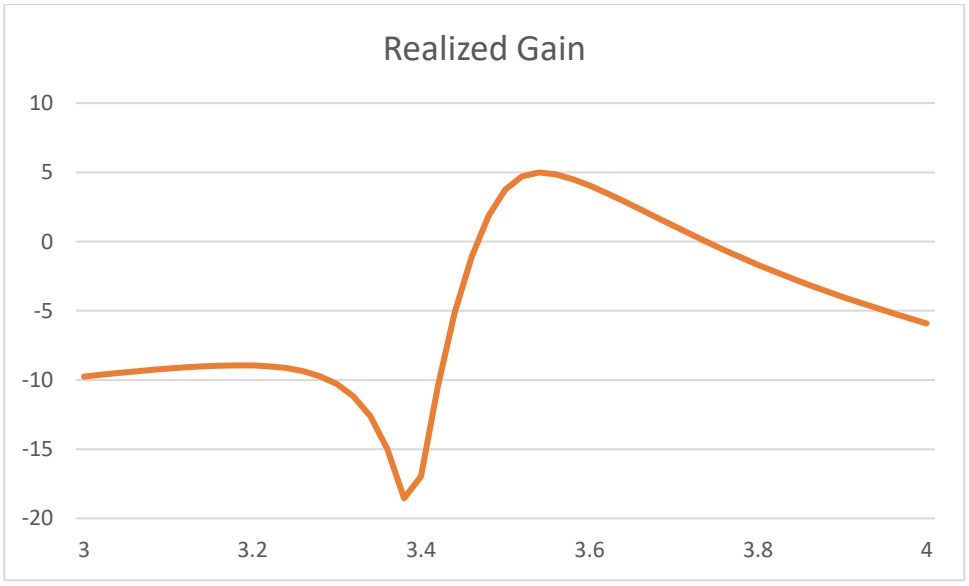

Figure 4-34 Realized Gain of dual polarized filtering antenna when Port 2 is excited

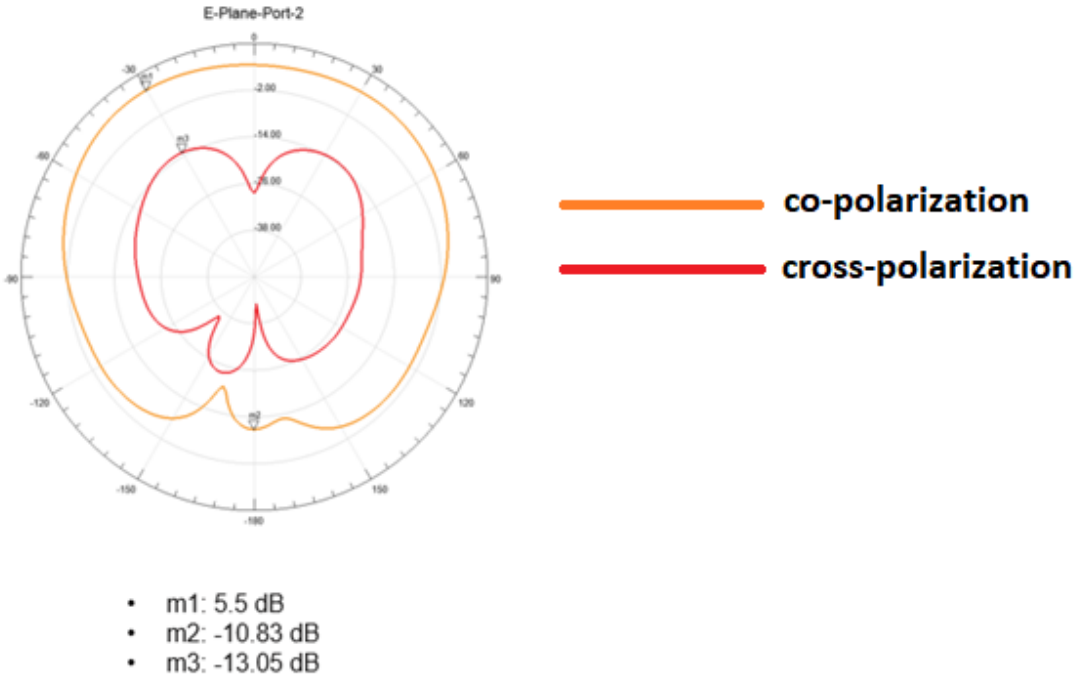

Figure 4-35 DR Filtering Antenna Radiation Pattern E-Plane when Port 2 is excited

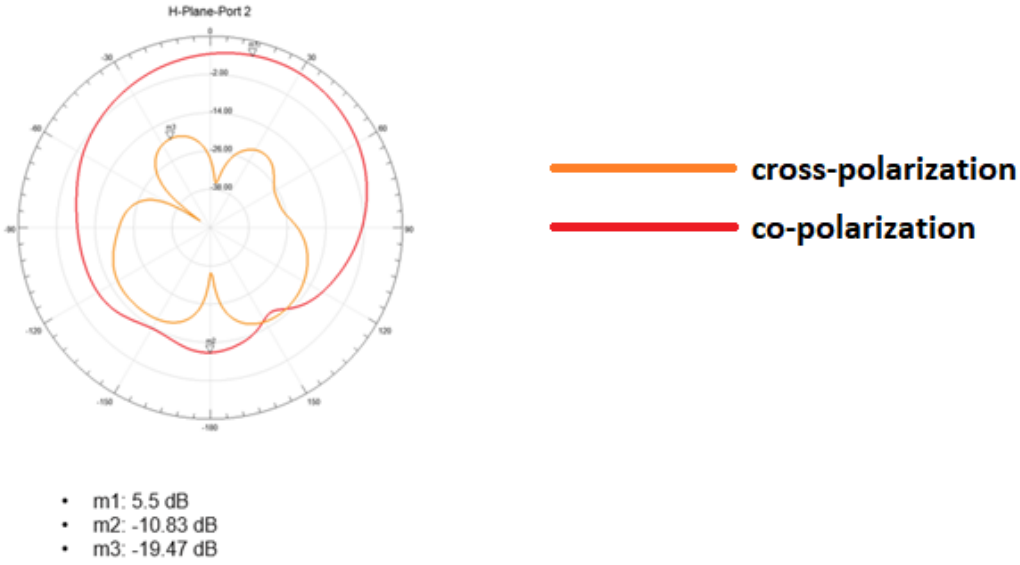

Figure 4-36 DR Filtering Antenna Radiation Pattern H-Plane when Port 2 is excited

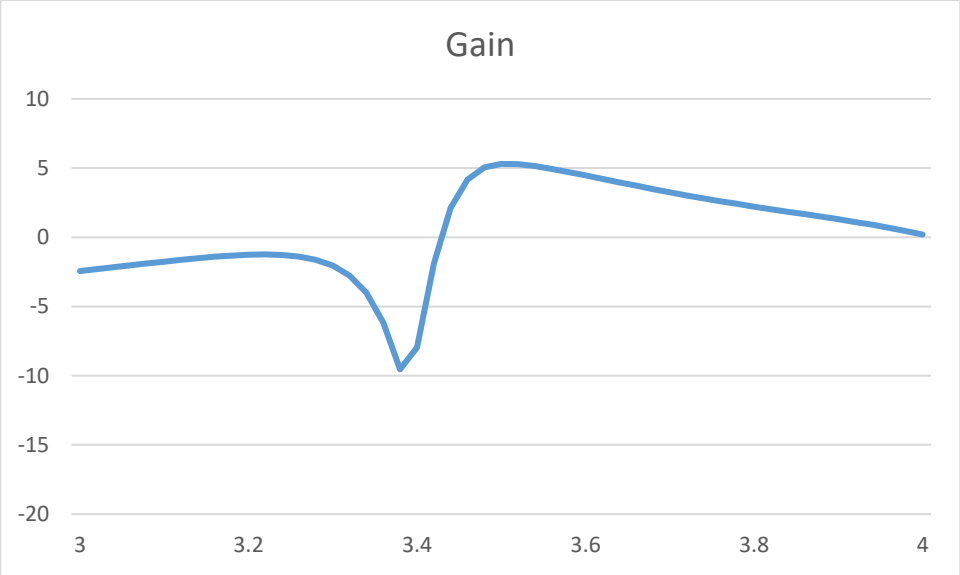

Figure 4-37 Gain of DR filtering antenna when Port 2 is excited

4.3 Summary

In this chapter, linearly polarized and dual polarized filtering antennas have been investigated using fusion method. First DRA antennas are designed. Then the filtering function is introduced by inserting conducting posts in the DRA antenna. Parametric studies are performed to study how transmission zeroes can be adjusted to realize different bandwidth. Both dielectric constant 10 and dielectric constant 20 are used in linearly polarized filter antennas. Due to the high Q factor, the bandwidth is narrow for dielectric constant of 20. Dual polarized filtering antenna is designed using dielectric constant of 10

only. Due to DRA size limitation, only transmission zeros below the passband are achieved for the dual polarized antenna.

In Chapter 3, filtering antenna is achieved by using the synthesis method. Filter and antenna are designed separately. Then last resonator of the filter is replaced by the antenna. The disadvantage is that the overall size is larger comparing to the fusion method due to the filter part of the structure. However, tuning of the responses are easier, and there is larger tuning range and more flexibilities for design parameters. In Chapter 4, fusion method has been applied to the filtering antenna. Instead of having combination of filter and antenna like in Chapter 3, a rectangular dielectric resonator with three posts can achieve filtering responses. The design is also easy to fabricate. However, the disadvantage are the limitation to the achievable bandwidth and the difficulty in tuning due to the size of the DRA and the structural complexity. Design of dual polarization is shown to be even more challenging.

Chapter 5

Conclusion and Future Work

This thesis focuses on different methods of realizing filtering antenna using rectangular dielectric resonator antenna (DRA). Both synthesis method and fusion method have been applied to the designs.

In the filter antenna integration method, high dielectric constant material is used for compact design, which results in narrow bandwidth. The emphasis is on controlling and increasing the antenna bandwidth. Four designs of DRA to increase bandwidth have been proposed. Low dielectric constant posts are inserted in DRA in different orientations. Parametric studies have been performed, showing that the bandwidth can be readily controlled by adjusting DRA height and post radius. An integrated design of DRA with a 3-pole waveguide filter shows that, after inserting an air post in the antenna, the bandwidth is increased to 300 MHz, which is significantly higher than the design without air post of 200 MHz bandwidth.

Fusion method is also considered in this thesis to design the filtering antenna using rectangular DRA. Instead of combining a filter and an antenna, the fusion method focuses on the modification of the antenna and does not require additional filtering circuits. Conducting posts are inserted in the DRA to realize radiation cancelation. Transmission zeros, which results in filtering responses, have been achieved for both linear polarization and dual polarizations. Simulation results and parametric studies are presented. The

advantage of fusion method is the compact size. However, the complexity of the structure limits the bandwidth and tuning range.

The following future work can be investigated:

- Fabrication and measurement of both DR filtering antenna designs can be performed.
- For the fusion method, method to achieve wider bandwidth can be explored, especially for high dielectric constant materials.
- Investigation can be carried out to implement dual polarized filtering antenna design with transmission zeros above the passband that is easy to fabricate.

Appendices

Appendix A. Figure Reprint Permissions

Thesis / Dissertation Reuse
The IEEE does not require individuals working on a thesis to obtain a formal reuse license, however, you may print out this statement to be used as a permission grant:

Requirements to be followed when using any portion (e.g., figure, graph, table, or textual material) of an IEEE copyrighted paper in a thesis:

1) In the case of textual material (e.g., using short quotes or referring to the work within these papers) users must give full credit to the original source (author, paper, publication) followed by the IEEE copyright line © 2011 IEEE.
2) In the case of illustrations or tabular material, we require that the copyright line © [Year of original publication] IEEE appear prominently with each reprinted figure and/or table.
3) If a substantial portion of the original paper is to be used, and if you are not the senior author, also obtain the senior author's approval.

Requirements to be followed when using an entire IEEE copyrighted paper in a thesis:

1) The following IEEE copyright/ credit notice should be placed prominently in the references: © [year of original publication] IEEE. Reprinted, with permission, from [author names, paper title, IEEE publication title, and month/year of publication]
2) Only the accepted version of an IEEE copyrighted paper can be used when posting the paper or your thesis on-line.
3) In placing the thesis on the author's university website, please display the following message in a prominent place on the website: In reference to IEEE copyrighted material which is used with permission in this thesis, the IEEE does not endorse any of [university/educational entity's name goes here]'s products or services. Internal or personal use of this material is permitted. If interested in reprinting/republishing IEEE copyrighted material for advertising or promotional purposes or for creating new collective works for resale or redistribution, please go to http://www.ieee.org/publications_standards/publications/rights/rights_link.html to learn how to obtain a License from RightsLink.

If applicable, University Microfilms and/or ProQuest Library, or the Archives of Canada may supply single copies of the dissertation.

Bibliography

[1] W. -J. Wu, Y. -Z. Yin, S. -L. Zuo, Z. -Y. Zhang and J. -J. Xie, "A New Compact Filter-Antenna for Modern Wireless Communication Systems," in *IEEE Antennas and Wireless Propagation Letters*, vol. 10, pp. 1131-1134, 2011.

[2] A. X. Chen, F. Zhao, L. Yan and W. Zhang, "A compact filtering antenna with flat gain response within the passband", *IEEE Antennas Wireless Propag. Lett.*, vol. 12, pp. 857-860, 2013.

[3] D. Yang, H. Zhai, C. Guo and H. Li, "A Compact Single-Layer Wideband Microstrip Antenna With Filtering Performance," *in IEEE Antennas and Wireless Propagation Letters*, vol. 19, no. 5, pp. 801-805, May 2020.

[4] W.A. Edson, "Microwave filters using ghost-mode resonance," *Proc. IRE*, vol. 19, pp. 2, 1961.

[5] S. Long, M. McAllister and Liang Shen, "The resonant cylindrical dielectric cavity antenna," in *IEEE Transactions on Antennas and Propagation*, vol. 31, no. 3, pp. 406-412, May 1983.

[6] K. W. Leung, E. H. Lim and X. S. Fang, "Dielectric Resonator Antennas: From the Basic to the Aesthetic," in Proceedings of the IEEE, vol. 100, no. 7, pp. 2181-2193, July 2012.

[7] S. Chaudhuri, M. Mishra, R. S. Kshetrimayum, R. K. Sonkar, H. Chel and V. K. Singh, "Rectangular DRA Array for 24 GHz ISM-Band Applications," in *IEEE Antennas and Wireless Propagation Letters*, vol. 19, no. 9, pp. 1501-1505, Sept. 2020.

[8] Z. Chen et al., "Millimeter-Wave Rectangular Dielectric Resonator Antenna Array With Enlarged DRA Dimensions, Wideband Capability, and High-Gain Performance," in *IEEE Transactions on Antennas and Propagation*, vol. 68, no. 4, pp. 3271-3276, April 2020.

[9] Y. M. Pan, K. W. Leung and K. Lu, "Study of Resonant Modes in Rectangular Dielectric Resonator Antenna Based on Radar Cross Section," in *IEEE Transactions on Antennas and Propagation*, vol. 67, no. 6, pp. 4200-4205, June 2019.

[10] Z. Chen and H. Wong, "Wideband Glass and Liquid Cylindrical Dielectric Resonator Antenna for Pattern Reconfigurable Design," in *IEEE Transactions on Antennas and Propagation*, vol. 65, no. 5, pp. 2157-2164, May 2017.

[11] A. Tadjalli, A. Sebak and T. Denidni, "Modes of elliptical cylinder dielectric resonator and its resonant frequencies," *IEEE Antennas and Propagation Society Symposium*, 2004., Monterey, CA, USA, 2004, pp. 2039-2042 Vol.2.

[12] C. . -E. Zebiri et al., "Offset Aperture-Coupled Double-Cylinder Dielectric Resonator Antenna With Extended Wideband," in *IEEE Transactions on Antennas and Propagation*, vol. 65, no. 10, pp. 5617-5622, Oct. 2017

[13] M. Khalily, M. R. Kamarudin and M. H. Jamaluddin, "A Novel Square Dielectric Resonator Antenna With Two Unequal Inclined Slits for Wideband Circular Polarization," in *IEEE Antennas and Wireless Propagation Letters*, vol. 12, pp. 1256-1259, 2013.

[14] A. Khalajmehrabadi, M. K. A. Rahim, N. A. Murad and M. R. Kamarudin, "Square circular polarized dielectric resonator antenna with a rotated notch," *2012 6th*

European Conference on Antennas and Propagation (EUCAP), Prague, Czech Republic, 2012, pp. 2819-2822.

[15] M. Yang, Y. Pan and W. Yang, "A Singly Fed Wideband Circularly Polarized Dielectric Resonator Antenna," in *IEEE Antennas and Wireless Propagation Letters*, vol. 17, no. 8, pp. 1515-1518, Aug. 2018.

[16] Basile et al., "Design and Manufacturing of Super-Shaped Dielectric Resonator Antennas for 5G Applications Using Stereolithography," in *IEEE Access*, vol. 8, pp. 82929-82937, 2020.

[17] M. Simeoni, R. Cicchetti, A. Yarovoy and D. Caratelli, "Plastic-Based Supershaped Dielectric Resonator Antennas for Wide-Band Applications," in *IEEE Transactions on Antennas and Propagation*, vol. 59, no. 12, pp. 4820-4825, Dec. 2011.

[18] M. Simeoni, R. Cicchetti, A. Yarovoy and D. Caratelli, "Supershaped dielectric resonator antennas," *2009 IEEE Antennas and Propagation Society International Symposium*, North Charleston, SC, USA, 2009, pp. 1-4.

[19] A. Petosa, *Dielectric Resonator Antenna Handbook*, Norwood, MA: Artech House, 2007.

[20] R. D. Gupta and M. S. Parihar, "Differentially Fed Wideband Rectangular DRA With High Gain Using Short Horn," in IEEE Antennas and Wireless Propagation Letters, vol. 16, pp. 1804-1807, 2017.

[21] B. Ghosh, D. Bhattacharya, P. D. Sinha and D. H. Werner, "Design of Circular Waveguide Annular Slot-Coupled Two-Layer DRA for Linear and Circular Polarizations," in *IEEE Antennas and Wireless Propagation Letters*, vol. 19, no. 6, pp. 1012-1016, June 2020.

[22] K. W. Leung and K. K. So, "Rectangular waveguide excitation of dielectric resonator antenna", *IEEE Trans. Antennas Propag.*, vol. 51, no. 9, pp. 2477-2481, Sep. 2003.

[23] K. W. Leung, H. Y. Lo, K. K. So and K. M. Luk, "High-permittivity dielectric resonator antenna excited by a rectangular waveguide", *Microw. Opt. Technol. Lett.*, vol. 34, no. 3, pp. 157-158, Aug. 2002.

[24] A. Rashidian, M. Tayfeh Aligodarz, L. Shafai and D. M. Klymyshyn, "On the Matching of Microstrip-Fed Dielectric Resonator Antennas," in *IEEE Transactions on Antennas and Propagation*, vol. 61, no. 10, pp. 5291-5296, Oct. 2013.

[25] S. -J. Guo, L. -S. Wu, K. W. Leung and J. -F. Mao, "Microstrip-Fed Differential Dielectric Resonator Antenna and Array," in *IEEE Antennas and Wireless Propagation Letters*, vol. 17, no. 9, pp. 1736-1739, Sept. 2018.

[26] B. Rana and S. K. Parui, "Microstrip Line Fed Wideband Circularly-Polarized Dielectric Resonator Antenna Array for Microwave Image Sensing," in *IEEE Sensors Letters*, vol. 1, no. 3, pp. 1-4, June 2017, Art no. 3500604.

[27] R. Chair, S. L. S. Yang, A. A. Kishk, Kai Fong Lee and Kwai Man Luk, "Aperture fed wideband circularly polarized rectangular stair shaped dielectric resonator antenna," in *IEEE Transactions on Antennas and Propagation*, vol. 54, no. 4, pp. 1350-1352, April 2006.

[28] R. Chair, A. A. Kishk, K. F. Lee and C. E. Smith, "Broadband aperture coupled flipped staired pyramid and conical dielectric resonator antennas," *IEEE Antennas and Propagation Society Symposium*, 2004., Monterey, CA, USA, 2004, pp. 1375-1378 Vol.2.

[29] A. H. Majeed, A. S. Abdullah, F. Elmegri, K. H. Sayidmarie, R. A. Abd-Alhameed and J. M. Noras, "Aperture-Coupled Asymmetric Dielectric Resonators Antenna for Wideband Applications," in *IEEE Antennas and Wireless Propagation Letters,* vol. 13, pp. 927-930, 2014.

[30] A. B. Kakade and B. Ghosh, "Mode Excitation in the Coaxial Probe Coupled Three-Layer Hemispherical Dielectric Resonator Antenna," in *IEEE Transactions on Antennas and Propagation,* vol. 59, no. 12, pp. 4463-4469, Dec. 2011.

[31] I. A. Eshrah, A. A. Kishk, A. B. Yakovlev and A. W. Glisson, "Excitation of dielectric resonator antennas by a waveguide probe: modeling technique and wide-band design," in *IEEE Transactions on Antennas and Propagation*, vol. 53, no. 3, pp. 1028-1037, March 2005.

[32] H. -C. Li, D. -S. La and C. Zhang, "Wide-/Dual-Band Omnidirectional Dielectric Resonator Antenna with Filtering Function," 2021 IEEE 4th International Conference on Electronic Information and Communication Technology (ICEICT), Xi'an, China, 2021, pp. 369-372.

[33] W. M. Abdel Wahab, D. Busuioc and S. Safavi-Naeini, "Low Cost Planar Waveguide Technology-Based Dielectric Resonator Antenna (DRA) for Millimeter-Wave Applications: Analysis, Design, and Fabrication," in *IEEE Transactions on Antennas and Propagation,* vol. 58, no. 8, pp. 2499-2507, Aug. 2010.

[34] C. X. Mao, Y. Zhang, X. Y. Zhang, P. Xiao, Y. Wang and S. Gao, "Filtering Antennas: Design Methods and Recent Developments," in *IEEE Microwave Magazine*, vol. 22, no. 11, pp. 52-63, Nov. 2021.

[35] H. Cheng, Y. Yusuf and X. Gong, "Vertically Integrated Three-Pole Filter/Antennas for Array Applications," in *IEEE Antennas and Wireless Propagation Letters*, vol. 10, pp. 278-281, 2011.

[36] M. M. Fakharian, P. Rezaei, A. A. Orouji and M. Soltanpur, "A Wideband and Reconfigurable Filtering Slot Antenna," in *IEEE Antennas and Wireless Propagation Letters*, vol. 15, pp. 1610-1613, 2016.

[37] Y. Yusuf, H. Cheng and X. Gong, "A Seamless Integration of 3-D Vertical Filters With Highly Efficient Slot Antennas," in *IEEE Transactions on Antennas and Propagation*, vol. 59, no. 11, pp. 4016-4022, Nov. 2011.

[38] H. Tang, C. Tong and J.-X. Chen, "Differential dual-polarized filtering dielectric resonator antenna", *IEEE Trans. Antennas Propag.*, vol. 66, no. 8, pp. 4298-4302, Aug. 2018.

[39] H. Chu, H. Hong, X. Zhu, P. Li and Y. -X. Guo, "Implementation of Synthetic Material in Dielectric Resonator-Based Filtering Antennas," in *IEEE Transactions on Antennas and Propagation*, vol. 66, no. 7, pp. 3690-3695, July 2018.

[40] L. Li and G. Liu, "A Differential Microstrip Antenna With Filtering Response," in *IEEE Antennas and Wireless Propagation Letters*, vol. 15, pp. 1983-1986, 2016.

[41] C. -Y. Hsieh, C. -H. Wu and T. -G. Ma, "A Compact Dual-Band Filtering Patch Antenna Using Step Impedance Resonators," in *IEEE Antennas and Wireless Propagation Letters*, vol. 14, pp. 1056-1059, 2015.

[42] C. -K. Lin and S. -J. Chung, "A compact edge-fed filtering microstrip antenna with 0.2 dB equal-ripple response," *2009 European Microwave Conference (EuMC)*, Rome, Italy, 2009, pp. 378-380.

[43] Y. Yusuf and X. Gong, "Compact Low-Loss Integration of High- Q 3-D Filters With Highly Efficient Antennas," in *IEEE Transactions on Microwave Theory and Techniques*, vol. 59, no. 4, pp. 857-865, April 2011.

[44] Z.Maqsood, "Compact integrated designs of microwave filters and antennas with dual-polarization," Electronic Thesis and Dissertations [1428], Ontario Tech University, 2021.

[45] W. Duan, X. Y. Zhang, Y. -M. Pan, J. -X. Xu and Q. Xue, "Dual-Polarized Filtering Antenna With High Selectivity and Low Cross Polarization," in *IEEE Transactions on Antennas and Propagation*, vol. 64, no. 10, pp. 4188-4196, Oct. 2016.

[46] S. J. Yang, Y. F. Cao, Y. M. Pan, Y. Wu, H. Hu and X. Y. Zhang, "Balun-Fed Dual-Polarized Broadband Filtering Antenna Without Extra Filtering Structure," in *IEEE Antennas and Wireless Propagation Letters*, vol. 19, no. 4, pp. 656-660, April 2020.

[47] C. X. Zhao, Y. M. Pan and G. D. Su, "Design of Filtering Dielectric Resonator Antenna Arrays Using Simple Feeding Networks," in *IEEE Transactions on Antennas and Propagation*, vol. 70, no. 8, pp. 7252-7257, Aug. 2022.

[48] P. Sarkar, R. Ghatak, M. Pal and D. R. Poddar, "Compact UWB Bandpass Filter With Dual Notch Bands Using Open Circuited Stubs," in *IEEE Microwave and Wireless Components Letters*, vol. 22, no. 9, pp. 453-455, Sept. 2012.

[49] C. F. Ding, X. Y. Zhang, Y. Zhang, Y. M. Pan and Q. Xue, "Compact Broadband Dual-Polarized Filtering Dipole Antenna With High Selectivity for Base-Station Applications," in *IEEE Transactions on Antennas and Propagation*, vol. 66, no. 11, pp. 5747-5756, Nov. 2018.

[50] J. Wu, Z. Zhao, Z. Nie and Q. -H. Liu, "A Printed Unidirectional Antenna With Improved Upper Band-Edge Selectivity Using a Parasitic Loop," in *IEEE Transactions on Antennas and Propagation*, vol. 63, no. 4, pp. 1832-1837, April 2015.

[51] P. F. Hu, Y. M. Pan, X. Y. Zhang and S. Y. Zheng, "A Compact Filtering Dielectric Resonator Antenna With Wide Bandwidth and High Gain," in *IEEE Transactions on Antennas and Propagation*, vol. 64, no. 8, pp. 3645-3651, Aug. 2016.

[52] X. Y. Zhang, W. Duan and Y.-M. Pan, "High-gain filtering patch antenna without extra circuit", *IEEE Trans. Antennas Propag.*, vol. 63, no. 12, pp. 5883-5888, Dec. 2015.

[53] Sewoong Kwon, Byoung Moo Lee, Young Joong Yoon, Woo Young Song and Jong-Gwan Yook, "A harmonic suppression antenna for an active integrated antenna," in *IEEE Microwave and Wireless Components Letters*, vol. 13, no. 2, pp. 54-56, Feb. 2003.

[54] F. J. Huang, T. C. Yo, C. M. Lee and C. H. Luo, "Design of circular polarization antenna with harmonic suppression for rectenna application", *IEEE Antenna Wireless Propag. Lett.*, vol. 11, pp. 592-595, 2012.

[55] Q. X. Chu, C. X. Mao and H. Zhu, "A compact notched band UWB slot antenna with sharp selectivity and controllable bandwidth", *IEEE Trans. Antennas Propag.*, vol. 61, no. 8, pp. 3961-3966, Aug. 2013.

[56] Y. M. Pan, P. F. Hu, K. W. Leung and X. Y. Zhang, "Compact Single-/Dual-Polarized Filtering Dielectric Resonator Antennas," in *IEEE Transactions on Antennas and Propagation*, vol. 66, no. 9, pp. 4474-4484, Sept. 2018.

[57] Y. -T. Liu, K. W. Leung, J. Ren and Y. -X. Sun, "Linearly and Circularly Polarized Filtering Dielectric Resonator Antennas," in *IEEE Transactions on Antennas and Propagation*, vol. 67, no. 6, pp. 3629-3640, June 2019.

[58] H. I. Kremer, K. W. Leung and M. W. K. Lee, "Compact Wideband Low-Profile Single- and Dual-Polarized Dielectric Resonator Antennas Using Dielectric and Air Vias," in *IEEE Transactions on Antennas and Propagation*, vol. 69, no. 12, pp. 8182-8193, Dec. 2021.

[59] Y. Li and K. -M. Luk, "Wideband Perforated Dense Dielectric Patch Antenna Array for Millimeter-Wave Applications," in *IEEE Transactions on Antennas and Propagation*, vol. 63, no. 8, pp. 3780-3786, Aug. 2015.

[60] W. M. Abdel-Wahab and S. Safavi-Naeini, "Improvement of aperture coupling in SIW-fed DRA using embedded metallic posts," *Proceedings of the 2012 IEEE International Symposium on Antennas and Propagation*, Chicago, IL, USA, 2012, pp. 1-2.

[61] C. Tong, H. I. Kremer, N. Yang and K. W. Leung, "Compact Wideband Circularly Polarized Dielectric Resonator Antenna With Dielectric Vias," in *IEEE Antennas and Wireless Propagation Letters*, vol. 21, no. 6, pp. 1100-1104, June 2022.

[62] R. Kumar Mongia and A. Ittipiboon, "Theoretical and experimental investigations on rectangular dielectric resonator antennas," in *IEEE Transactions on Antennas and Propagation*, vol. 45, no. 9, pp. 1348-1356, Sept. 1997.